NAVAL POSTGRADUATE SCHOOL
Monterey, California

THESIS

EXPERIMENTAL INVESTIGATION OF VORTEX SHEDDING IN FLOW OVER SECOND-GENERATION, CONTROLLED-DIFFUSION, COMPRESSOR BLADES IN CASCADE

by

Peter J. Brown

March 2002

Thesis Advisor:	Garth V. Hobson
Second Reader:	Raymond P. Shreeve

Report Documentation Page

Report Date	Report Type	Dates Covered (from... to)
29 Mar 2002	N/A	-

Title and Subtitle Experimental Investigation of Vortex Shedding in Flow Over Second-Generation, Controlled-Diffusion, Compressor BLades In Cascade	**Contract Number**
	Grant Number
	Program Element Number
Author(s) Brown, Peter	**Project Number**
	Task Number
	Work Unit Number
Performing Organization Name(s) and Address(es) Naval Postgraduate School Monterey, California	**Performing Organization Report Number**
Sponsoring/Monitoring Agency Name(s) and Address(es)	**Sponsor/Monitor's Acronym(s)**
	Sponsor/Monitor's Report Number(s)
Distribution/Availability Statement Approved for public release, distribution unlimited	
Supplementary Notes The original document contains color images.	
Abstract	
Subject Terms	
Report Classification unclassified	**Classification of this page** unclassified
Classification of Abstract unclassified	**Limitation of Abstract** UU
Number of Pages 106	

REPORT DOCUMENTATION PAGE			Form Approved OMB No. 0704-0188
Public reporting burden for this collection of information is estimated to average 1 hour per response, including the time for reviewing instruction, searching existing data sources, gathering and maintaining the data needed, and completing and reviewing the collection of information. Send comments regarding this burden estimate or any other aspect of this collection of information, including suggestions for reducing this burden, to Washington headquarters Services, Directorate for Information Operations and Reports, 1215 Jefferson Davis Highway, Suite 1204, Arlington, VA 22202-4302, and to the Office of Management and Budget, Paperwork Reduction Project (0704-0188) Washington DC 20503.			
1. AGENCY USE ONLY ***(Leave blank)***	**2. REPORT DATE** March 2002	**3. REPORT TYPE AND DATES COVERED** Master's Thesis	
4. TITLE AND SUBTITLE: Experimental Investigation of Vortex Shedding in Flow Over Second-Generation, Controlled-Diffusion, Compressor Blades in Cascade			**5. FUNDING NUMBERS**
6. AUTHOR(S) Brown, Peter Jeffrey			
7. PERFORMING ORGANIZATION NAME(S) AND ADDRESS(ES) Naval Postgraduate School Monterey, CA 93943-5000			**8. PERFORMING ORGANIZATION REPORT NUMBER**
9. SPONSORING / MONITORING AGENCY NAME(S) AND ADDRESS(ES)			**10. SPONSORING / MONITORING AGENCY REPORT NUMBER**
11. SUPPLEMENTARY NOTES The views expressed in this thesis are those of the author and do not reflect the official policy or position of the Department of Defense or the U.S. Government.			
12a. DISTRIBUTION / AVAILABILITY STATEMENT Approved for public release; distribution is unlimited			**12b. DISTRIBUTION CODE**

13. ABSTRACT ***(maximum 200 words)***

An investigation of vortex shedding downstream of a cascade of second-generation, controlled-diffusion, compressor stator blades, at off-design inlet-flow angles of 31, 33 and 35 degrees and Reynolds numbers, based on chord length, of 280,000, 380,000 and 640,000 is reported. The objective of the study was to characterize the flow and shedding through various complementary methods. Blade surface pressure measurements were taken from a fully instrumented blade, and distributions of pressure coefficients were determined. Five-hole probe wake surveys were performed at midspan, and the total pressure loss coefficients and axial velocity ratios were calculated. Upstream inlet-flow angle was set, and further characterized through two-component laser-Doppler velocimetry (LDV). Hot-wire anemometry measurements were performed at midspan, in the wake, and the reduced data were compared with two-component LDV surveys of the same regions. Plots of hot-wire vs. LDV turbulence data are reported in addition to power spectra documenting the shedding events.

Vortex shedding was determined to be a leading edge phenomenon as periodic shedding was only detected on the pressure side of the wake. The frequency and magnitude of shedding were found to be independent of incidence angle, and to increase with Reynolds number at constant incidence angle. The Strouhal number, based on leading edge diameter, was found to be in the range of 0.23-0.26, which is comparable to that of vortex shedding behind a circular cylinder in the Reynolds number range tested.

14. SUBJECT TERMS Controlled-diffusion, Compressor, Stator, Cascade, Turbomachinery, Hot-wire anemometry, Laser Doppler velocimetry, Vortex shedding			**15. NUMBER OF PAGES** 88
			16. PRICE CODE
17. SECURITY CLASSIFICATION OF REPORT Unclassified	**18. SECURITY CLASSIFICATION OF THIS PAGE** Unclassified	**19. SECURITY CLASSIFICATION OF ABSTRACT** Unclassified	**20. LIMITATION OF ABSTRACT** UL

NSN 7540-01-280-5500 Standard Form 298 (Rev. 2-89)
Prescribed by ANSI Std. 239-18

THIS PAGE INTENTIONALLY LEFT BLANK

EXPERIMENTAL INVESTIGATION OF VORTEX SHEDDING IN FLOW OVER SECOND-GENERATION, CONTROLLED-DIFFUSION, COMPRESSOR BLADES IN CASCADE

Peter J. Brown
Captain, United States Marine Corps
B.S., Chemistry, Texas Tech University, 1992

Submitted in partial fulfillment of the
requirements for the degree of

MASTER OF SCIENCE IN AERONAUTICAL ENGINEERING

from the

NAVAL POSTGRADUATE SCHOOL
March 2002

Author: Peter J. Brown

Approved by: Garth V. Hobson
Thesis Advisor

Raymond P. Shreeve
Second Reader

Max F. Platzer
Chairman, Department of Aeronautics and Astronautics

THIS PAGE INTENTIONALLY LEFT BLANK

ABSTRACT

An investigation of vortex shedding downstream of a cascade of second-generation, controlled-diffusion, compressor stator blades, at off-design inlet-flow angles of 31, 33 and 35 degrees and Reynolds numbers, based on chord length, of 280,000, 380,000 and 640,000 is reported. The objective of the study was to characterize the flow and shedding through various complementary methods. Blade surface pressure measurements were taken from a fully instrumented blade, and distributions of pressure coefficients were determined. Five-hole probe wake surveys were performed at midspan, and the total pressure loss coefficients and axial velocity ratios were calculated. Upstream inlet-flow angle was set, and further characterized through two-component laser-Doppler velocimetry (LDV). Hot-wire anemometry measurements were performed at midspan, in the wake and the reduced data were compared with two-component LDV surveys of the same regions. Plots of hot-wire vs. LDV data are reported in addition to power spectra documenting the shedding events.

Vortex shedding was determined to be a leading edge phenomenon as periodic shedding was only detected on the pressure side of the wake. The frequency and magnitude of shedding was found to be independent of incidence angle, and to increase with Reynolds number at constant incidence angle. The Strouhal number, based on leading edge diameter, was found to be in the range of 0.23-0.26, which is comparable to that of vortex shedding behind a circular cylinder in the Reynolds number range tested.

THIS PAGE INTENTIONALLY LEFT BLANK

TABLE OF CONTENTS

LIST OF FIGURES

THIS PAGE INTENTIONALLY LEFT BLANK

LIST OF TABLES

THIS PAGE INTENTIONALLY LEFT BLANK

LIST OF SYMBOLS

c	blade chord
C_{ac}	fraction of axial chord
C_P	coefficient of pressure
D	blade leading edge diameter
P_{local}	local blade surface pressure
$P_{t\infty}$	freestream stagnation pressure
P_∞	freestream static pressure
Re	Reynolds number
S	blade spacing
St	Strouhal number
U	axial velocity component
V	tangential velocity component
u'	axial turbulent fluctuating velocity
v'	tangential turbulent fluctuating velocity
Vref	reference velocity (test section inlet velocity)
β_1	cascade inlet-flow angle
β_2	cascade outlet-flow angle
β_{1w}	tunnel inlet wall angle
β_{2w}	tunnel outlet wall angle
ω	vortex shedding frequency

THIS PAGE INTENTIONALLY LEFT BLANK

GOVERNMENT DISCLAIMER

The use of trademark software packages used in this study does not imply government endorsement.

THIS PAGE INTENTIONALLY LEFT BLANK

I. INTRODUCTION

A. BACKGROUND

The continual demand for smaller and more powerful engines for today's civil and military aircraft has led to increased requirements for blade loading, improved performance at the design point and perhaps most importantly, the ability to operate at off-design conditions without adverse effects such as compressor stall. These demands have led to the development of controlled-diffusion (CD) blading. Controlled-diffusion blading allows blades to be specifically designed to produce a desired pressure distribution, while simultaneously avoiding boundary-layer separation on the suction side of the blade. This leads to higher blade loading and more turning for each blade row. The increased loading results in a higher pressure ratio with the same number of blades, or fewer blade rows for a desired pressure both of which can reduce size and weight for a desired thrust level.

Controlled-diffusion blading was made possible by the development of Computational Fluid Dynamics (CFD) techniques. Since CFD is an integral part of the blade design process, validation data must be gathered in order to continue the development for more efficient, higher performance blading.

Controlled-diffusion blading design also resulted in profiles which have relatively blunt leading and trailing edges, from which vortex shedding could occur at various off-design conditions. Vortex shedding in turbomachines can result in flow unsteadiness in excess of 20 kHz which is higher than either blade passing frequencies or background turbulence. These unsteady flow phenomena could lead to high cycle fatigue problems within engine components. The first step towards solving these high cycle fatigue problems is an understanding of all the unsteady flow processes within blade rows and the effect these will have on unsteady blade loading levels.

The CD compressor blades investigated in the current study were designed by Thomas F. Gelder of NASA Lewis Research Center, with a design inlet-flow angle of 36 degrees [Ref. 1]. The compressor stator profiles were Stator 67B blades, which together

with Rotor 67, comprised Compressor Stage 67B. The Stator 67B blades were second-generation CD blades, which were designed as an improvement over Stator 67A, a first-generation CD blade designed by Nelson Sanger [Ref. 2].

The present study was an investigation of flow through Compressor Stage 67B CD compressor blades in the Naval Postgraduate School (NPS) low-speed cascade wind tunnel (LSCWT). Hanson [Ref. 3] examined the flow through the mid-span section at a near-design inlet-flow angle of 36.3 degrees, using laser-Doppler velocimetry (LDV) and pressure probe measurements. Schnorenberg [Ref. 4] studied the off-design flow characteristics at an angle of 38 degrees, using LDV measurements, flow visualization, and blade surface pressure measurements to investigate the effect of Reynolds number on a separation region detected near mid-chord. Grove [Ref. 5] characterized the flow patterns at an inlet-flow angle of 39.5 degrees, with flow visualization, rake probe surveys, blade surface pressure measurements and LDV measurements. Nicholls [Ref. 6] characterized and compared the flow patterns over and around the blades after the replacement of the wind tunnel motor. The inlet-flow angle was found to have increased from 39.5 to 40 degrees with no reconfiguration of the tunnel. Carlson [Ref. 7] characterized the three-dimensional flow behavior in the end-wall region of the cascade using five-hole pressure probe and two-component LDV measurements. CFD studies were also initiated to compare blade surface pressure distributions at various inlet-flow angles and inlet boundary layer thickness. Most recently, Caruso [Ref. 8] conducted an off-design (38 degrees) investigation of the three-dimensional flow field ahead of and behind the blades using three-component LDV, and detailed the complex flow field including the corner vortex system.

B. PURPOSE

The objective of the present study was to locate, identify and characterize vortex shedding over the blades at three different off-design inlet-flow angles of 31, 33 and 35 degrees, and three Reynolds numbers based on chord length, of 280,000, 380,000 and 640,000. Various methods were used including surface pressure measurements, five-hole

probe wake surveys, two-component LDV inlet surveys which ensured correct inlet-flow angle settings, and hot-wire anemometry, which was correlated by LDV wake surveys. Sanger and Shreeve [Ref. 9] provided previous measurements on the set of first-generation, controlled-diffusion blades at negative incidence, which produced pure tones at discrete frequencies at a Strouhal number of 0.17 based on trailing edge diameter. The discrete frequencies were most distinct when the mean flow wake profile was most symmetric, i.e. the boundary layer growth was similar on both sides of the blade.

THIS PAGE INTENTIONALLY LEFT BLANK

II. TEST FACILITY AND INSTRUMENTATION

A. LOW-SPEED CASCADE WIND TUNNEL

The present study was conducted in the Low-Speed Cascade Wind Tunnel (LSCWT) located at the Naval Postgraduate School's Turbopropulsion Laboratory. The wind tunnel is powered by a 550-hp electric motor driving a turbo-vane blower, and is capable of producing a sustained maximum freestream Mach number of 0.4 in the test section. Figure 1 shows a schematic of the cascade in the Low Speed Turbomachinery Building (Bldg. 213) with the associated plenum chamber, drive system, and inlet and exhaust ducting. All aspects of the tunnel remain as previously documented by Nicholls [Ref. 6].

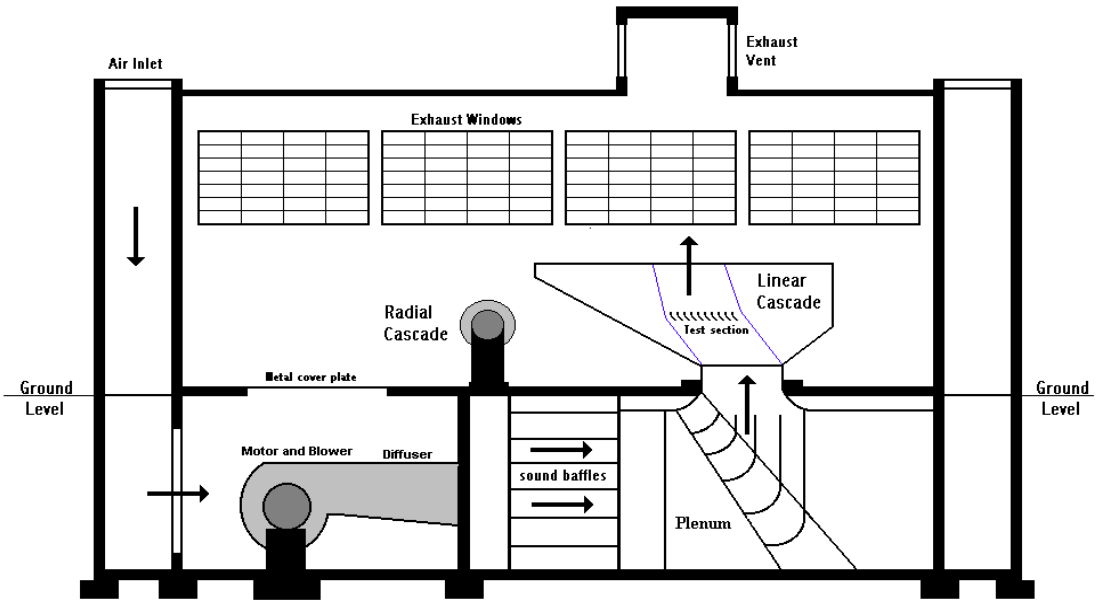

Figure 1. NPS Cascade Wind Tunnel Facility

B. TEST SECTION

The test section of the LSCWT contained 10 Stator 67B controlled-diffusion blades. The installation of the blades in the test section was detailed by Hansen [Ref. 3].

A detailed layout of the test section is shown in Figure 2. Reference 4 contains a description of the procedure used to adjust the inlet-flow angle.

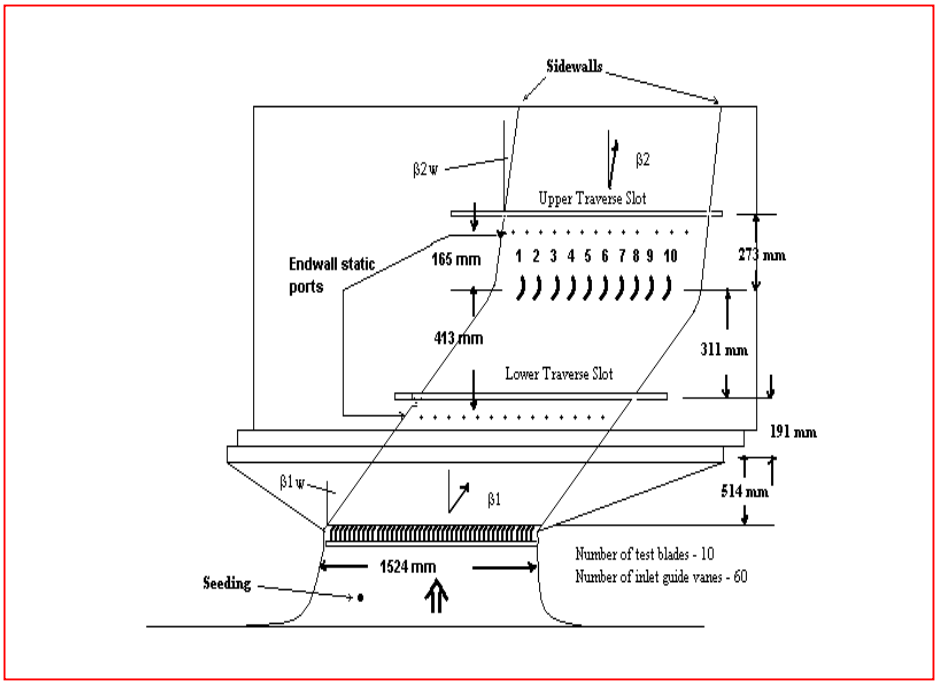

Figure 2. Test Section Schematic

The blades were scaled from the mid-span section of the Stator 67B [Ref. 1]. The coordinates used to machine the blades were documented by Hanson [Ref. 3]. Each blade was 254 mm in span, 127.25 mm in chord and set with blade spacing of 152.4 mm. The blade profile is shown in Figure 3.

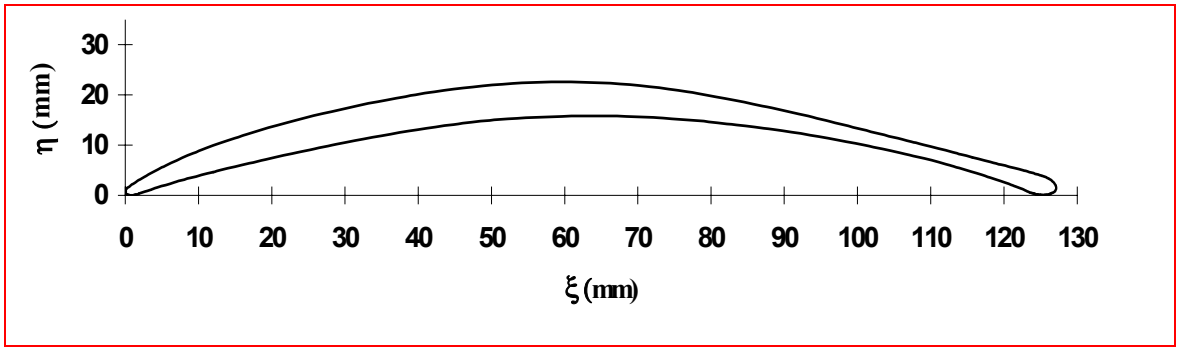

Figure 3. Blade Profile

Blades 2 and 8 (Figure 4) were partially instrumented with eight pressure ports, and blade 6 was fully instrumented with 42 pressure ports around the blade profile at midspan.

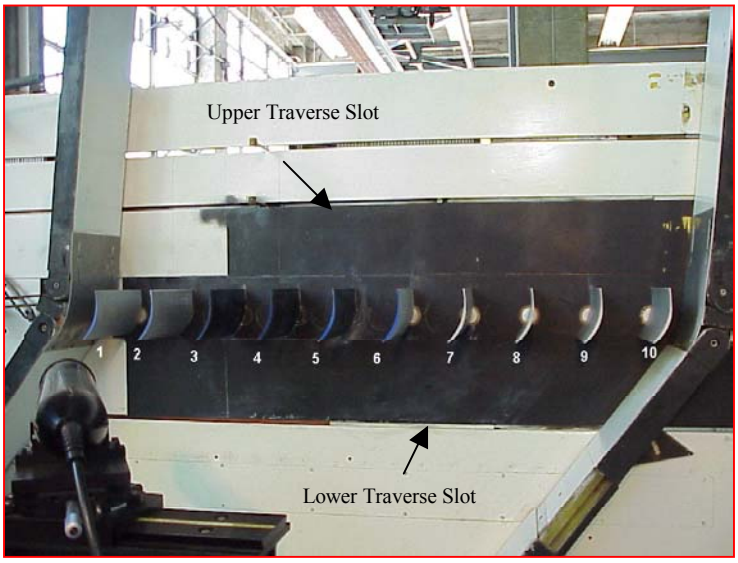

Figure 4. CD Blades Mounted in LSCWT

Five-hole probe measurements were conducted in the wake across blades 3 and 4. The probe was positioned in the upper traverse slot approximately 2 chord lengths downstream of the blade trailing edge. Hot-wire measurements were conducted across blade 4, using the upper traverse slot, but with the probe positioned approximately 1.3 mm (~ 1% chord) downstream of the blade trailing edge. LDV measurements were conducted across blades 3 and 4, which were anodized black to reduce laser light backscatter. Inlet-flow angle LDV measurements were conducted at 38.2 mm (~ 30% chord) upstream of the leading edge, and wake measurements were conducted at 13 mm (~ 10% chord) downstream of the trailing edge.

C. INSTRUMENTATION AND DATA ACQUISITION

1. Pressure Surveys

Surface pressure measurements were taken from the fully instrumented blade 6 and recorded as described by Grove [Ref. 5], to determine the pressure distribution over the surface of the blade and to locate areas of separation. Five-hole probe wake surveys were conducted to characterize wake flow. The probe used for the wake surveys was a

United Sensor conical five-hole probe with a probe diameter of 3.0 mm and port-hole size of 0.1 mm (Fig. 5).

Figure 5. United Sensor Conical Five-Hole Probe

The probe was used in a non null-yawed mode and did not require null yawing at each position before recording the pressure measurements. Grubb [Ref. 10] outlines probe calibration and functional limitations. Matlab codes used to analyze the nine pressure surveys were documented by Carlson [Ref. 7].

All pressures from the five-hole probe and instrumented blades were recorded using two 48-channel rotary pressure scanners as described by Carlson [Ref. 7]. Scanivalve ports and channel assignments are given in Appendix A.

a. ***Data Acquisition***

All pressure data were acquired using the HP75000 Series B VXI-Bus Mainframe controlled by HP-VEE software running on a PC. The acquisition system was documented by Grossman [Ref. 11]. The HP-VEE program used to control the Scanivalve rotary pressure scanners was documented by Nicholls [Ref. 6].

1. Hot-Wire Anemometry Instrumentation and Data Acquisition

Hot-wire anemometry measurements were conducted to characterize, in detail, the flow in the wake of the blades, and to resolve the frequency and magnitude of the unsteady flow downstream of the blades. Measurements were taken with 20 micron TSI Model 1210-20 hot-film probes (Figure 6) with individual serial numbers 014055 (31 degrees) and 72157 (33 and 35 degrees), supported by a custom-built probe holder shown in Figure 7. The probe holder stabilized the hot-film probes and allowed the probes to translate in the upper traverse slot in the LSCWT.

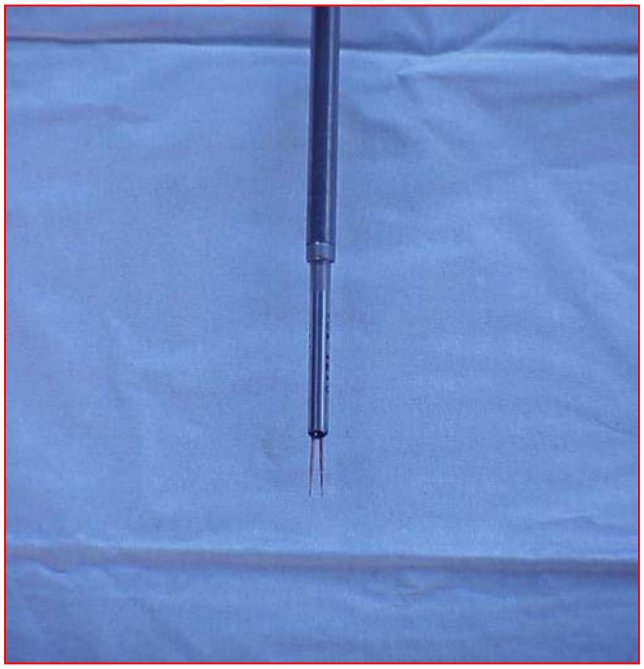

Figure 6. Hot-Film Probe

Figure 7. 20 Micron Hot-Film Probe Holder

Hot-wire data were acquired and reduced using an IFA 100 Intelligent Flow Analyzer, and TSI ThermalPro software version 4.50.03, running on a PC. Figure 8 shows the IFA 100 data acquisition system. Operational procedures can be found in Appendix B.

Figure 8. IFA 100 Data Acquisition System

3. LDV Instrumentation and Data Acquisition

LDV measurements were obtained using a TSI two-component fiber-optic system. The system included a five-watt Lexel Model 95 argon-ion laser, directed into a TSI Model 9201 Colorburst multicolor beam separator, transmitted by fiber-optic cables to two 83 mm probes. The reflected signals were collected by the probes and fed back to a TSI Model 9230 Colorlink, via a return fiber-optic cable. The laser, optics system, data acquisition system, laser flow seeding systems and traverse mechanism, were described by Caruso [Ref. 8]. All LDV data were acquired and reduced using TSI Find For Windows software, version 1.4. Figure 9 shows the fiber optic probes, traverse mechanism and data acquisition system of the LDV setup.

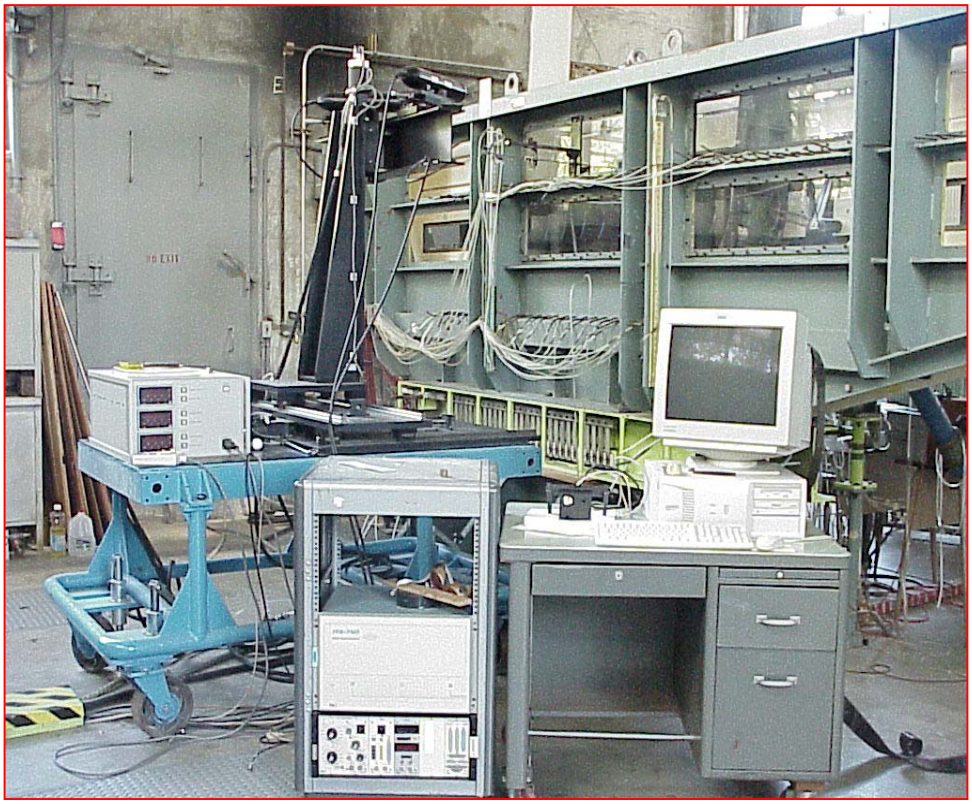

Figure 9. LDV Optics, Traverse and Data Acquisition System

THIS PAGE INTENTIONALLY LEFT BLANK

III. EXPERIMENTAL PROCEDURE

A. REYNOLDS NUMBER AND INLET-FLOW ANGLE VARIATION

In order to fully quantify the unsteady flow characteristics and make legitimate comparisons of frequency and magnitude, data were collected at three Reynolds numbers and three inlet-flow angles.

The tunnel was run at plenum gage pressures of 51 mm (2 inches), 102 mm (4 inches) and 305 mm (12 inches) of water, corresponding to Reynolds numbers based on chord length of 280,000, 380,000 and 640,000 respectively. The "low", "medium", and "high" Reynolds numbers corresponded to freestream Mach numbers of 0.09, 0.13 and 0.22 respectively.

The cascade inlet walls were initially set at $\beta_{1W} = 35°$ (-1°incidence) giving $\beta_1 = 35.2°$ and the tailboards were set at β_{2W}(West) = 3.5° and β_{2W}(East) = 3.8°. Subsequent reconfigurations of the tunnel positioned the inlet walls at $\beta_{1W} = 33°$ (-3° incidence) giving $\beta_1 = 32.8°$ with tailboard settings of 2.8° (West) and 3.1° (East); and finally, $\beta_{1W} = 31°$ (-5° incidence) giving $\beta_1 = 31.2°$, with tailboards set at 2.2° (West) and 2.1° (East).

B. PRESSURE MEASUREMENTS

1. Blade Surface Pressure Measurements

The cascade tunnel was allowed to reach an equilibrium plenum temperature prior to all surveys. Blade surface pressure measurements were taken from the fully instrumented blade number 6, using the HP Automated Data Acquisition System and Scanivalve #1, as described in Grossman [Ref. 11], and the HP-VEE Software program "Test_Scanners_Pressures3" documented by Nicholls [Ref. 6]. Inlet total and static pressures were recorded to non-dimensionalize the blade surface pressure measurements as a coefficient of pressure; i.e., $C_p = (p_{local} - p_\infty) / (p_{t\infty} - p_\infty)$. Pressure distributions were recorded for each of the three Reynolds numbers at nominally 31, 33 and 35 degrees inlet-flow angle to examine the effects of varying tunnel speed and incidence angle.

2. Five-Hole Probe Pressure Measurements

The five-hole probe was mounted in a traverse mechanism in the upper traverse slot of the tunnel (Fig. 4). The probe was centered at midspan of the blades and aligned with the leading edge of blade 3. The probe was traversed across one full blade passage (152.4 mm) in 6.35 mm increments. A two-minute time delay prior to recording each data point allowed pressure stabilization in the tubing to the Scanivalve. The probe was rotated 4 degrees off axial for all inlet-flow angles and Reynolds numbers to center the yaw measurements with respect to the range over which the probe was calibrated.

Pressures were measured at all three Reynolds numbers at 31, 33 and 35 degrees inlet-flow angle using Scanivalve #2, and recorded with the plenum temperature and probe yaw angle using an HP-VEE program called "Test_Scanners_Fivehole" documented in Nicholls [Ref. 6].

C. HOT-WIRE ANEMOMETRY

1. IFA 100 and Hot-Wire Calibration

The cable resistance was measured on the IFA 100 with the shorting probe inserted in place of the hot-film probe. Then the hot-film probe resistance was measured by replacing the shorting probe with the hot-film probe. Operating resistance, which was probe specific, and the bridge compensation were set, and the no-flow voltage was noted. The tunnel was started, allowed to reach equilibrium temperature at 305 mm (12 inches) of H_2O, and cable compensation was adjusted, noting the voltage at the high Reynolds number. From the high Reynolds number voltage, no-flow voltage, and probe resistance, span, offset and gain were calculated and set on the IFA 100.

The actual *in situ* calibration run of the tunnel consisted of recording plenum pressure, plenum temperature, pitot pressure and voltage data at each of seven discrete plenum pressure settings (0", 0.4", 4", 8", 10", 12" and 14"). During the run, the hot-film probe was positioned as close as possible to a downstream pitot tube to ensure the same velocity. The calibration curves and King's Law coefficients were calculated by the TSI software and saved in a calibration file. A complete description of the calibration and operational procedures is presented in Appendix B.

2. Hot-Wire Wake Surveys

Data acquisition files were created with the appropriate calibration information and specific probe data. Data were taken by traversing the hot-film probe across 76.2 mm passages (38.1 mm either side of centerline of the trailing edge) downstream of blade 4. The probe was traversed at the minimum attainable increment of 1.27 mm, producing 60 discrete data points per survey. A survey was conducted for each Reynolds number (280,000, 380,000 and 640,000) at each inlet-flow angle (31, 33 and 35 degrees). At each point in the survey, 8000 samples were recorded at a rate of 40 K samples per second. Atmospheric pressure and temperature, as well as plenum pressure and temperature were recorded for each run. Raw data were reduced using the TSI ThermalPro software version 4.50.03, and data were normalized to a reference velocity calculated for the particular inlet-flow angle and Reynolds number.

D. LDV MEASUREMENTS

1. Inlet Guide Vane Adjustment

The tunnel was reconfigured three times to nominal off-design inlet-flow angles of 31, 33 and 35 degrees. After each reconfiguration, prior to any data collection, LDV inlet surveys were conducted at Station 1, over 1 full passage (152.4 mm), to determine the mean flow angle downstream of the inlet guide vanes (β_1). Inlet guide vanes were adjusted until the mean flow angle was within 0.2 degrees of the desired inlet-flow angle of the blades.

2. Tunnel Calibration

Plenum pressure, plenum temperature and atmospheric pressure were recorded, while axial and tangential velocity components were measured with the LDV traversing across blades 3 and 4 at Station 1. The tunnel reference velocity was determined as the mean of the resultant vector magnitude. Each run was non-dimensionalized by the reference velocity to allow surveys under differing atmospheric conditions to be compared.

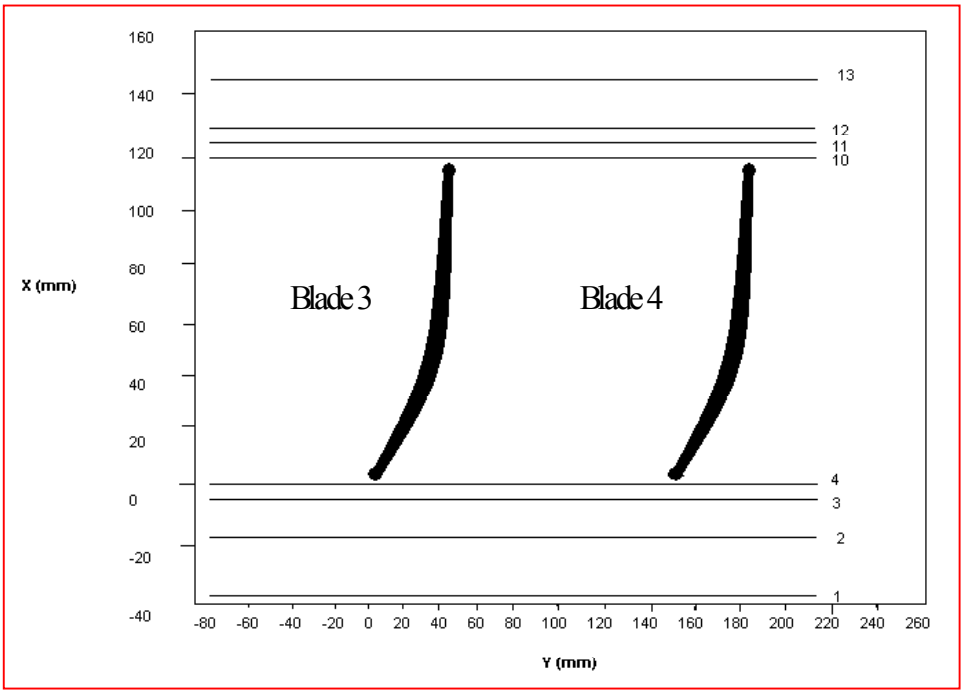

Figure 10. LDV Survey Locations

3. LDV Probe Volume Alignment

The LDV probe volume was aligned prior to surveys using an alignment tool. A description of the coordinates for the alignment tool is documented in Hansen [Ref. 3]. LDV surveys were performed at midspan, and all survey positions were measured from a reference position at the leading edge of blade 3.

4. Particle Seeding

Vegetable oil was used as the seeding material for the present study. The seed particle generator used was a TSI Model 9306 6-jet atomizer modified as shown and described in Caruso [Ref. 8]. The four adjustable wands provided adequate seeding coverage for the survey area.

5. LDV Surveys

A total of 23 two-dimensional LDV surveys were completed in the present study. These included 9 inlet and 14 wake surveys at Reynolds numbers of 280,000, 380,000

and 640,000 at each of the three inlet-flow angles 31, 33 and 35 degrees. The wake surveys were both coarse and fine. All surveys were conducted at midspan.

Data output included axial and tangential velocities, turbulence intensities, Reynolds stresses and Reynolds stress correlation coefficient. All data were processed using Find For Windows software version 1.4, and runs were non-dimensionalized using the reference velocity calculated for each run.

a. *Inlet Surveys*

Inlet-flow surveys were conducted at Station 1, from the leading edge of blade 3 to the leading edge of blade 4 (152.4 mm), in 6.35 mm increments. Prior to each set of surveys, the laser beams were tuned using a Newport Model 815 digital power meter. Surveys were conducted at 2 watts of laser power for all three Reynolds numbers at each inlet-flow angle for a total of 9 surveys. Five MHz of frequency shifting was used for data acquisition and all histograms used 1000 points.

b. *Wake Surveys*

Coarse wake surveys were conducted at Station 12, from the leading edge of blade 3 to the leading edge of blade 4 (152.4 mm), in 6.35 mm increments. Prior to each set of surveys, the laser beams were tuned as in the inlet surveys. Surveys were conducted at 2 watts of laser power and 5 MHz of frequency shift for all three Reynolds numbers at each inlet-flow angle for a total of 9 surveys. All histograms used 1000 points.

Fine wake surveys were run to correlate hot-wire data. In order to position the LDV probe volume to correspond with the initial wake position of the hot-wire data, the laser beams were focused on the hot-film probe in the tunnel, and the coordinates set as a zero point. The LDV was then traversed in 1.27 mm increments (the same 1/20" used in the hot-wire anemometry), to the final wake point of interest. The surveys were conducted at a Reynolds number of 380,000 at 31, 33 and 35 degrees, and also 280,000 and 640,000 at 33 degrees. Each of the 5 surveys resulted in 15-25 data points depending upon wake size. Surveys were conducted at 2 watts of laser power and 5 MHz of frequency shift. All histograms used 1000 points.

THIS PAGE INTENTIONALLY LEFT BLANK

IV. RESULTS AND DISCUSSION

A. SURFACE PRESSURE MEASUREMENTS

Surface pressure measurements were taken from the fully instrumented blade 6 at each of the three Reynolds numbers at each inlet-flow angle. The blade surface pressure measurements were non-dimensionalized using inlet total and static pressures. The surface pressure distributions are presented in terms of the coefficient of pressure (C_P) plotted against fraction of the blade chord (x/c).

The three surface pressure distributions for an inlet-flow angle of 35 degrees (-1° incidence) are shown in figure 11.

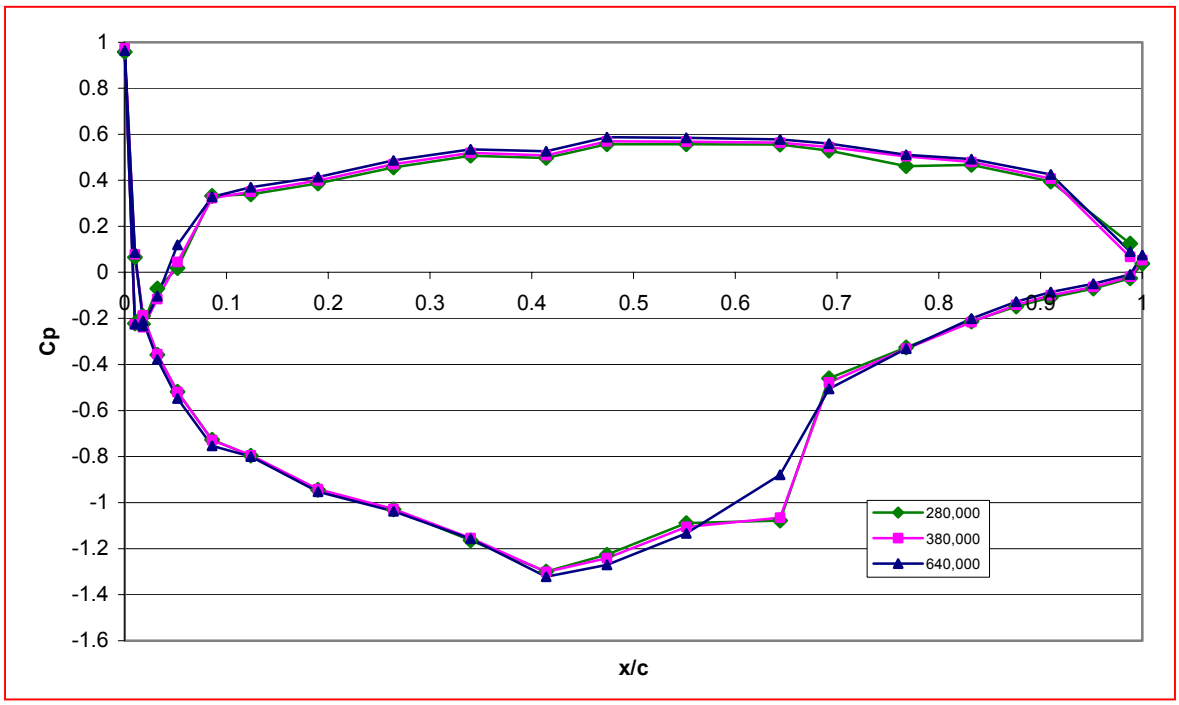

Figure 11. C_P vs x/c for 35° Inlet-Flow Angle

The suction side C_P is shown to decrease almost immediately at the leading edge to a value of -0.75. The acceleration of the flow continued to 0.41 x/c where the C_P reached its minimum value of -1.32. From 0.41, the suction side pressure distribution increased with no sign of separation until 0.55 x/c. Between 0.55 and 0.68 x/c, the adverse pressure gradient caused laminar flow separation on the blade surface at the low

and medium Reynolds numbers. At the high Reynolds number, the boundary layer underwent transition ahead of the bubble which energized the velocity profile at the blade surface, and partially suppressed the separation bubble. The observed behavior was similar to that measured at positive incidence by Schnorenberg [Ref. 4]. The C_P distribution over the pressure side after an initial spike, was smooth and constant to the trailing edge, with no evidence of separation. Near the trailing edge, the positive gradient was caused by the thickened profile of the elliptic trailing edge.

The three surface pressure distributions for an inlet-flow angle of 33 degrees (-3° incidence) are shown in Figure 12.

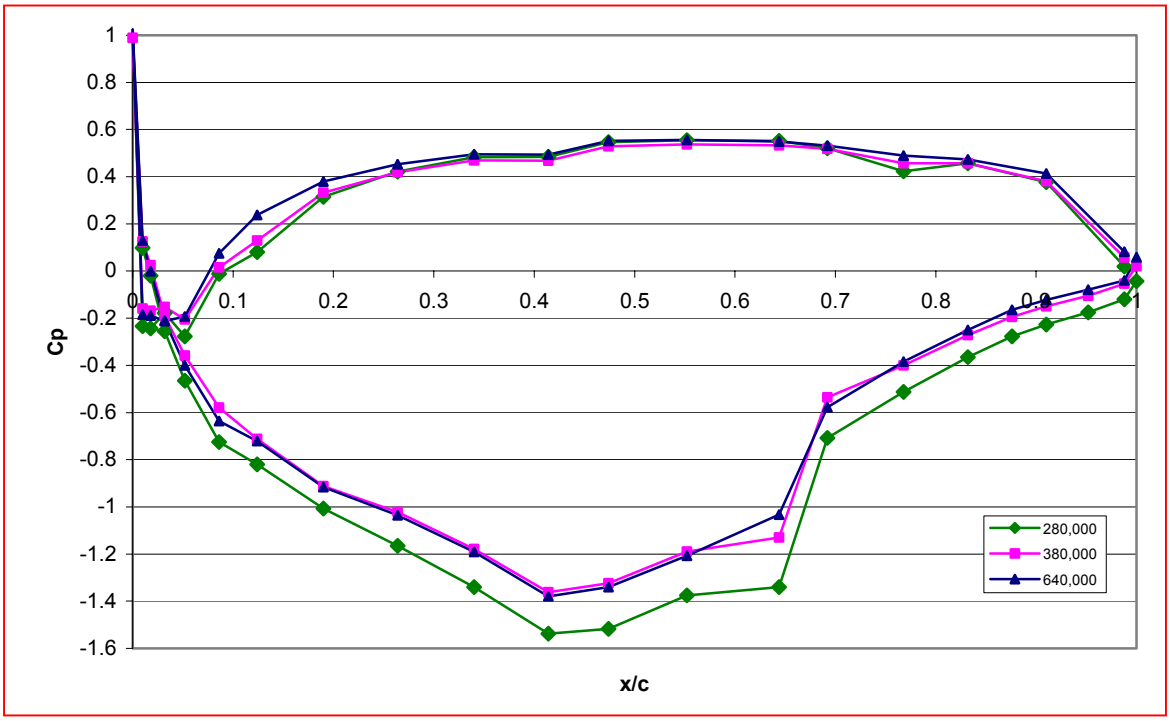

Figure 12. C_P vs x/c for 33° Inlet-Flow Angle

The suction side C_P is seen to decrease at the leading edge to a value of -0.68. The acceleration of the flow continued again to 0.41 x/c where the C_P reached its minimum value of -1.37. From 0.41, the suction side pressure distribution increased with no sign of separation until 0.55 x/c. Between 0.55 and 0.68 x/c, an adverse pressure gradient existed causing laminar flow separation on the blade. The C_P distribution on the

pressure side showed that the initial spike at x/c ≈ 0.01 had grown, in extent, giving rise to a pressure plateau between x/c = 0.01 and x/c = 0.05. This was indicative of a pressure side, leading edge separation bubble at all three Reynolds numbers.

The three surface pressure distributions for an inlet-flow angle of 31 degrees (-5° incidence) are shown in Figure 13.

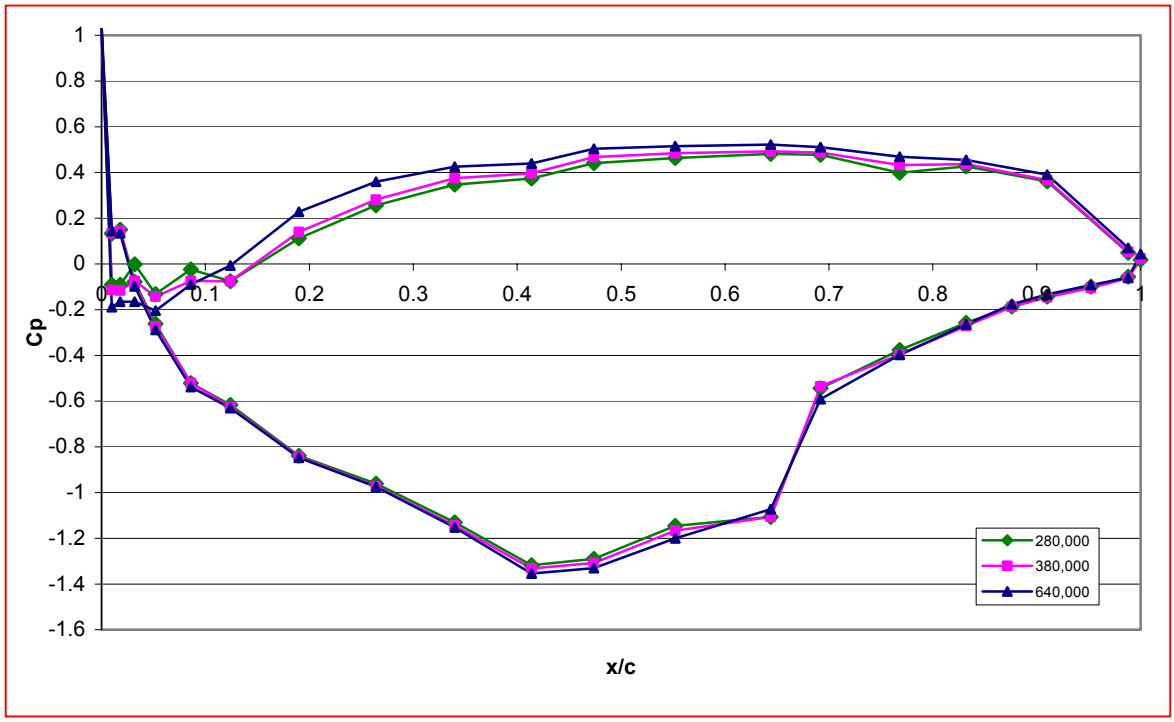

Figure 13. C_P vs x/c for 31° Inlet-Flow Angle

The suction side C_P decreased at the leading edge to a value of -0.58. Acceleration of the flow continued to 0.41 x/c where the C_P reached its minimum value of -1.35. From 0.41 x/c to 0.55 x/c the C_P increased linearly, showing no sign of separation. Between 0.55 and 0.68, an adverse pressure gradient existed, causing laminar flow separation on the blade. The C_P distribution on the pressure side showed that the initial spike at x/c ≈ 0.01 had grown even larger, and the pressure plateau extended between x/c = 0.01 and x/c = 0.125; again indicative of a pressure side, leading edge separation bubble at all three Reynolds numbers. The C_P distribution over the pressure side showed an even larger area of separation than seen at 33°, and then was smooth and

constant to the trailing edge. The location and magnitude of the separation bubble on the suction side with change in Reynolds number became constant.

Overall, the flow seemed more two-dimensional with decreasing incidence angle. The initial suction C_P became more positive with decreasing incidence angle. The pressure side separation bubble appeared larger with decreasing incidence angle. The suction side turbulent flow separation bubble location was relatively constant (0.65-0.70 x/c), as was the minimum C_P (~ -1.35).

B. FIVE-HOLE PROBE MEASUREMENTS

Downstream five-hole probe surveys were taken across one full blade passage at all three Reynolds numbers at each inlet-flow angle. A total of 25 data points, with a uniform spacing of 6.35mm, were recorded during each survey. Loss coefficients and Axial Velocity Ratios (AVRs) were calculated for each survey using the formulas documented in Appendix A of Carlson [Ref. 7] and are presented in Table 1 with the representative inlet-flow angles and Reynolds numbers to be discussed in detail, highlighted in blue.

Inlet Flow Angle	**Re=280,000**	**Re=380,000**	**Re=640,000**
31 degrees			
AVR	1.009	1.027	1.077
Loss Coefficient	0.079	0.069	0.088
33 degrees			
AVR	1.010	1.029	1.082
Loss Coefficient	0.014	0.048	0.088
35 degrees			
AVR	1.003	1.007	1.070
Loss Coefficient	0.020	0.040	0.044

Table 1. Five-Hole Probe AVR and Loss Coefficients

The flow was well behaved at a constant inlet-flow angle as indicated by an increased AVR and loss coefficient with increased Reynolds number. At a constant Reynolds number of 380,000, AVR remained relatively constant as expected, and the loss coefficient showed an increasing trend as inlet-flow angle decreased, also as expected.

The pressure differences being measured at the low Reynolds number (280,000) were very small (on the order of one 1/100" H_2O), making the loss coefficient calculations suspect, and only the medium and high Reynolds number data were used for comparison and trend analysis.

Figure 14 shows the pitchwise, non-dimensionalized stagnation pressure distribution for the first of the representative data sets; 33 degrees inlet-flow angle and Reynolds number of 380,000.

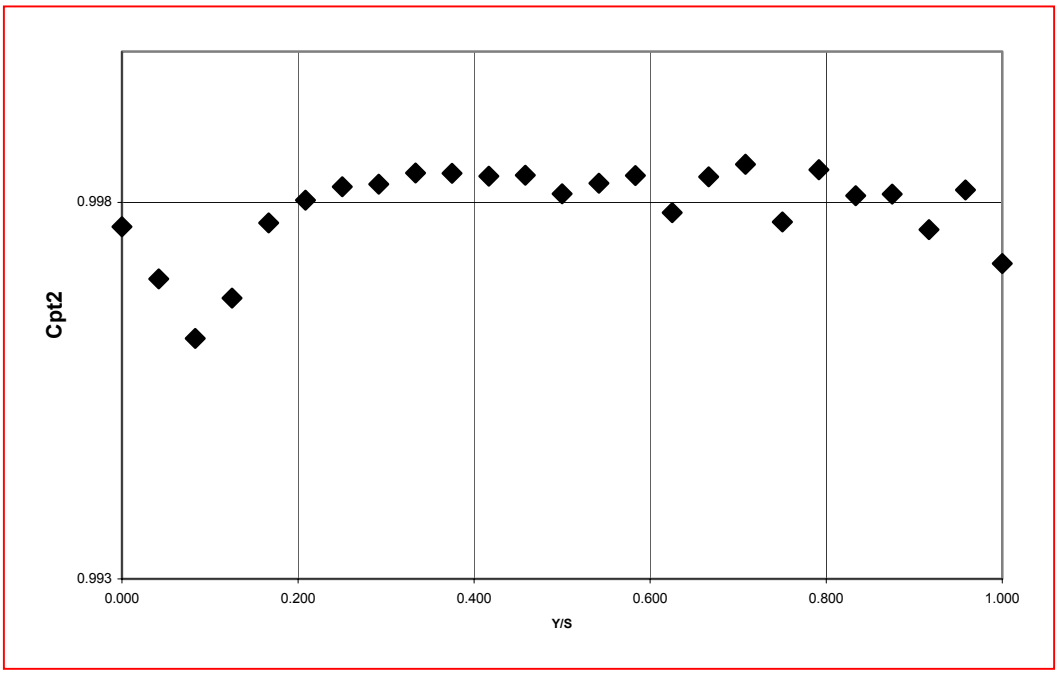

Figure 14. Non-Dimensional Pressure Distribution at 33° & Re = 380,000

Individual survey plots similar to Fig. 14, for the remaining eight five-hole probe pressure surveys and the five-hole probe equations are presented in Appendix C. Reduced data for all nine five-hole probe pressure surveys are presented in Appendix D. The five-hole probe data reduction in MATLAB is documented in Carlson [Ref. 7].

C. INLET-FLOW SURVEYS

LDV measurements were taken at midspan across 1 blade passage (152.4 mm) to characterize the inlet-flow and to determine and set the inlet-flow angle (β_1). Inlet surveys were taken at Station 1 (0.3 C_{ac} upstream), for all three Reynolds numbers at each

inlet-flow angle. All turbulence intensities were calculated using two standard deviations of data refinement. Plots are presented in Figures 15 and 16, and the reduced data for the five surveys are presented in Appendix E.

1. LDV Inlet Survey at 31° Inlet-flow Angle and Re = 380,000

The station 1 survey was used to determine and set the inlet-flow angle to ensure uniform upstream flow as close as possible to the desired blade inlet-flow angle setting. The inlet angle at each point across the blade passage from blade 3 to blade 4 is plotted vs. blade spacing (Y/S) in Figure 15, and the average inlet-flow angle was determined to be 31.2 degrees. A 3.5° variation in flow angle from blade to blade was seen as a result of the potential effect of the blades on the approaching flow.

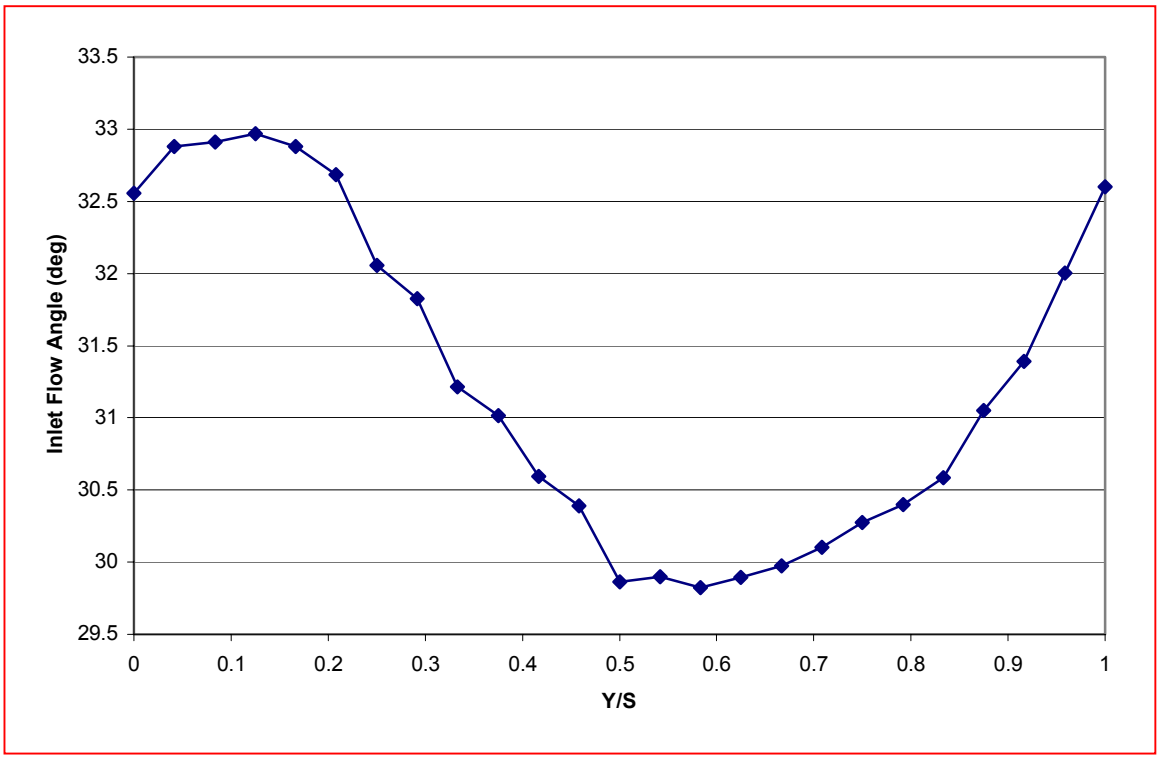

Figure 15. Inlet Flow Angle Distribution at 31° and Re = 380,000

The Station 1 survey results for 31° at the medium Reynolds number are shown in Figure 16. The survey indicated nearly uniform velocity across the blade space, with the wave-like features of the velocity ratios as result of the upstream influence of the blades. The "ripple effect" (3 per blade) in the turbulence intensity was a result of the downstream influence of the unmixed wakes of the inlet guide vanes. Turbulence intensities varied from 1.6 to 2.25%. The Reynolds-stress correlation coefficient was positive, but very small, indicating that turbulent fluctuations were uncorrelated.

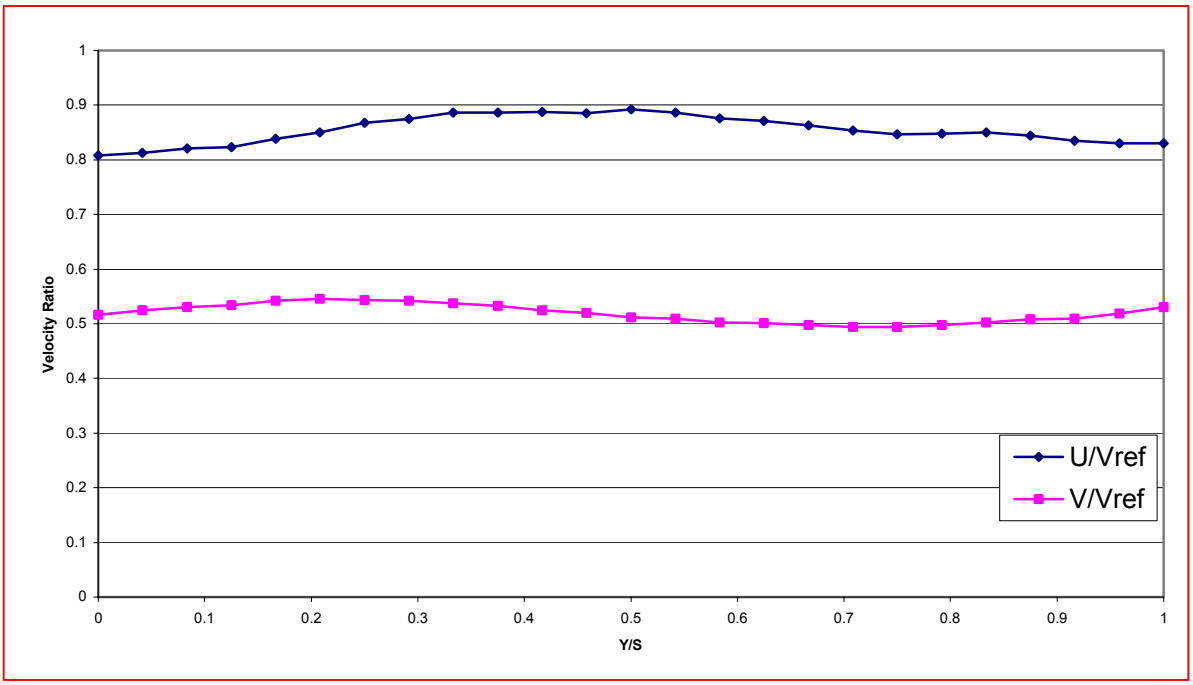

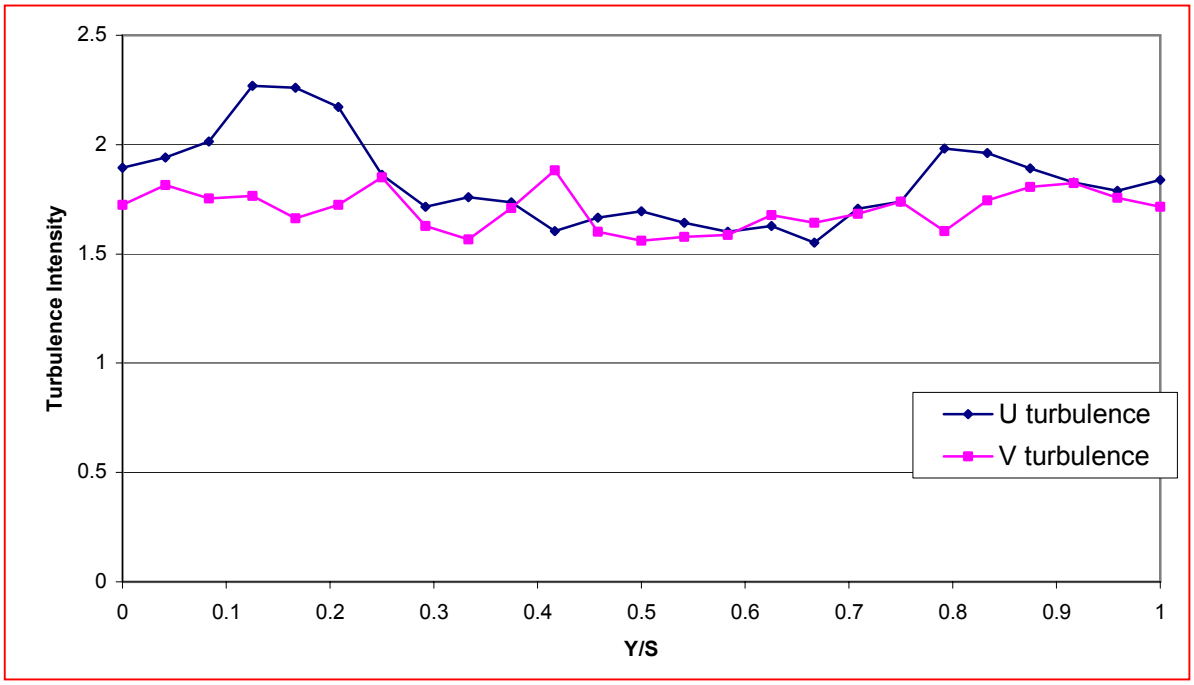

Figure 16. Station 1 LDV Inlet Survey at 31° and Re = 380,000

D. WAKE FLOW SURVEYS

Wake surveys were conducted both by hot-wire anemometry and LDV. Hot -wire surveys were taken across a 76.2 mm passage (38.1 mm either side of centerline), 1.3 mm downstream of the trailing edge of blade 4. Surveys were taken for all three Reynolds numbers at all three inlet-flow angles. Non-dimensionalized, reduced data are presented in the form of mean flow plots, turbulence intensity plots and frequency spectra. Data are discussed here only for the representative inlet-flow angles and Reynolds numbers (31°, 33° and 35° at Re=380,000 and 33° at Re=280,000 and 640,000). The reduced hot-wire data can be found in Appendix F, and the LDV data in Appendix G.

LDV surveys were conducted at Station 12, 13 mm downstream of the trailing edges of blades 3 and 4. Coarse wake surveys covered a full 152.4 mm blade passage in 6.35 mm increments. Fine wake surveys were conducted to coincide with the wake points previously established in the hot-wire anemometry (procedure described in section III), at 1.27 mm increments, to encompass the entire wake region. LDV surveys were primarily used to correlate hot-wire data, but were also used to analyze the Reynolds-stress correlation coefficient.

1. Hot-Wire and LDV Surveys at 31° and Re = 380,000

The hot-wire and LDV wake surveys are shown combined in Figure 17. The freestream velocity profiles showed that a maximum was reached on either side of the wake, decreasing to a minimum at the center of the wake passage. The pressure-side entry into the wake was visibly steeper than the suction side, but otherwise, the wake was relatively symmetric and well defined. The turbulence intensity profiles showed good correlation with the mean flow profile as the maximum turbulence intensity (point 31) occurred at the location of the maximum gradient of the mean flow profile on the pressure side of the blade. The pressure-side separation was clearly evident in the rising turbulence intensity prior to the maximum, as opposed to the clean exit from the wake on the suction side, where the freestream turbulence intensity levels were recovered. The Reynolds-stress plots indicated significant shear on the pressure-side entry to the wake, also suggesting leading edge, pressure side, vortex shedding.

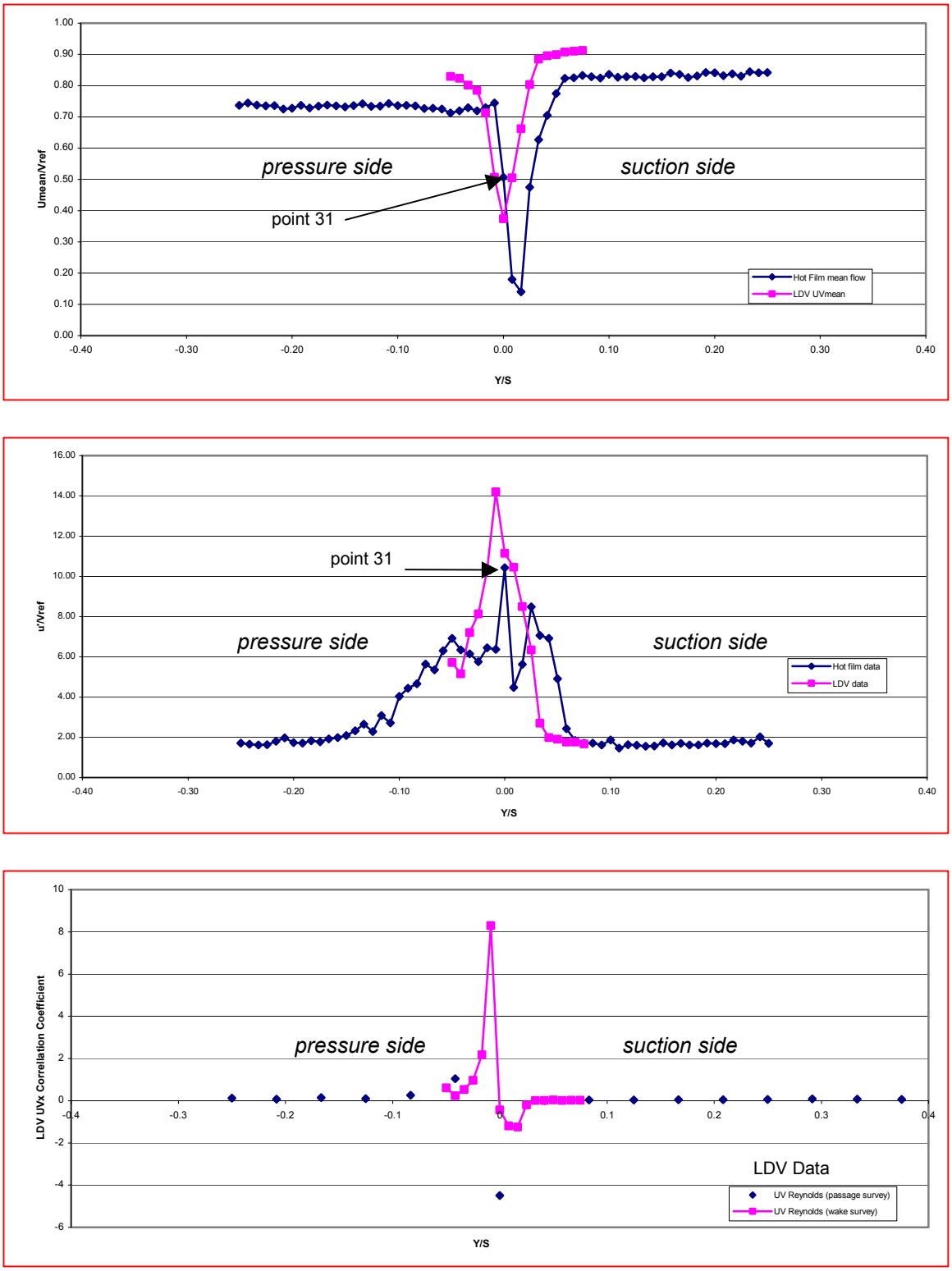

Figure 17. Hot-Wire and LDV Surveys at 31° and Re = 380,000

The positional shift in LDV data vs. hot-wire data was a product of the inability to exactly position the probe volume on the hot-film probe during position calibration. The difference in magnitude of the plots could be caused by the fact that the hot-wire was calibrated downstream of the blade row, while the LDV data was non-dimensionalized with an upstream reference velocity. In general, this led to more conservative values in the hot-wire measurements.

Figure 18 shows the FFT of point 31 as a frequency/power spectrum plot. Frequency/power spectra were generated for every point in the survey, and were analyzed for indications of vortex shedding, based on the mean flow and turbulence intensity information from the hot-wire and LDV surveys. Strouhal numbers were calculated as $St = \omega D/U_{mean}$, based on a leading edge diameter (D) of 4.0 mm, then used to verify peaks corresponding to areas of likely vortex shedding. Figure 18 corresponds to 1.27 mm on the pressure side of the blade 4 centerline. The Strouhal number calculated, for the minor peak at 1870 Hz, was 0.25, which was similar to results predicted in Roshko [Ref. 12]. Point 31 was the only point on the pressure side to display a frequency spike. There was no detectable shedding on the suction side of the blade. The minor peak at 1870 Hz also corresponded to the location of maximum turbulence intensity in Figure 17. One reason for this peak not being distinct could be that it was diminished due to increased pressure side turbulence levels that also originated at the leading edge (-0.13<Y/S<-0.01 in Figure 17).

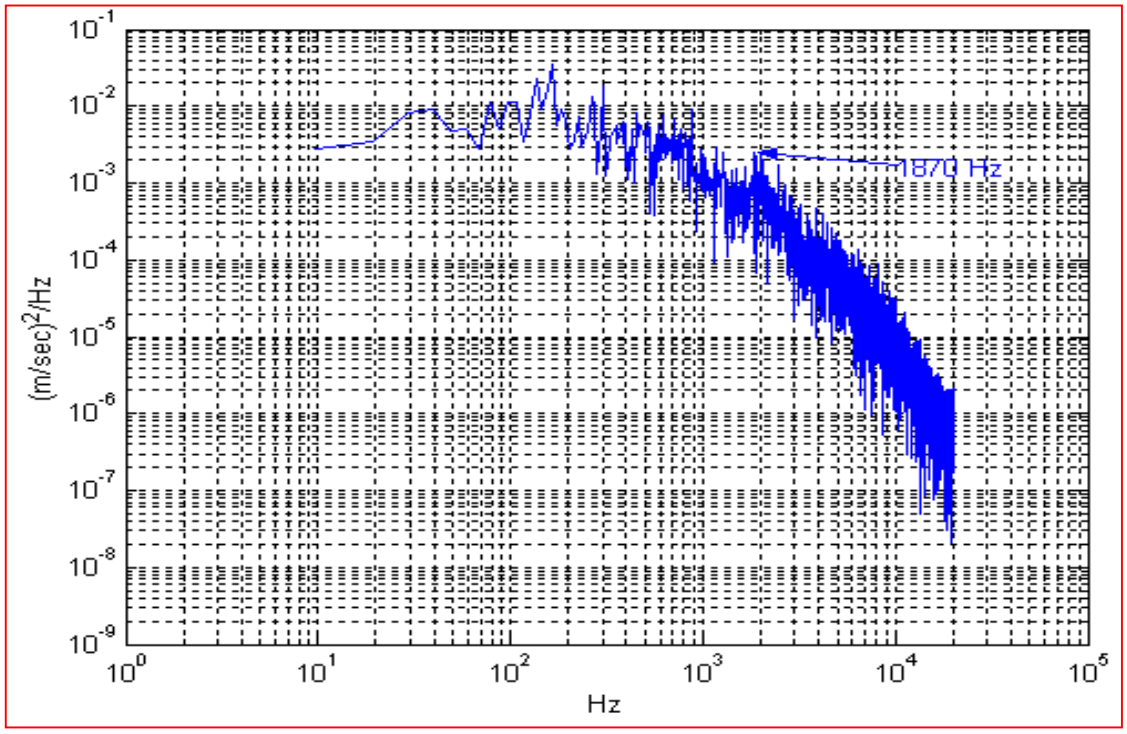

Figure 18. Power Spectrum (Point 31) at 31° and Re = 380,000

2. Hot-Wire and LDV Surveys at 33° and Re = 380,000

The hot-wire and LDV wake surveys are shown combined in Figure 19. The freestream velocity profiles showed better correlation on both sides of the wake. The pressure-side entry into the wake was still steeper than the suction side, but the wake was symmetric and well defined. The turbulence intensity profiles showed better correlation with both maximum turbulence intensities corresponding to the location of the maximum gradient of the mean flow profile on the pressure side of the blade. The pressure-side turbulence rise was steeper and delayed, indicating a smaller area of separation as expected. The Reynolds-stress plots indicated less significant shear on the pressure-side entry to the wake.

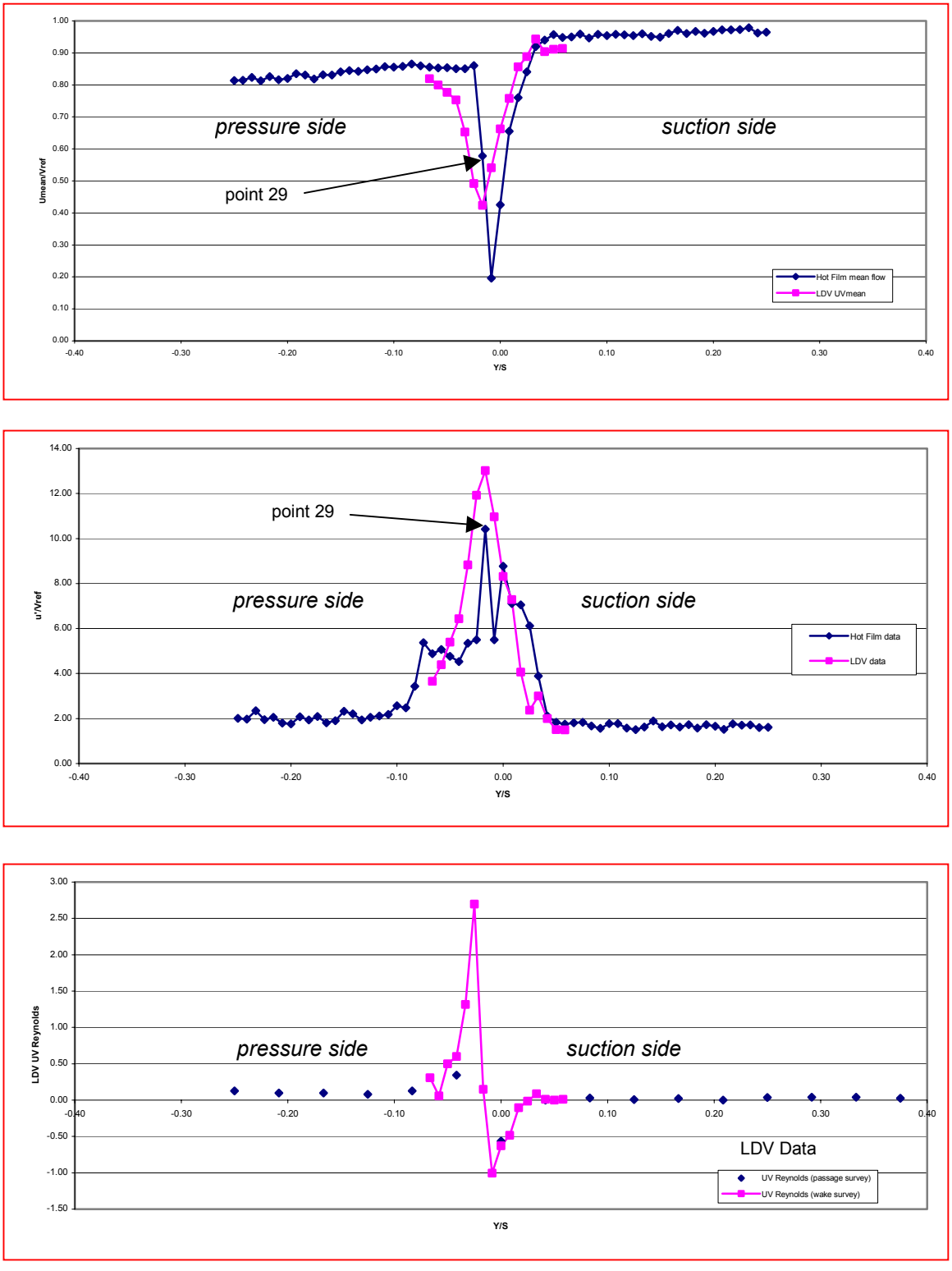

Figure 19. Hot-Wire and LDV Surveys at 33° and Re = 380,000

Figure 20 shows the FFT of point 29 as a frequency/power spectrum plot. Frequency/power spectra were generated for every point in the survey, and were analyzed for indications of vortex shedding, based on the mean flow and turbulence intensity information from the hot-wire and LDV surveys. Figure 20 shows the spectrum corresponding to 1.27 mm on the pressure side of the blade 4 centerline. The Strouhal number calculated, for the peak at 2050 Hz, was 0.24, also similar to results predicted in Roshko [Ref. 12]. Point 29 was the only point on the pressure side to display a frequency spike. There was no detectable shedding on the suction side of the blade. The peak at 2050 Hz also corresponded to the location of maximum turbulence intensity in Figure 19. This peak also lacked distinctness due to increased pressure side turbulence levels that originated at the leading edge (-0.1<Y/S<-0.01 in Figure 19).

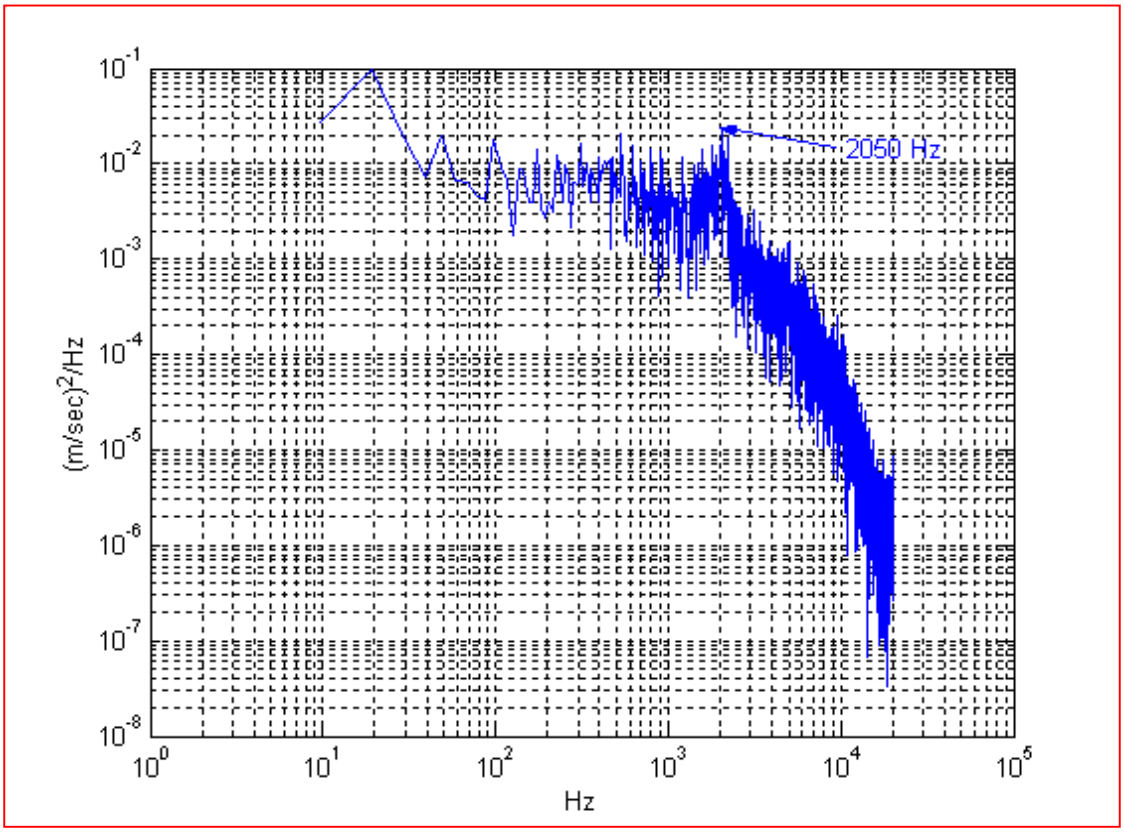

Figure 20. Power Spectrum (Point 29) at 33° and Re = 380,000

3. Hot-Wire and LDV Surveys at 35° and Re = 380,000

The hot-wire and LDV wake surveys are shown combined in Figure 21. The freestream velocity profiles showed a positional correlation on both sides of the wake with a magnitude difference as a result of calibration location differences between hot-wire and LDV. The pressure-side entry into the wake was still steeper than the suction side, but the wake was symmetric and well defined. The turbulence intensity profiles showed shape similarity with LDV maximum turbulence intensity corresponding to the location of the maximum gradient of the mean flow profile on the pressure side of the blade. The pressure-side turbulence rise was steeper and delayed, indicating a smaller area of separation, as expected at only one-degree off-design incidence angle. The Reynolds-stress plots indicated almost insignificant shear on the pressure-side entry to the wake. There was little difference in intensity of Reynolds stress between the full passage survey and the wake survey.

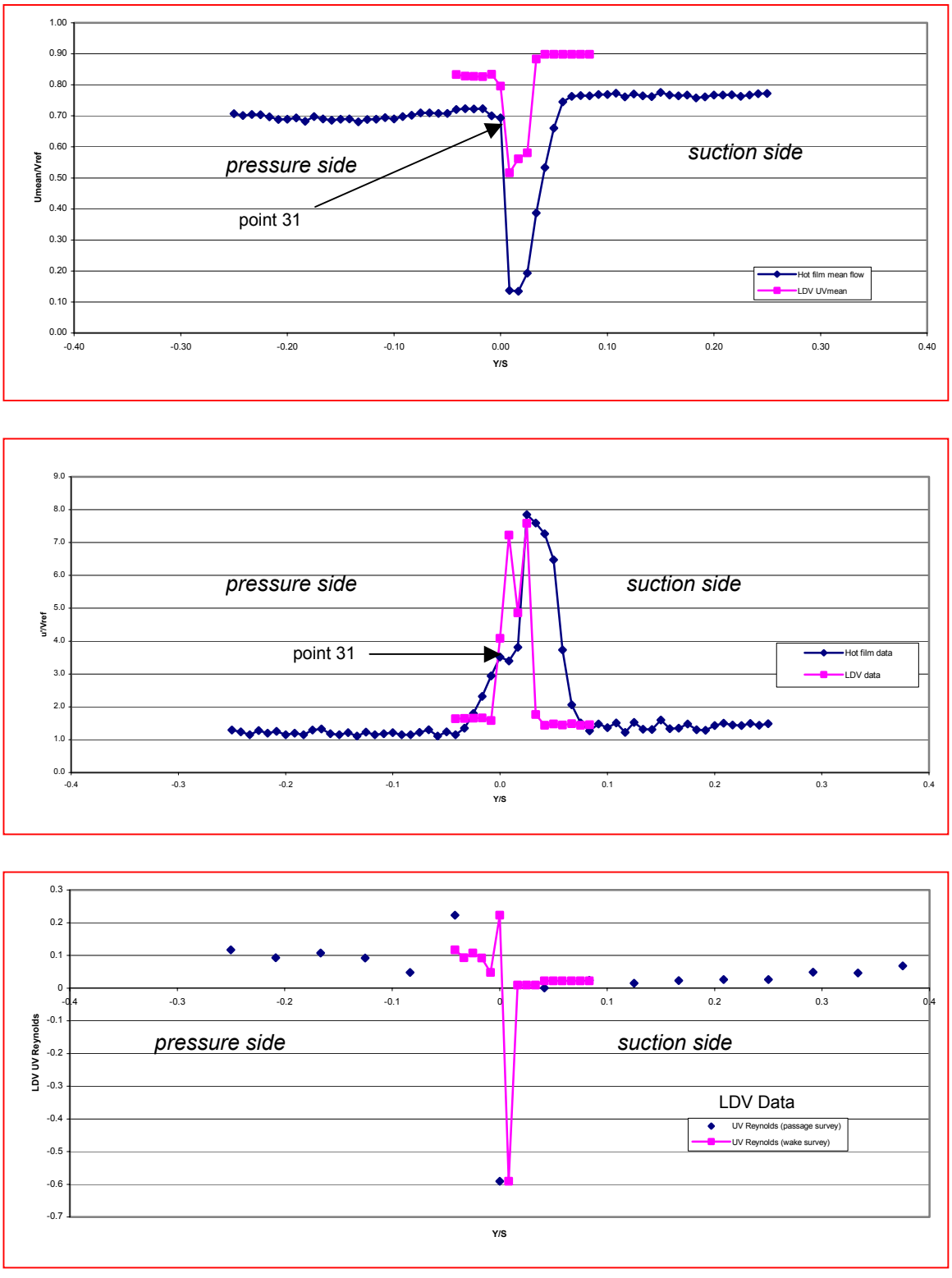

Figure 21. Hot-Wire and LDV Surveys at 35° and Re = 380,000

Figure 22 shows the FFT of point 31 as a frequency/power spectrum plot. Frequency/power spectra were generated for every point in the survey, and were analyzed for indications of vortex shedding, based on the mean flow and turbulence intensity information from the hot-wire and LDV surveys. Figure 22 corresponds to 1.27 mm on the pressure side of the blade 4 centerline. The Strouhal number calculated, for the peak at 1880 Hz, was 0.26, which was slightly higher than, but similar to results predicted in Roshko [Ref. 12]. Point 31 was the only point on the pressure side to display a frequency spike. There was no detectable shedding on the suction side of the blade. The peak at 1880 Hz did not correspond to the location of maximum turbulence intensity in Figure 21. This peak again lacked distinctness due to increased pressure side turbulence levels that originated at the leading edge (-0.05<Y/S<-0.01 in Figure 19).

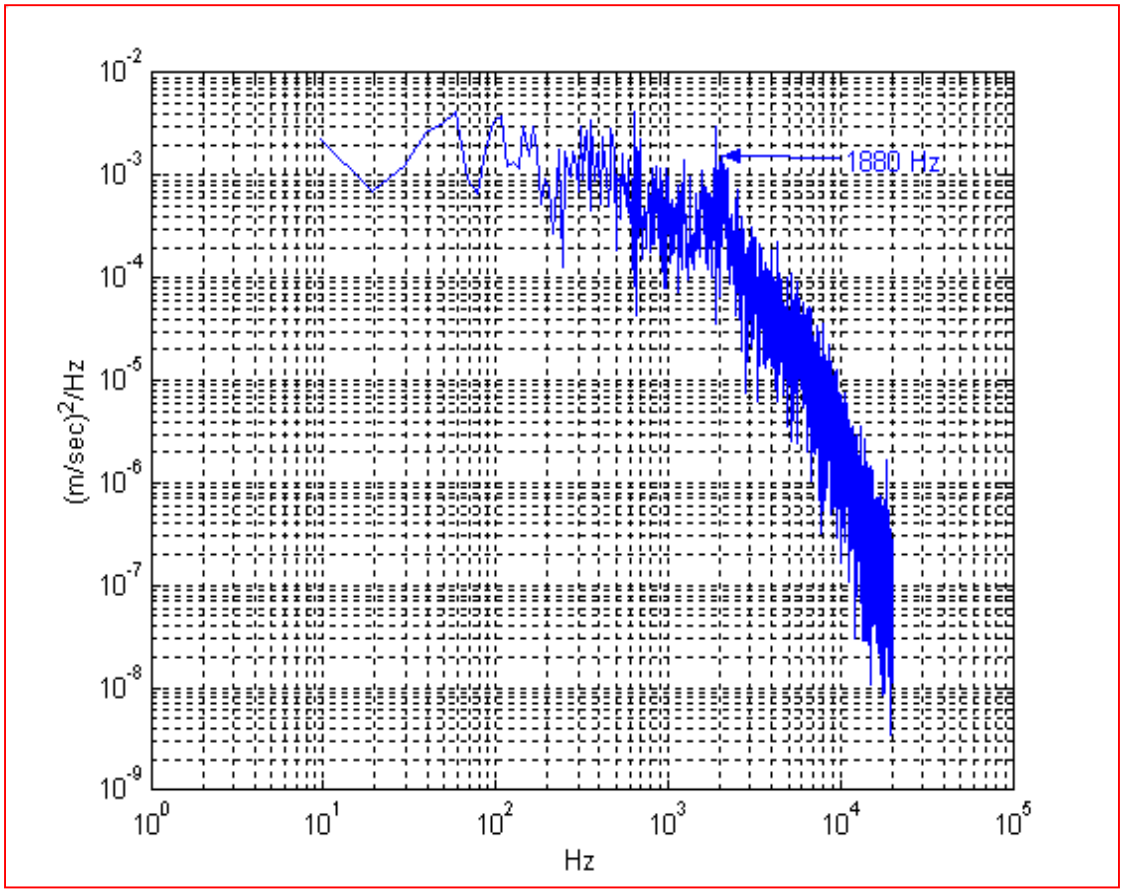

Figure 22. Power Spectrum (Point 31) at 35° and Re = 380,000

4. Hot-Wire and LDV Surveys at 33° and Re = 280,000

The hot-wire and LDV wake surveys are shown combined in Figure 23. The freestream velocity profiles showed reasonable correlation in magnitude with a maximum on both sides of the wake and a positional shift as a result of location differences between hot-wire and LDV probe volume, as discussed previously. The pressure-side entry into the wake was steeper than the suction side, but the wake was very symmetric and well defined. Both the LDV and the hot-wire measurements reached the same freestream values outside the wake. The turbulence intensity profiles showed the same peak location, although the hot-wire turbulence intensity profile was much broader. The maximum turbulence intensity in both profiles corresponded to the location of the maximum gradient of the mean flow profile on the pressure side of the blade. The pressure-side turbulence rise was shallow and wide similar to the profile shown for 33° and Re = 380,000 in Figure 19. The Reynolds-stress plots indicated low, but not negligible, shear on the pressure-side entry to the wake. There was little difference in intensity of Reynolds stress between the full passage survey and the wake survey.

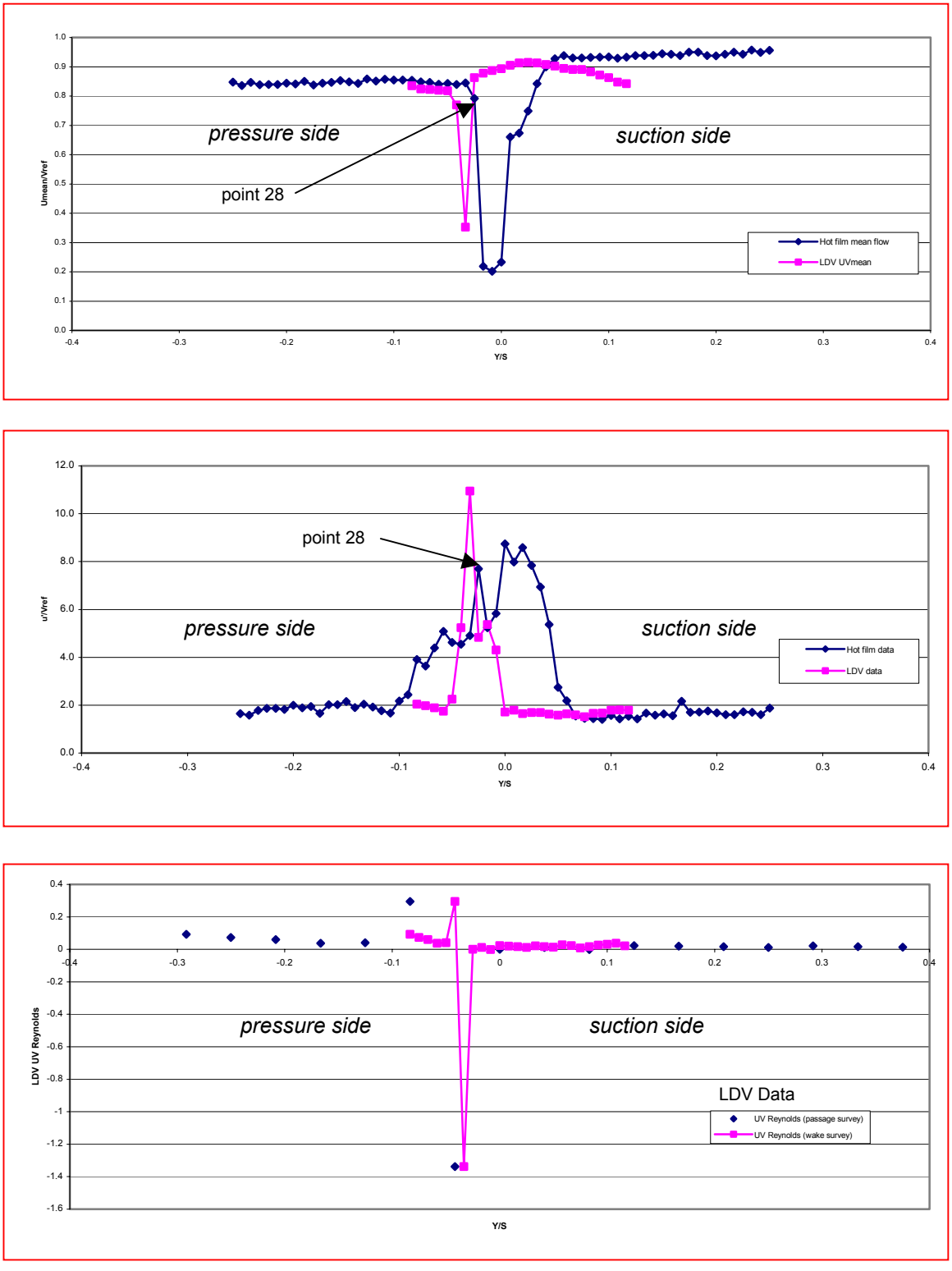

Figure 23. Hot-Wire and LDV Surveys at 33° and Re = 280,000

Figure 24 shows the FFT of point 28 as a frequency/power spectrum plot. Frequency/power spectra were generated for every point in the survey, and were analyzed for indications of vortex shedding, based on the mean flow and turbulence intensity information from the hot-wire and LDV surveys. Figure 24 corresponds to 1.27 mm on the pressure side of the blade 4 centerline. The Strouhal number calculated was 0.25, which was well within results predicted in Roshko [Ref. 12]. Point 28 was the only point on the pressure side to display a frequency spike. There was no detectable shedding on the suction side of the blade. With inlet-flow angle constant at 33°, and Reynolds number decreased from 380,000 to 280,000, the shedding peak frequency decreased significantly from 1880 Hz to 1480 Hz (~ 21%). The minor peak at 1480, was diminished due to pressure side turbulence, but corresponded to the point of maximum LDV turbulence intensity in Figure 23.

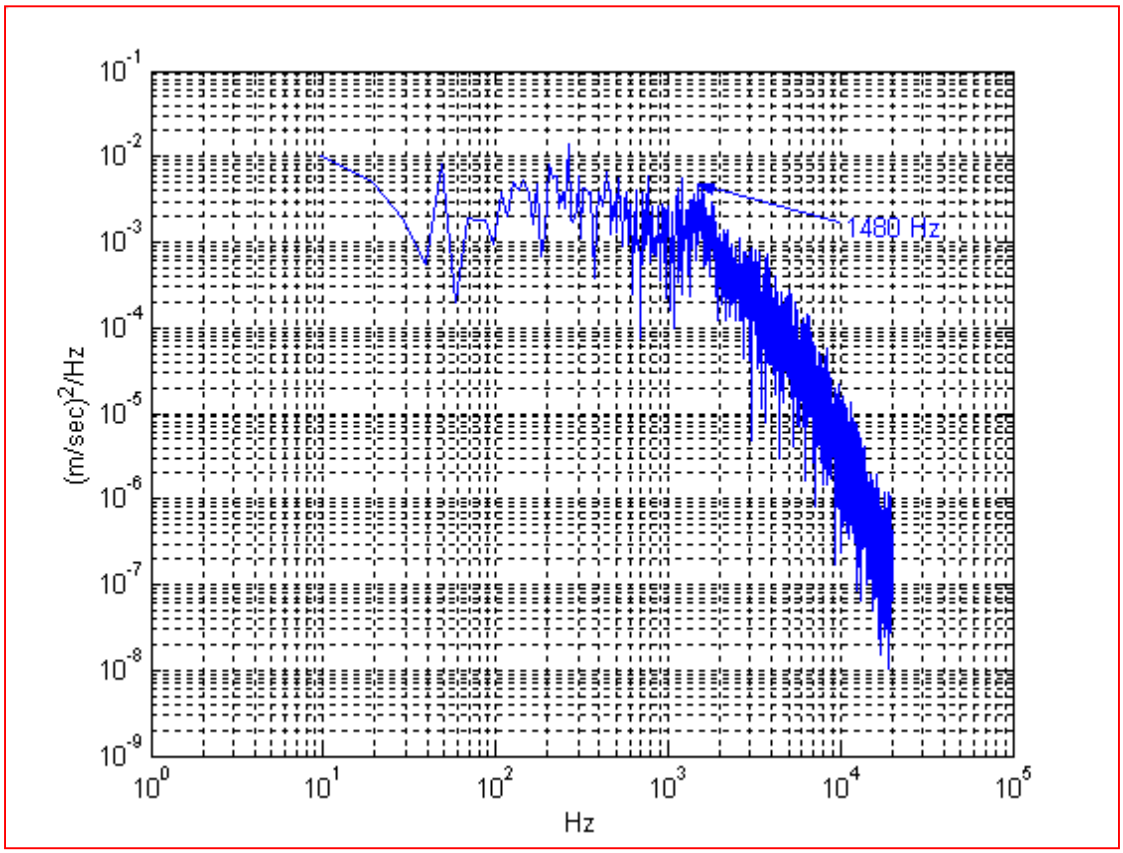

Figure 24. Power Spectrum (Point 28) at 33° and Re = 280,000

5. Hot-Wire and LDV Surveys at 33° and Re = 640,000

The hot-wire and LDV wake surveys are shown combined in Figure 25. The freestream velocity profiles showed reasonable correlation in magnitude, with a maximum on both sides of the wake and a positional shift as a result of location differences between hot-wire and LDV probe volume, as discussed previously. The pressure-side and suction-side entries into the wake were relatively symmetric, and the wake was well defined. Both the LDV and the hot-wire measurements reached the same freestream values outside the wake. The turbulence intensity profiles showed excellent correlation, including the "double-humped' profile. The maximum turbulence intensity in both profiles corresponded to the location of the maximum gradient of the mean flow profile on the pressure side of the blade. The pressure-side turbulence rise was shallow and wide, similar to the other 33° profiles. The Reynolds-stress plots indicated low, but not negligible, shear on the pressure-side entry to the wake.

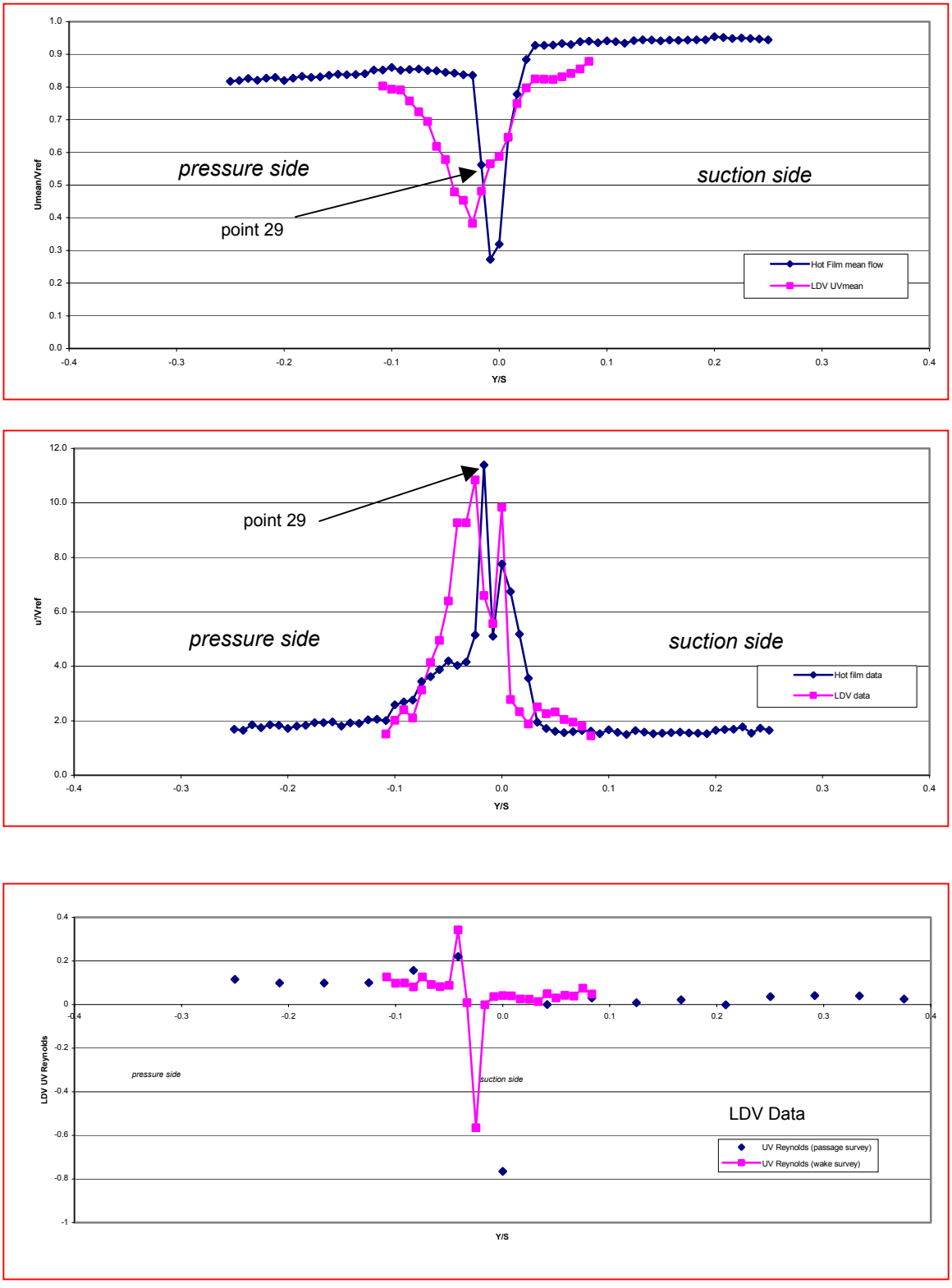

Figure 25. Hot-Wire and LDV Surveys at 33° and Re = 640,000

Figure 26 shows the FFT of point 29 as a frequency/power spectrum plot. Frequency/power spectra were generated for every point in the survey, and were analyzed for indications of vortex shedding, based on the mean flow and turbulence intensity information from the hot-wire and LDV surveys. The major peak in Figure 26 corresponds to 1.27 mm on the pressure side of the blade 4 centerline. The Strouhal number calculated was 0.24, which was within results predicted in Roshko [Ref. 12]. Point 29 displayed the greatest magnitude spike on the pressure side. There was no detectable shedding on the suction side of the blade. The peak frequency increased significantly from 1880 Hz to 3550 Hz (~89%) when Reynolds number was raised from 380,000 to 640,000 at 33°.

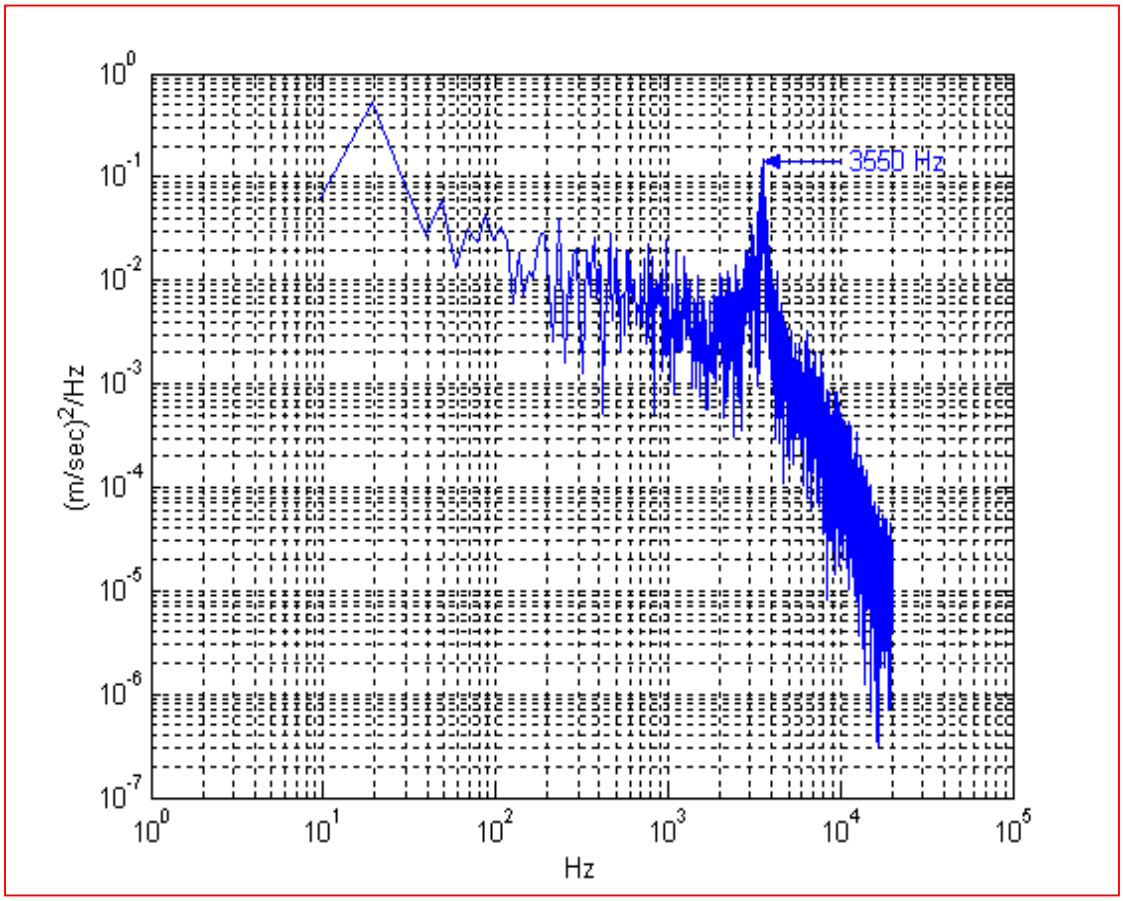

Figure 26. Power Spectrum (Point 29) at 33° and Re = 640,000

E. SUMMARY

Overall, vortex shedding was documented aft of the blades at a constant Reynolds number while varying inlet-flow angle, and at a constant inlet-flow angle and varying Reynolds number. As the inlet-flow angle was increased from 31° to 33° and then to 35° at constant Reynolds number, the shedding peak frequency remained relatively constant while leading edge, pressure side turbulence decreased. With inlet-flow angle held constant at 33°, and Reynolds number increased from 280,000 to 380,000 and then to 640,000, the shedding peak frequency increased significantly from 1480 Hz to 2050 Hz to 3550 Hz (~ 140%). Vortex shedding was found to be at its peak intensity and frequency at 33° and a Reynolds number of 640,000. However, the Strouhal number associated with these three test cases remained relatively constant (0.24-0.26).

A CFD prediction of the vortex-shedding phenomenon was produced by Hah [Ref 13], and is presented in Figure 27. The color-coding represents Mach number differences from blue (low) to red (high). In the snapshot presented, the leading edge, pressure-side, separation bubble (the vortex shedding detected) can be seen just aft of midchord.

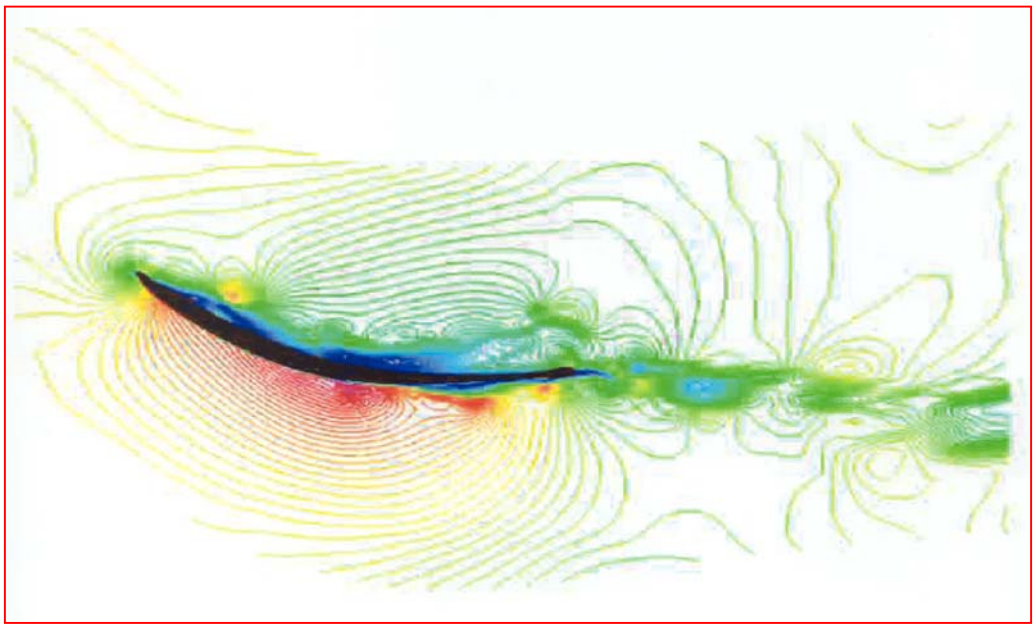

Figure 27. CFD Prediction of Shedding Over a CD Compressor Blade

V. CONCLUSIONS AND RECOMMENDATIONS

A. CONCLUSIONS

Second-generation controlled-diffusion compressor blade sections, which modeled the midspan section of NASA's stator 67B, were investigated in the LSCWT. The objective of the study was to locate, identify and characterize vortex shedding aft of the blades at three different off-design negative incidence angles, corresponding to inlet-flow angles of 31, 33 and 35 degrees, at Reynolds numbers of 280,000, 380,000 and 640,000, using multiple experimental techniques.

Blade surface pressure distributions were measured at midspan for each Reynolds number at each inlet-flow angle. A suction-side, laminar-flow separation was found at each Reynolds number and each inlet-flow angle. A pressure-side, leading-edge separation bubble was evident at 33°, at all Reynolds numbers, which grew larger as inlet-flow angle was decreased at all Reynolds numbers.

The loss coefficients and axial velocity ratios were calculated from the five-hole probe wake surveys at midspan, which documented the total pressure losses due to midspan boundary layer growth. The trends in losses and AVR were as expected at all inlet-flow angles and all Reynolds numbers.

The wake flow was characterized through hot-wire and 2-component LDV measurements at midspan downstream of the CD blades. Leading-edge, pressure-side vortex shedding was documented, corresponding to mean flow profile points of maximum gradient, and turbulence intensity profile points of maximum intensity. Analysis of Reynolds stress in the wake showed a dependence on Reynolds number and inlet-flow angle. Vortex shedding frequency and intensity were found to be a function of Reynolds number at constant inlet-flow angle, and independent of inlet-flow angle at constant Reynolds number. Peak vortex shedding occurred at 33° and Re = 640,000, where the pressure-side turbulence intensity due to incidence angle was not strong enough to significantly diminish the high frequency peak. Strouhal numbers calculated,

based on the leading edge diameter, ranged from 0.23 to 0.26, with a Strouhal number of 0.25 for the peak vortex shedding at 33° inlet-flow angle and Re = 640,000.

B. RECOMMENDATIONS

Data produced here should be compared to CFD predictions. Further experiments should be carried out at off-design negative incidence angles to determine the inlet-flow angle and Reynolds number most likely to produce peak vortex shedding. A detailed investigation will require a hot-wire data acquisition system and traverse mechanism with enhanced resolution, as well as an LDV system with a higher power laser.

Unsteady instantaneous global flowfield surveys should be conducted with a particle image velocimetry (PIV) system in an attempt to fully capture the multiple vortex shedding from the blade leading and trailing edges.

APPENDIX A: TABLES OF SCANIVALVE PORTS AND CHANNEL ASSIGNMENTS

Scanivalve #1

Blade Pressure Measurements

1	Atmosphere	25	3 Suct. Side
2	Calibration	26	4 Suct. Side
3	Plenum Press	27	5 Suct. Side
4	18 Press side	28	6 Suct. Side
5	17 Press side	29	7 Suct. Side
6	16 Press side	30	8 Suct. Side
7	15 Press side	31	9 Suct. Side
8	14 Press side	32	10 Suct. Side
9	13 Press side	33	11 Suct. Side
10	12 Press side	34	12 Suct. Side
11	11 Press side	35	13 Suct. Side
12	10 Press side	36	14 Suct. Side
13	9 Press side	37	15 Suct. Side
14	8 Press side	38	16 Suct. Side
15	7 Press side	39	17 Suct. Side
16	6 Press side	40	18 Suct. Side
17	5 Press side	41	19 Suct. Side
18	4 Press side	42	20 Suct. Side
19	3 Press side	43	TE
20	2 Press side	44	Blade 8, 1 Suct.
21	1 Press side	45	Blade 8, 2 Suct.
22	LE	46	Blade 8, 3 Suct.
23	1 Suct. Side	47	Blade 8, 4 Suct.
24	2 Suct. Side	48	Blade 8, 5 Suct.

Scanivalve #2

5-hole Probe Measurements

1	Atmosphere	25	Not Used
2	Calibration	26	Not Used
3	Plenum Press	27	Not Used
4	P Wall Static	28	Not Used
5	5-hole P1	29	Not Used
6	5-hole P2	30	Not Used
7	5-hole P3	31	Not Used
8	5-hole P4	32	Not Used
9	5-hole P5	33	Not Used
10	P Prandtl tot	34	Not Used
11	P Prandtl stat	35	Not Used
12	Not Used	36	Not Used
13	Not Used	37	Not Used
14	Not Used	38	Not Used
15	Not Used	39	Not Used
16	Not Used	40	Not Used
17	Not Used	41	Not Used
18	Not Used	42	Not Used
19	Not Used	43	Not Used
20	Not Used	44	Not Used
21	Not Used	45	Not Used
22	Not Used	46	Not Used
23	Not Used	47	Not Used
24	Not Used	48	Not Used

THIS PAGE INTENTIONALLY LEFT BLANK

APPENDIX B: HOT-WIRE ANEMOMETRY AND IFA 100 OPERATION AND DATA ACQUISITION PROCEDURES

Hot-wire Calibration Procedure

IFA 100 Setup

1. Record atmospheric temperature and pressure.
2. Measure cable resistance (R_C) with shorting probe inserted in probe holder.

   [RES MEAS]⇒zero with operating resistance control

   [RES MEAS]

   [ENTER]
3. Remove shorting probe, insert hot-film probe and repeat step 2 to find R_O, but DO NOT PRESS [ENTER].
4. Press [OPER RES]⇒adjust to operating resistance on probe box.
5. [BRIDGE COMP]⇒adjust to 115 for 20μm probe⇒[RUN] Record no-flow voltage (E_O) which should appear next to channel output (~1.15).
6. Run tunnel up to 12" H_2O, then turn cable comp knob counterclockwise until OSC light comes on then turn clockwise until it goes off plus another half turn. Note voltage (E_M) before turning tunnel off.
7. Using E_M, estimate GAIN, OFFSET and SPAN:

   $GAIN=5/E_M-2$ $OFFSET=E_M - 5/R_O$ $SPAN=10/E_M-E_O$
8. [OFFSET]⇒enter offset⇒[ENTER]

   [GAIN]⇒enter gain mantissa and exponent⇒[ENTER]

ThermalPro Software Setup

1. In IFA100 software,
   [COMMUNICATIONS]⇒[REMOTE]⇒[SEND]⇒[CLOSE]

   [CALIBRATION]⇒[PROBE DATA]⇒[OPEN CAL FILE]⇒[SAVE]

   [CALIBRATE]⇒check LP filter at 100,000, then on IFA 100, press LOCAL and OUTPUT DISPLAY then send back to remote as above.

   Set dP at 0.00⇒[ACQUIRE]⇒Nozzle 1 OK

2. Now that the first calibration point has been taken at 0", turn tunnel on and take remaining 6 calibration points at 0.4", 4", 8", 10", 12" and 14" H_2O. Each point will require a dP reading from the manometer connected to the pitot tube placed as close as possible to the hot-film probe for the *in situ* calibration.

SAMPLE CALIBRATION SHEET

Ta:_____	**Plenum P**	**Pitot P**	**Plenum T**	**Voltage**
Pa:_____	**0"**			
R_C:_____	**0.4"**			
R_O:_____	**4"**			
R_{OP}:_____	**8"**			
Bridge:_____	**10"**			
E_O:_____	**12"**			
E_M:_____	**14"**			
Offset:_____				
Gain:_____	**King's Law Coefficients:**		**A:**	**1.74628**
Probe#:_____			**B:**	**0.57914**
			1/n:	**0.57000**

3. After the calibration is complete, [NEXT SCREEN]⇒[CURVES] [POLYNOMIAL]⇒[PLOT]⇒[KING"S LAW]⇒[PLOT]copy the coefficients, then [CLOSE]⇒[SAVE]. Now you are ready for the acquisition menu.

Hot-Wire Data Acquisition Procedure

1. In ThermalPro Software,

   [ACQUISITION]⇒[PROBE TABLE]⇒[CLEAR TABLE]⇒ [ADD PROBE] enter probe ID number (in form of .cl file), check resistance, gain and offset. [NEXT SCREEN]⇒[CONTINUE]⇒[RENAME] enter new experiment name, then check settings (LP filter-100,000, size-8K, rate-40Khz, time-0.2 secs), and set x coordinate. Select [OUTPUT DISPLAY] on IFA 100 and check for proper no-flow voltage. [NEXT SCREEN] now you are ready to take data by hitting the [TRIGGER] key. After data point is taken, [CLOSE], traverse probe, change x coordinate and repeat.

2. Data reduction is done using the [POST ANALYSIS] pulldown menu in the IFA 100 software in the following order: [VELOCITY ANALYSIS]-select raw files and reduce mean flow and turbulence intensity data. [FLOW FIELD]-select .s files and create and plot mean flow and turbulence intensity profiles. [SPECTRUM CORRELATION]-select .v files plot FFT's of data as frequency vs. power.

IFA 100 and HWA Schematic Diagram

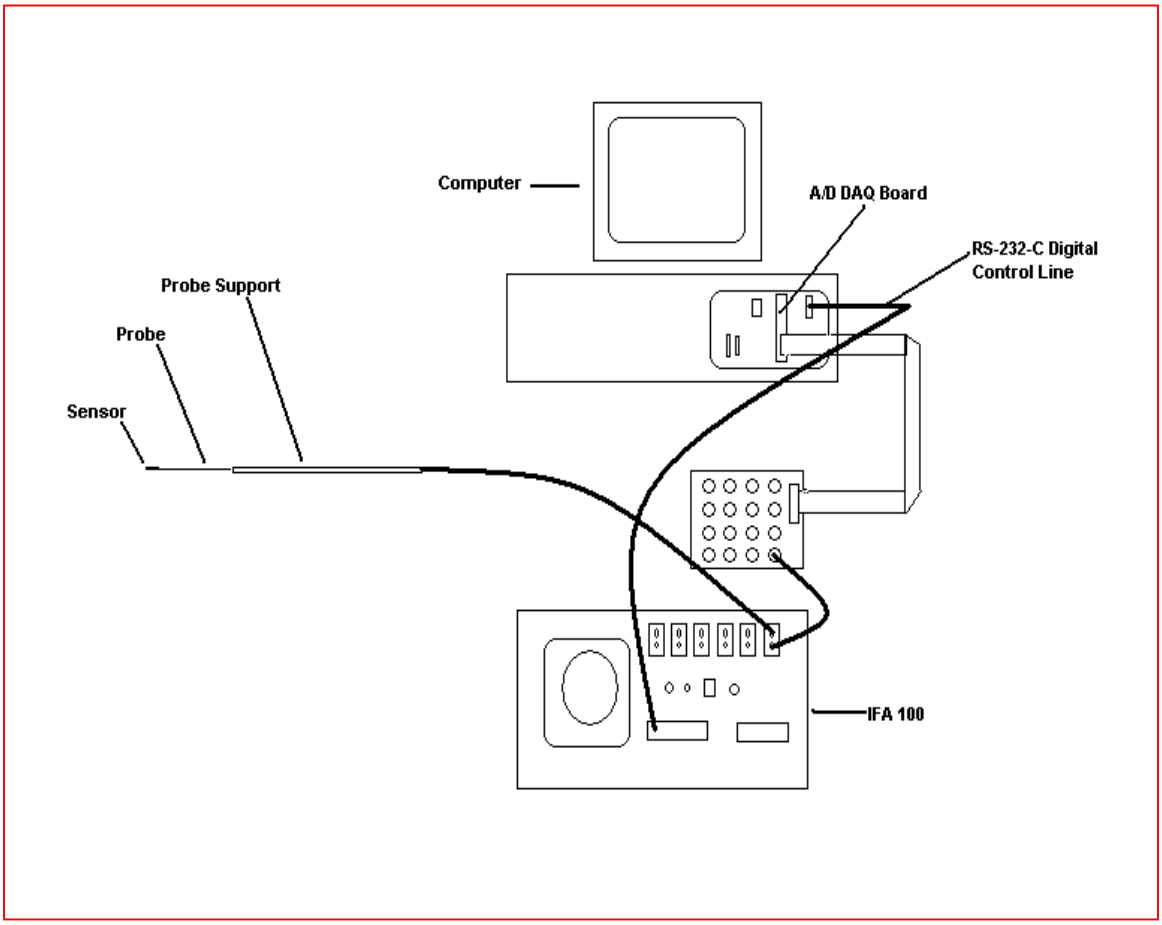

The United Electronic Industries Power DAQ A/D Board Model PD2-MFS-4-1M/12, was a 4-channel, simultaneous sample and hold at 1megasample per second.

THIS PAGE INTENTIONALLY LEFT BLANK

APPENDIX C: FIVE-HOLE PROBE EQUATIONS AND PLOTS

The five-hole probe data were reduced using the following equations:

Non-dimensional Velocity: $X = \frac{V}{V_t}$ where $V_t = \sqrt{2C_p T_t}$ where T_t is the stagnation temperature and C_p is specific heat at constant pressure.

Mach No. sensitivity: $\beta = \frac{p_1 - p_{avg}}{p_1}$ where $p_{avg} = \frac{p_2 + p_3 + p_4 + p_5}{4}$

and subscripts 1-5 denote the ports on the probe.

Pitch Sensitivity: $\gamma = \frac{p_4 - p_5}{p_1 - p_{avg}}$

Yaw Sensitivity: $\delta = \frac{p_2 - p_3}{p_1 - p_{avg}}$

AVR: $\frac{\int_0^S c_{z2}\,dx}{\int_0^S c_{z1}\,dx}$

where c_{z1} and c_{z2} are the components of velocity normal to the leading edge plane of the cascade at the lower and upper traverse locations respectively.

Loss Coefficient: $\omega = \frac{\overline{C_{pt1}} - \overline{C_{pt2}}}{\overline{C_{pt1}} - \overline{C_{ps1}}}$ where $\overline{C_{pt1}} = \frac{P_t}{P_{plenum}}$, $\overline{C_{ps1}} = \frac{P_s}{P_{plenum}}$ and

$$\overline{C_{pt2}} = \frac{1}{AVRc_{z1}S}\int_0^s \frac{P_{t2}}{P_{plenum}} c_{z2}\,dx$$

Here, subscripts 1 and 2 denote upstream and downstream of the cascade test section. Furthermore, 't' denotes Prandtl probe total pressure, 's' denotes Prandtl probe static pressure, and $P_{t2} = P_1$ on the five-hole probe.

Centerline Non-Dimensional Pressure Distribution Plots

Inlet-flow Angle (IFA) = 31° and Re = 280,000

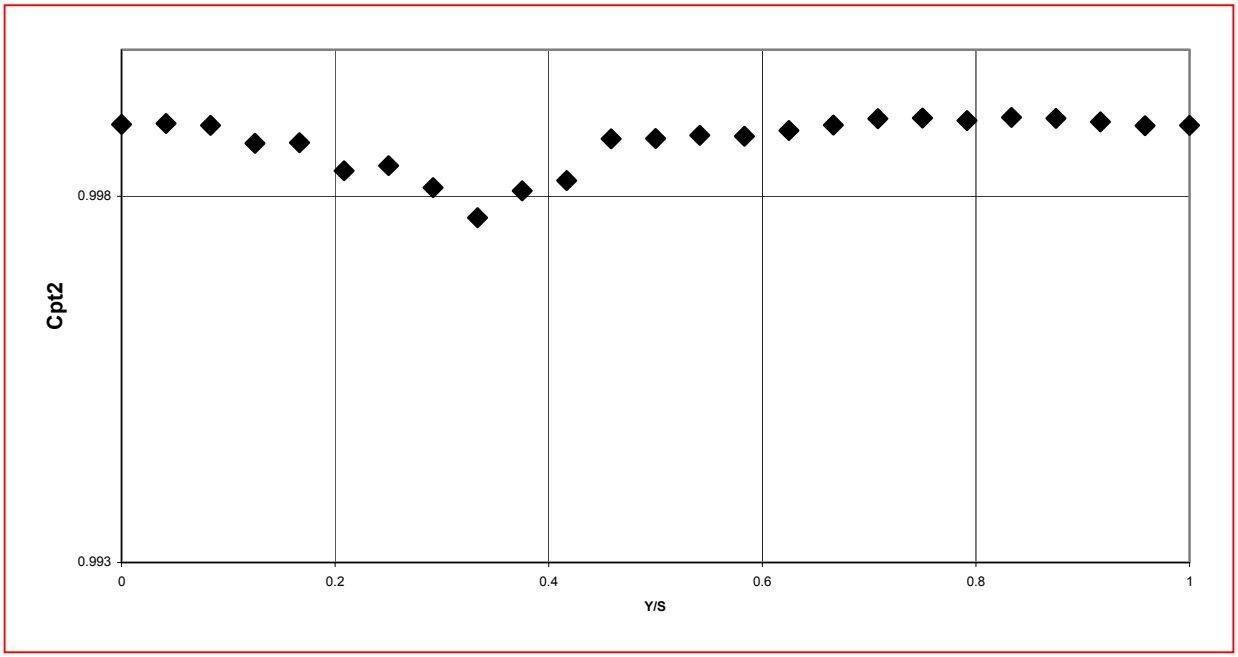

IFA = 31° and Re = 380,000

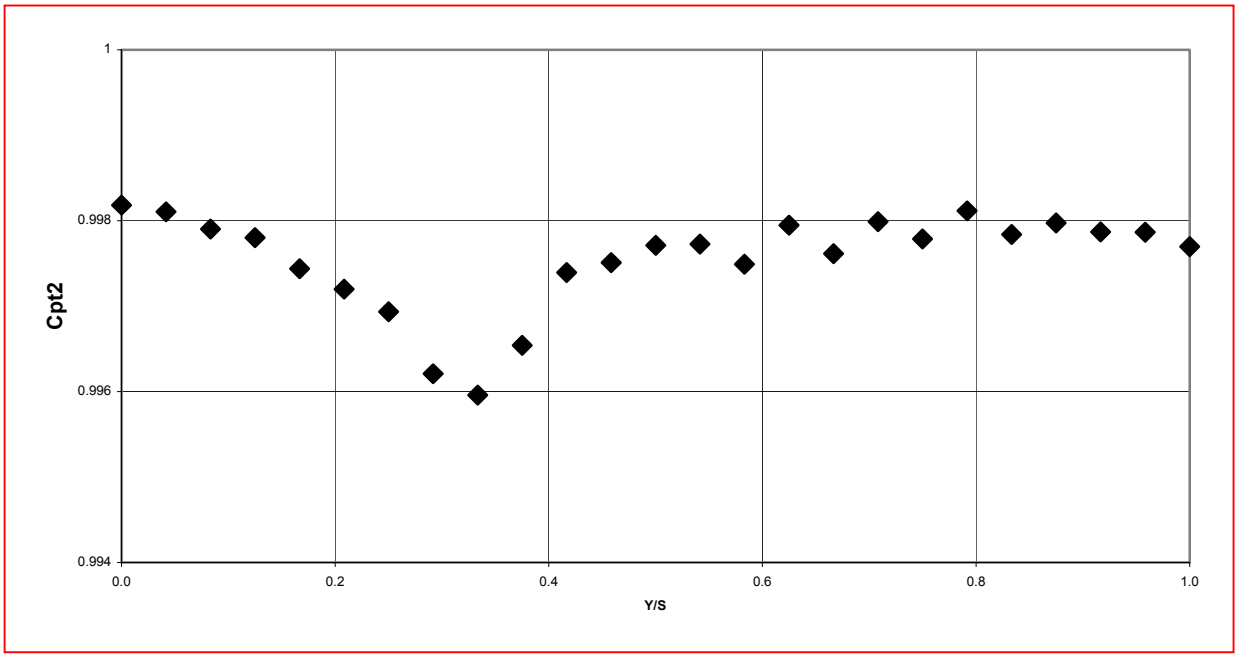

IFA = 31° and Re = 640,000

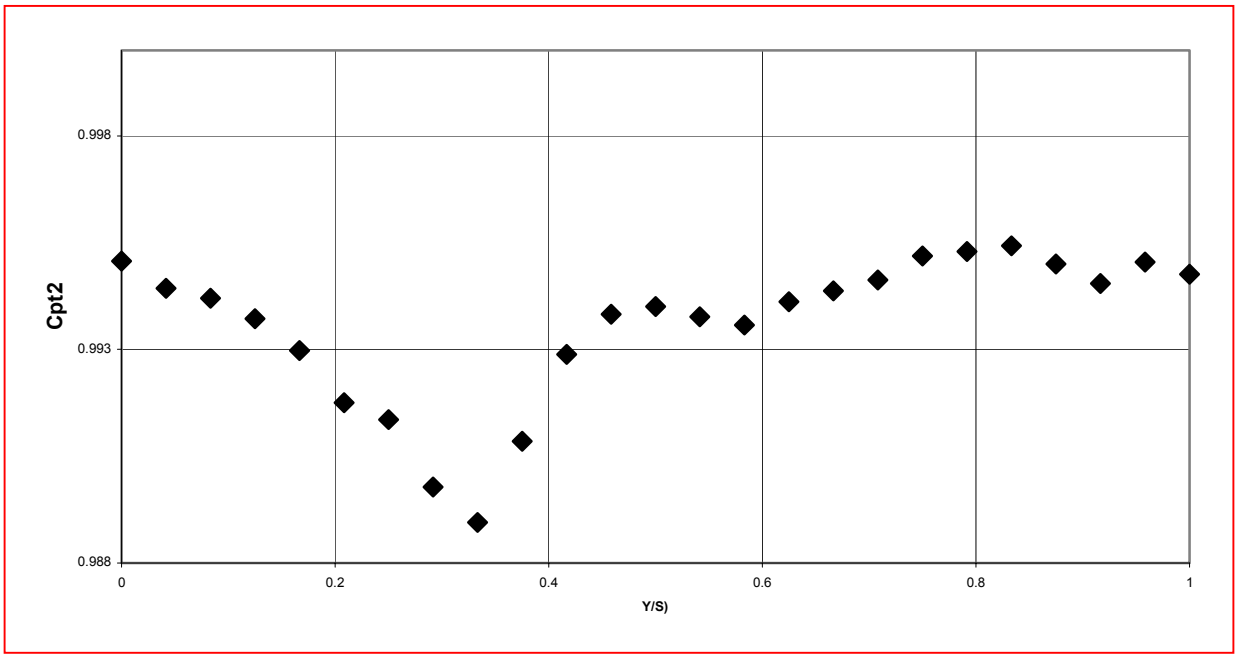

IFA = 33° and Re = 280,000

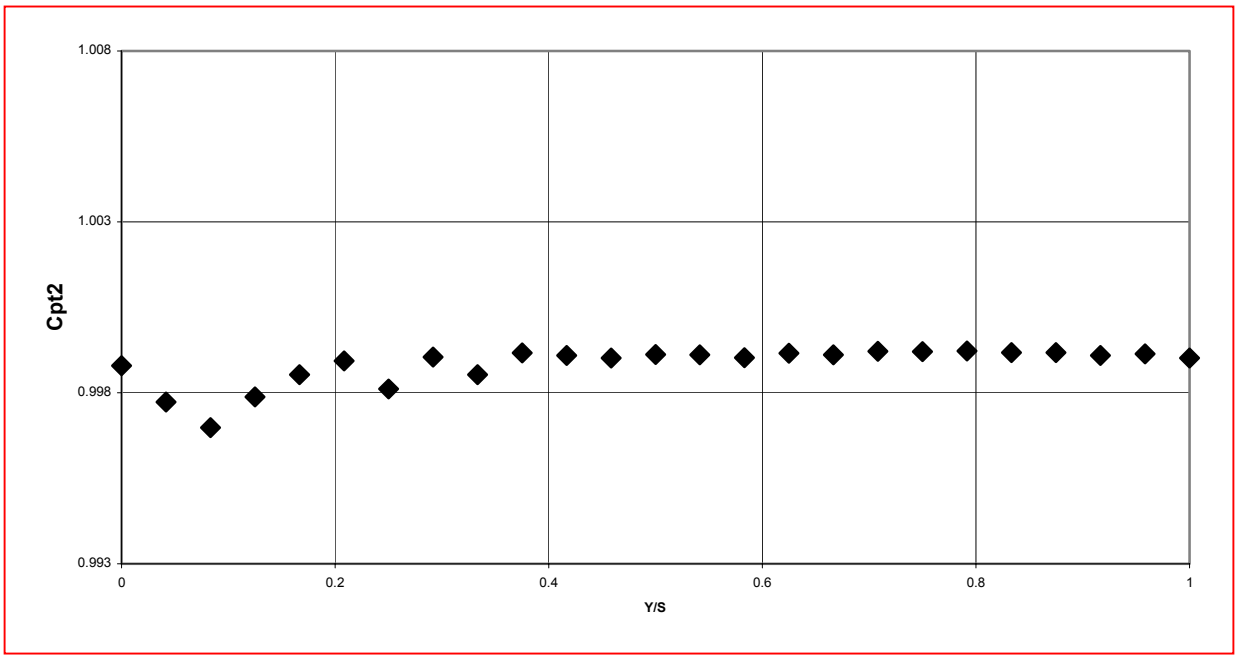

IFA = 33° and Re = 640,000

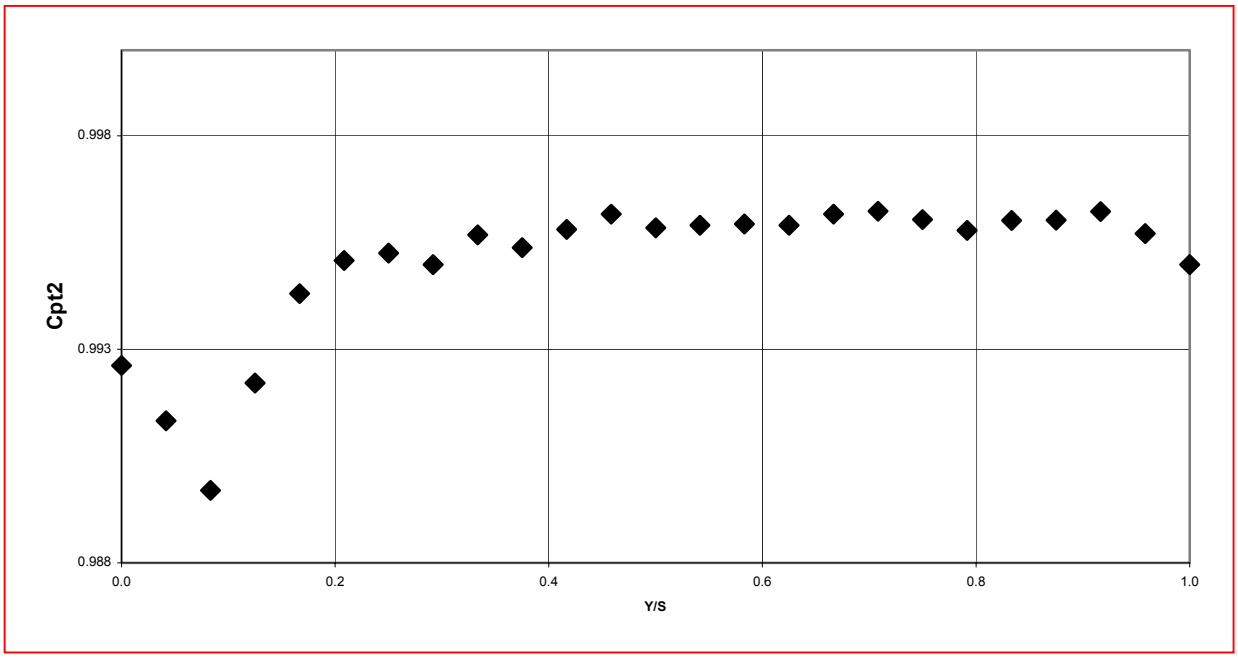

IFA = 35° and Re = 280,000

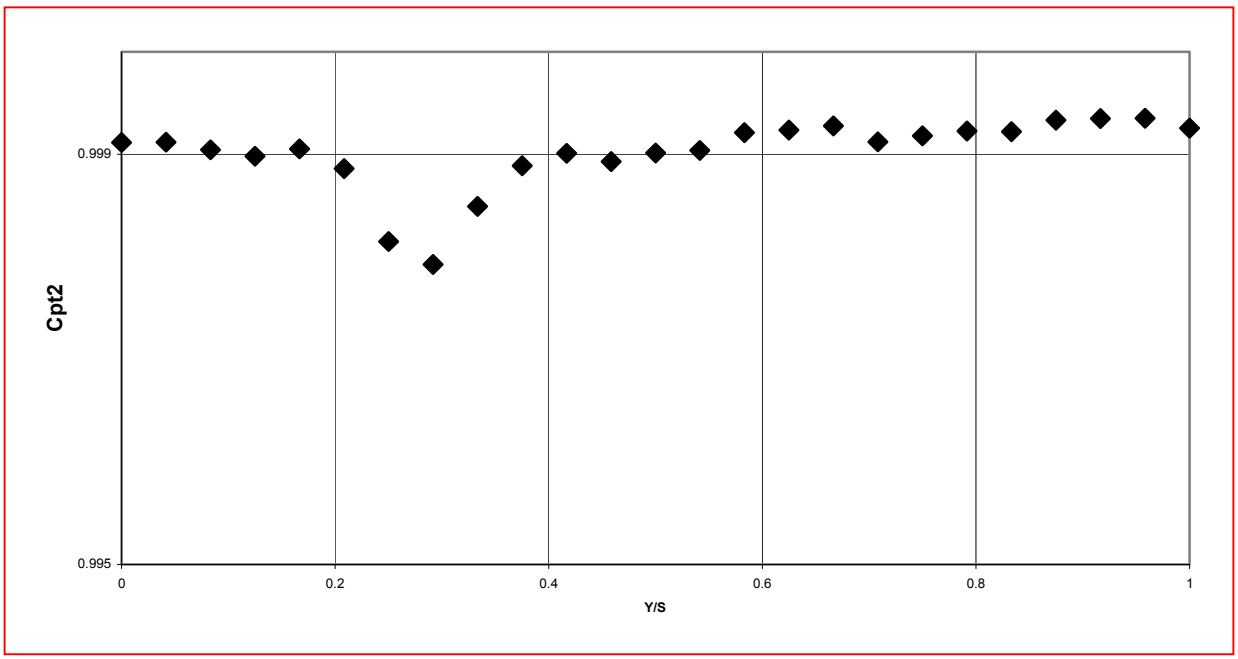

IFA = 35° and Re = 380,000

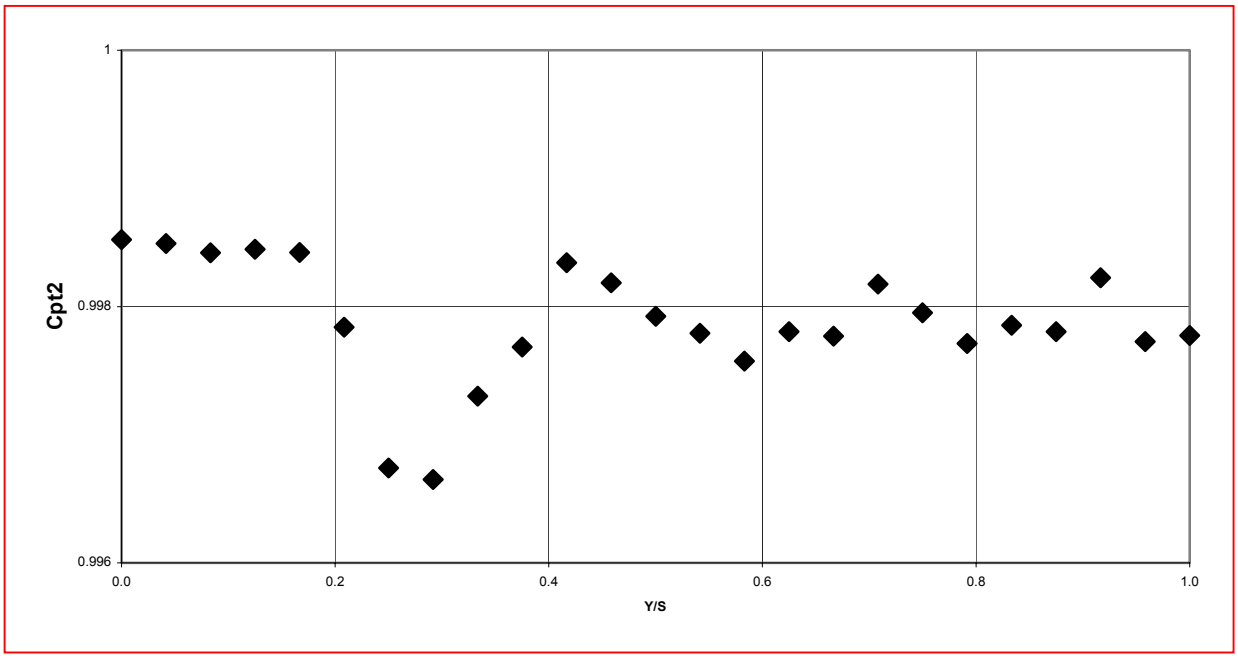

IFA = 35° and Re = 640,000

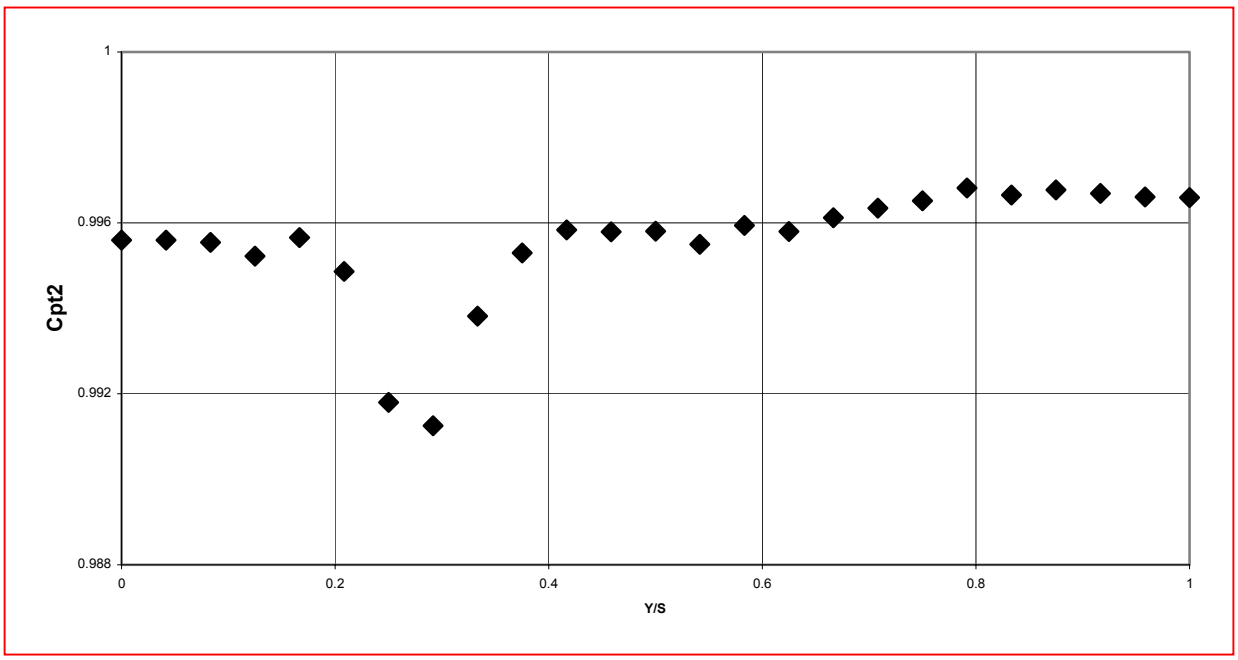

THIS PAGE INTENTIONALLY LEFT BLANK

APPENDIX D: FIVE-HOLE PROBE DATA

Five-hole Probe Reduced Data for IFA = 31° and Re = 280,000

Y/S	Cpt1	Cpt2	Cps1	P1	P2	P3	P4	P5	Pavg	Beta	Gamma	Delta	X	PSI
0.000	0.996	0.999	0.994	410.866	409.092	409.115	409.100	409.208	409.128	0.004	-0.062	-0.013	0.033	3.129
0.042	0.999	0.999	0.994	410.851	409.095	409.108	409.102	409.176	409.120	0.004	-0.043	-0.008	0.033	3.405
0.083	0.999	0.999	0.994	410.838	409.079	409.094	409.088	409.168	409.107	0.004	-0.046	-0.009	0.033	3.348
0.125	0.999	0.998	0.994	410.424	409.085	409.092	409.083	409.174	409.108	0.003	-0.069	-0.005	0.029	3.230
0.167	0.999	0.999	0.994	410.783	409.203	409.154	409.118	409.206	409.170	0.004	-0.054	0.030	0.032	2.246
0.208	0.999	0.998	0.994	410.709	409.096	409.113	409.109	409.200	409.130	0.004	-0.058	-0.011	0.031	3.343
0.250	0.999	0.998	0.994	410.617	409.088	409.108	409.108	409.203	409.127	0.004	-0.064	-0.013	0.031	3.377
0.292	0.999	0.998	0.994	410.507	409.079	409.104	409.106	409.191	409.120	0.003	-0.061	-0.018	0.030	3.672
0.333	0.999	0.998	0.994	410.346	409.090	409.103	409.107	409.159	409.115	0.003	-0.042	-0.010	0.028	4.141
0.375	0.999	0.998	0.994	410.469	409.096	409.109	409.109	409.149	409.116	0.003	-0.029	-0.009	0.029	4.263
0.417	0.999	0.997	0.994	410.093	409.200	409.180	409.173	409.183	409.184	0.002	-0.011	0.022	0.024	4.906
0.458	0.999	0.999	0.994	410.754	409.087	409.105	409.101	409.160	409.113	0.004	-0.036	-0.011	0.032	3.725
0.500	0.999	0.999	0.994	410.755	409.070	409.094	409.095	409.131	409.097	0.004	-0.022	-0.015	0.032	4.040
0.542	0.999	0.999	0.994	410.787	409.068	409.087	409.085	409.151	409.098	0.004	-0.039	-0.011	0.032	3.593
0.583	0.999	0.999	0.994	410.784	409.059	409.080	409.087	409.131	409.089	0.004	-0.026	-0.013	0.032	3.869
0.625	0.999	0.999	0.994	410.795	409.134	409.071	409.067	409.143	409.104	0.004	-0.045	0.037	0.032	2.231
0.667	0.999	0.999	0.994	410.843	409.051	409.068	409.066	409.136	409.080	0.004	-0.040	-0.010	0.033	3.461
0.708	0.999	0.998	0.994	410.371	409.039	409.062	409.065	409.141	409.077	0.003	-0.059	-0.017	0.029	3.815
0.750	0.999	0.999	0.994	410.877	409.035	409.057	409.053	409.138	409.071	0.004	-0.047	-0.012	0.033	3.311
0.792	0.999	0.999	0.994	410.867	409.025	409.050	409.058	409.119	409.063	0.004	-0.034	-0.014	0.033	3.588
0.833	0.999	0.999	0.994	410.865	409.023	409.041	409.044	409.124	409.058	0.004	-0.044	-0.010	0.033	3.334
0.875	0.999	0.999	0.994	410.875	409.024	409.053	409.059	409.120	409.064	0.004	-0.034	-0.016	0.033	3.630
0.917	0.999	0.999	0.994	410.856	409.025	409.042	409.048	409.107	409.056	0.004	-0.033	-0.010	0.033	3.545
0.958	0.999	0.999	0.994	410.845	409.079	409.028	409.040	409.096	409.061	0.004	-0.032	0.028	0.033	2.744
1.000	0.999	0.999	0.994	410.835	409.024	409.041	409.055	409.102	409.056	0.004	-0.027	-0.010	0.033	3.694

Five-hole Probe Reduced Data for IFA = 31° and Re = 380,000

Y/S	Cpt1	Cpt2	Cps1	P1	P2	P3	P4	P5	Pavg	Beta	Gamma	Delta	X	PSI
0.000	0.996	0.998	0.989	412.411	409.000	409.002	409.000	409.101	409.026	0.008	-0.030	-0.001	0.046	1.636
0.042	0.998	0.998	0.989	412.392	409.028	409.032	409.025	409.120	409.051	0.008	-0.028	-0.001	0.046	1.699
0.083	0.998	0.998	0.989	412.301	409.013	409.033	409.016	409.110	409.043	0.008	-0.029	-0.006	0.045	1.869
0.125	0.998	0.998	0.989	412.285	409.043	409.053	409.055	409.130	409.070	0.008	-0.023	-0.003	0.045	1.899
0.167	0.999	0.997	0.989	412.101	409.042	409.031	409.006	409.097	409.044	0.007	-0.030	0.004	0.044	1.869
0.208	0.998	0.997	0.989	412.012	409.048	409.079	409.062	409.138	409.082	0.007	-0.026	-0.011	0.043	2.304
0.250	0.998	0.997	0.989	411.906	409.093	409.144	409.134	409.208	409.145	0.007	-0.027	-0.018	0.041	2.608
0.292	0.998	0.996	0.989	411.644	409.002	409.006	408.992	409.065	409.016	0.006	-0.028	-0.001	0.040	2.448
0.333	0.998	0.996	0.989	411.494	409.123	409.048	409.042	409.069	409.070	0.006	-0.011	0.031	0.038	2.229
0.375	0.998	0.997	0.989	411.738	409.224	409.236	409.231	409.276	409.241	0.006	-0.018	-0.005	0.039	2.793
0.417	0.998	0.997	0.989	412.098	409.055	409.053	409.055	409.073	409.059	0.007	-0.006	0.001	0.044	2.170
0.458	0.998	0.998	0.989	412.141	409.048	409.081	409.076	409.097	409.075	0.007	-0.007	-0.011	0.044	2.340
0.500	0.998	0.998	0.989	412.210	409.095	409.152	409.161	409.218	409.157	0.007	-0.019	-0.019	0.044	2.384
0.542	0.999	0.998	0.989	412.219	409.048	409.070	409.072	409.080	409.068	0.008	-0.003	-0.007	0.044	2.217
0.583	0.998	0.997	0.989	412.131	409.024	409.065	409.069	409.084	409.061	0.007	-0.005	-0.013	0.044	2.397
0.625	0.998	0.998	0.989	412.280	409.081	409.105	409.115	409.154	409.114	0.008	-0.012	-0.007	0.045	2.126
0.667	0.998	0.998	0.989	412.204	409.003	409.029	409.030	409.048	409.027	0.008	-0.006	-0.008	0.045	2.180
0.708	0.998	0.998	0.989	412.347	409.076	409.120	409.117	409.152	409.116	0.008	-0.011	-0.014	0.045	2.181
0.750	0.998	0.998	0.989	412.275	408.995	409.017	409.021	409.043	409.019	0.008	-0.007	-0.007	0.045	2.061
0.792	0.998	0.998	0.989	412.421	409.067	409.141	409.142	409.192	409.136	0.008	-0.015	-0.022	0.046	2.246
0.833	0.998	0.998	0.989	412.336	409.057	409.077	409.082	409.104	409.080	0.008	-0.007	-0.006	0.045	2.052
0.875	0.998	0.998	0.989	412.351	408.992	409.002	409.011	409.032	409.009	0.008	-0.006	-0.003	0.046	1.906
0.917	0.998	0.998	0.989	412.290	409.001	409.048	409.059	409.081	409.047	0.008	-0.007	-0.015	0.045	2.219
0.958	0.998	0.998	0.989	412.290	409.002	409.020	409.031	409.046	409.024	0.008	-0.005	-0.005	0.045	2.044
1.000	0.998	0.998	0.989	412.242	409.059	409.116	409.123	409.175	409.118	0.008	-0.017	-0.018	0.044	2.321

Five-hole Probe Reduced Data for IFA = 31° and Re = 640,000

Y/S	Cpt1	Cpt2	Cps1	P1	P2	P3	P4	P5	Pavg	Beta	Gamma	Delta	X	PSI
0.000	0.996	0.995	0.967	419.199	408.961	409.061	408.950	409.020	408.998	0.024	-0.007	-0.010	0.085	-0.036
0.042	0.996	0.994	0.966	419.106	408.985	408.971	408.947	408.976	408.970	0.024	-0.003	0.001	0.085	-0.255
0.083	0.996	0.994	0.967	418.908	408.995	408.964	408.928	408.964	408.963	0.024	-0.004	0.003	0.084	-0.312
0.125	0.996	0.994	0.967	418.762	409.007	408.971	408.911	408.955	408.961	0.023	-0.004	0.004	0.083	-0.337
0.167	0.996	0.993	0.967	418.417	408.982	408.936	408.855	408.893	408.916	0.023	-0.004	0.005	0.082	-0.391
0.208	0.996	0.992	0.967	417.933	408.975	408.956	408.802	408.893	408.907	0.022	-0.010	0.002	0.080	-0.371
0.250	0.996	0.991	0.967	417.655	408.950	408.960	408.836	408.857	408.901	0.021	-0.002	-0.001	0.079	-0.313
0.292	0.996	0.990	0.967	416.980	408.977	408.941	408.882	408.864	408.916	0.019	0.002	0.004	0.076	-0.429
0.333	0.996	0.989	0.967	416.671	409.055	409.000	408.933	408.902	408.972	0.018	0.004	0.007	0.074	-0.468
0.375	0.996	0.991	0.967	417.433	409.085	409.010	408.985	408.949	409.007	0.020	0.004	0.009	0.077	-0.530
0.417	0.996	0.993	0.967	418.252	409.113	408.973	408.800	408.919	408.952	0.022	-0.013	0.015	0.081	-0.611
0.458	0.996	0.994	0.967	418.701	409.111	409.014	408.868	408.958	408.988	0.023	-0.009	0.010	0.083	-0.468
0.500	0.996	0.994	0.967	418.801	409.106	409.051	408.908	409.006	409.017	0.023	-0.010	0.006	0.083	-0.377
0.542	0.996	0.994	0.967	418.693	409.084	409.051	408.882	409.054	409.018	0.023	-0.018	0.003	0.083	-0.344
0.583	0.996	0.994	0.967	418.655	409.059	409.102	408.821	409.133	409.029	0.023	-0.032	-0.004	0.083	-0.186
0.625	0.996	0.994	0.967	418.870	409.062	409.151	408.859	409.143	409.054	0.023	-0.029	-0.009	0.083	-0.078
0.667	0.996	0.994	0.967	418.941	409.023	409.171	408.731	408.913	408.960	0.024	-0.018	-0.015	0.084	0.045
0.708	0.996	0.995	0.967	419.042	409.007	409.127	408.589	409.041	408.941	0.024	-0.045	-0.012	0.085	0.021
0.750	0.996	0.995	0.967	419.311	408.938	409.055	408.643	409.172	408.952	0.025	-0.051	-0.011	0.086	0.044
0.792	0.996	0.995	0.967	419.259	408.980	409.060	408.435	408.997	408.868	0.025	-0.054	-0.008	0.086	-0.018
0.833	0.996	0.995	0.967	419.454	408.939	409.028	408.346	409.220	408.883	0.025	-0.083	-0.008	0.087	0.059
0.875	0.996	0.995	0.967	419.221	408.956	409.014	408.602	409.006	408.895	0.025	-0.039	-0.006	0.086	-0.083
0.917	0.996	0.995	0.967	419.001	408.924	409.050	408.605	409.119	408.924	0.024	-0.051	-0.012	0.085	0.036
0.958	0.997	0.995	0.967	419.132	408.976	409.026	408.566	409.192	408.940	0.024	-0.061	-0.005	0.085	-0.090
1.000	0.996	0.995	0.967	419.141	409.000	409.062	408.795	409.005	408.965	0.024	-0.021	-0.006	0.085	-0.105

Five-hole Probe Reduced Data for IFA = 33° and Re = 280,000

Y/S	Cpt1	Cpt2	Cps1	P1	P2	P3	P4	P5	Pavg	Beta	Gamma	Delta	X	PSI
0.000	1.018	1.004	0.994	412.756	409.136	409.089	409.108	409.186	409.130	0.009	-0.022	0.013	0.048	1.202
0.042	0.999	1.006	0.994	413.617	409.137	409.046	409.053	409.109	409.086	0.011	-0.012	0.020	0.055	0.363
0.083	0.998	0.997	0.994	410.000	409.172	409.062	409.065	409.105	409.101	0.002	-0.045	0.123	0.025	-1.371
0.125	0.998	0.997	0.994	410.037	409.187	409.080	409.092	409.127	409.121	0.002	-0.038	0.117	0.025	-0.665
0.167	0.999	0.999	0.994	410.649	409.102	408.931	408.964	409.034	409.008	0.004	-0.043	0.104	0.032	-0.418
0.208	0.999	0.999	0.994	410.824	409.085	408.952	408.976	409.035	409.012	0.004	-0.032	0.073	0.033	1.163
0.250	0.999	0.998	0.994	410.466	409.086	409.028	408.924	408.958	408.999	0.004	-0.024	0.039	0.030	3.068
0.292	0.999	0.999	0.994	410.856	409.098	409.026	409.034	409.073	409.058	0.004	-0.021	0.040	0.033	2.637
0.333	0.999	0.999	0.994	410.638	408.833	408.774	408.765	408.789	408.790	0.004	-0.013	0.032	0.033	2.993
0.375	0.999	0.999	0.994	410.900	409.059	408.944	408.949	409.007	408.990	0.005	-0.031	0.061	0.034	1.583
0.417	0.999	0.999	0.994	410.855	409.058	409.007	409.007	409.054	409.031	0.004	-0.025	0.028	0.033	2.846
0.458	0.999	0.999	0.994	410.796	409.206	408.961	408.941	409.026	409.033	0.004	-0.048	0.139	0.033	-2.287
0.500	0.999	0.999	0.994	410.836	409.110	408.958	408.940	409.018	409.007	0.004	-0.043	0.083	0.033	0.462
0.542	0.999	0.999	0.994	410.840	409.070	408.949	408.923	409.025	408.992	0.004	-0.055	0.065	0.034	0.816
0.583	0.999	0.999	0.994	410.808	409.145	408.949	408.924	409.019	409.009	0.004	-0.053	0.109	0.033	-0.933
0.625	0.998	0.999	0.994	410.834	409.066	409.074	409.095	409.163	409.099	0.004	-0.040	-0.005	0.032	3.412
0.667	0.999	0.999	0.994	410.832	409.075	408.956	408.921	409.000	408.988	0.004	-0.043	0.065	0.034	1.175
0.708	0.999	0.999	0.994	410.855	409.056	408.942	408.912	409.002	408.978	0.005	-0.048	0.061	0.034	1.147
0.750	0.999	0.999	0.994	410.860	409.070	408.935	408.905	408.996	408.977	0.005	-0.048	0.072	0.034	0.726
0.792	0.999	0.999	0.994	410.843	408.919	408.929	408.902	408.982	408.933	0.005	-0.042	-0.005	0.034	3.149
0.833	0.999	0.999	0.994	410.822	409.007	408.919	408.890	408.981	408.949	0.005	-0.049	0.047	0.034	1.621
0.875	0.999	0.999	0.994	410.824	409.003	408.910	408.887	408.972	408.943	0.005	-0.045	0.049	0.034	1.638
0.917	0.999	0.999	0.994	410.786	409.011	408.921	408.899	408.980	408.953	0.004	-0.044	0.049	0.033	1.713
0.958	0.999	0.999	0.994	410.813	409.016	408.905	408.890	408.964	408.944	0.005	-0.040	0.059	0.034	1.441
1.000	0.999	0.999	0.994	410.742	409.013	408.916	408.899	408.976	408.951	0.004	-0.043	0.054	0.033	1.596

Five-hole Probe Reduced Data for IFA = 33° and Re = 380,000

Y/S	Cpt1	Cpt2	Cps1	P1	P2	P3	P4	P5	Pavg	Beta	Gamma	Delta	X	PSI
0.000	1.008	0.998	0.989	411.937	409.084	409.056	409.011	409.104	409.064	0.007	-0.032	0.010	0.042	1.908
0.042	0.998	0.997	0.989	411.653	408.954	408.906	408.928	409.013	408.950	0.007	-0.032	0.018	0.041	1.918
0.083	0.998	0.996	0.989	411.304	408.998	408.875	408.862	408.949	408.921	0.006	-0.037	0.052	0.038	1.271
0.125	0.998	0.997	0.989	411.502	409.120	409.048	409.017	409.090	409.069	0.006	-0.030	0.030	0.039	1.955
0.167	0.998	0.998	0.989	411.961	408.972	408.896	408.920	409.000	408.947	0.007	-0.027	0.025	0.043	1.477
0.208	0.998	0.998	0.989	412.089	408.948	408.935	408.934	408.996	408.953	0.008	-0.020	0.004	0.044	1.879
0.250	0.998	0.998	0.989	412.131	409.009	409.037	409.021	409.089	409.039	0.008	-0.022	-0.009	0.044	2.147
0.292	0.998	0.998	0.989	412.190	408.928	408.917	408.881	408.941	408.917	0.008	-0.018	0.003	0.045	1.761
0.333	0.998	0.998	0.989	412.194	408.932	408.949	408.929	408.979	408.947	0.008	-0.016	-0.006	0.045	1.978
0.375	0.998	0.998	0.989	412.221	408.925	408.955	408.909	408.958	408.937	0.008	-0.015	-0.009	0.046	2.014
0.417	0.998	0.998	0.989	412.180	408.889	408.939	408.885	408.956	408.917	0.008	-0.022	-0.015	0.045	2.092
0.458	0.998	0.998	0.989	412.187	408.943	409.049	409.009	409.075	409.019	0.008	-0.021	-0.033	0.045	2.488
0.500	0.998	0.998	0.989	412.104	408.861	408.935	408.850	408.930	408.894	0.008	-0.025	-0.023	0.045	2.243
0.542	0.997	0.998	0.989	412.138	408.987	409.059	409.003	409.082	409.032	0.008	-0.025	-0.023	0.044	2.345
0.583	0.998	0.998	0.989	412.190	408.853	408.914	408.803	408.952	408.881	0.008	-0.045	-0.019	0.046	1.909
0.625	0.998	0.998	0.989	411.963	408.862	408.948	408.873	408.974	408.914	0.007	-0.033	-0.028	0.044	2.412
0.667	0.997	0.998	0.990	412.160	408.931	409.032	408.987	409.069	409.005	0.008	-0.026	-0.032	0.045	2.435
0.708	0.998	0.999	0.989	412.217	408.882	408.941	408.862	408.922	408.902	0.008	-0.018	-0.018	0.046	2.117
0.750	0.997	0.998	0.989	412.039	408.966	409.044	408.979	409.026	409.004	0.007	-0.016	-0.026	0.044	2.539
0.792	0.998	0.998	0.989	412.164	408.861	408.921	408.843	408.847	408.868	0.008	-0.001	-0.018	0.046	2.265
0.833	0.998	0.998	0.990	412.061	408.978	409.040	408.961	409.013	408.998	0.007	-0.017	-0.020	0.044	2.416
0.875	0.998	0.998	0.989	412.019	408.925	409.009	408.941	408.997	408.968	0.007	-0.018	-0.028	0.044	2.533
0.917	0.997	0.998	0.989	411.996	408.914	408.972	408.933	408.980	408.950	0.007	-0.015	-0.019	0.044	2.423
0.958	0.998	0.998	0.989	412.051	408.967	409.002	408.922	408.982	408.968	0.007	-0.019	-0.011	0.044	2.222
1.000	0.998	0.997	0.989	411.814	408.930	408.996	408.916	408.980	408.955	0.007	-0.023	-0.023	0.042	2.626

Five-hole Probe Reduced Data for IFA = 33° and Re = 640,000

Y/S	Cpt1	Cpt2	Cps1	P1	P2	P3	P4	P5	Pavg	Beta	Gamma	Delta	X	PSI
0.000	1.066	0.993	0.966	418.151	408.930	408.613	408.424	408.829	408.699	0.023	-0.043	0.034	0.082	-0.959
0.042	0.995	0.991	0.966	417.403	408.927	408.689	408.533	408.892	408.760	0.021	-0.042	0.028	0.078	-0.907
0.083	0.995	0.990	0.966	416.666	408.973	408.700	408.667	408.899	408.810	0.019	-0.030	0.035	0.075	-1.057
0.125	0.995	0.992	0.966	417.709	408.991	408.565	408.593	408.845	408.748	0.021	-0.028	0.047	0.080	-1.277
0.167	0.995	0.994	0.966	418.652	408.992	407.960	408.150	409.096	408.549	0.024	-0.094	0.102	0.084	-2.274
0.208	0.995	0.995	0.966	419.118	408.951	407.397	407.817	409.183	408.337	0.026	-0.127	0.144	0.087	-3.158
0.250	0.995	0.995	0.966	419.128	408.904	407.835	408.040	408.947	408.432	0.026	-0.085	0.100	0.087	-2.059
0.292	0.994	0.995	0.966	419.126	408.879	407.818	407.893	408.886	408.369	0.026	-0.092	0.099	0.087	-2.053
0.333	0.995	0.996	0.966	419.201	408.871	408.055	407.888	409.155	408.492	0.026	-0.118	0.076	0.087	-1.723
0.375	0.995	0.995	0.966	419.064	408.869	408.292	408.032	409.024	408.554	0.025	-0.094	0.055	0.086	-1.256
0.417	0.995	0.996	0.966	419.337	408.811	408.380	408.127	408.771	408.522	0.026	-0.059	0.040	0.087	-0.845
0.458	0.995	0.996	0.966	419.430	408.779	408.458	408.006	408.962	408.551	0.026	-0.088	0.029	0.088	-0.656
0.500	0.995	0.996	0.966	419.416	408.738	408.363	407.723	408.463	408.322	0.026	-0.067	0.034	0.089	-0.676
0.542	0.995	0.996	0.966	419.437	408.699	408.458	407.521	409.141	408.455	0.026	-0.147	0.022	0.088	-0.495
0.583	0.995	0.996	0.966	419.483	408.628	408.603	407.401	409.095	408.432	0.026	-0.153	0.002	0.088	0.000
0.625	0.995	0.996	0.966	419.440	408.668	408.561	407.824	409.058	408.528	0.026	-0.113	0.010	0.088	-0.237
0.667	0.995	0.996	0.966	419.587	408.656	408.460	407.595	409.163	408.469	0.026	-0.141	0.018	0.089	-0.368
0.708	0.995	0.996	0.966	419.587	408.708	408.334	407.395	409.091	408.382	0.027	-0.151	0.033	0.089	-0.736
0.750	0.995	0.996	0.966	419.509	408.704	408.320	407.336	409.116	408.369	0.027	-0.160	0.034	0.089	-0.786
0.792	0.995	0.996	0.966	419.467	408.734	408.352	407.307	409.148	408.385	0.026	-0.166	0.035	0.088	-0.807
0.833	0.995	0.996	0.966	419.551	408.767	408.252	407.322	409.216	408.389	0.027	-0.170	0.046	0.089	-1.098
0.875	0.995	0.996	0.966	419.533	408.796	408.159	407.366	409.183	408.376	0.027	-0.163	0.057	0.089	-1.350
0.917	0.995	0.996	0.966	419.576	408.816	408.061	407.248	409.253	408.345	0.027	-0.179	0.067	0.089	-1.651
0.958	0.995	0.996	0.966	419.376	408.845	407.863	407.260	409.272	408.310	0.026	-0.182	0.089	0.088	-2.245
1.000	0.995	0.995	0.966	419.046	408.833	408.343	408.097	409.088	408.590	0.025	-0.095	0.047	0.086	-1.102

Five-hole Probe Reduced Data for IFA = 35° and Re = 280,000

Y/S	Cpt1	Cpt2	Cps1	P1	P2	P3	P4	P5	Pavg	Beta	Gamma	Delta	X	PSI
0.000	0.997	0.999	0.994	410.891	409.121	409.141	409.159	409.131	409.138	0.004	0.016	-0.011	0.032	4.496
0.042	0.997	0.999	0.994	410.870	409.075	409.091	409.122	409.070	409.089	0.004	0.029	-0.009	0.032	4.613
0.083	0.999	0.999	0.994	410.846	409.165	409.065	409.110	409.073	409.103	0.004	0.021	0.057	0.032	3.068
0.125	0.999	0.999	0.994	410.846	409.084	409.099	409.131	409.114	409.107	0.004	0.010	-0.009	0.032	4.390
0.167	0.999	0.999	0.994	410.858	409.171	409.041	409.095	409.074	409.095	0.004	0.012	0.074	0.032	2.202
0.208	0.999	0.999	0.994	410.778	409.115	409.026	409.087	409.081	409.077	0.004	0.003	0.052	0.032	2.956
0.250	0.999	0.998	0.994	410.475	409.067	409.016	409.059	409.066	409.052	0.003	-0.004	0.036	0.029	3.793
0.292	0.999	0.998	0.994	410.379	409.072	409.000	409.073	409.068	409.053	0.003	0.004	0.055	0.028	3.569
0.333	0.999	0.998	0.994	410.598	409.086	409.003	409.085	409.083	409.064	0.004	0.001	0.054	0.030	3.134
0.375	0.999	0.999	0.994	410.756	409.136	408.992	409.082	409.094	409.076	0.004	-0.007	0.086	0.032	1.383
0.417	0.999	0.999	0.994	410.792	409.116	409.003	409.080	409.092	409.073	0.004	-0.007	0.066	0.032	2.195
0.458	0.999	0.999	0.994	410.751	409.047	408.986	409.069	409.076	409.044	0.004	-0.004	0.035	0.032	3.325
0.500	0.999	0.999	0.994	410.767	409.059	408.986	409.070	409.088	409.051	0.004	-0.010	0.043	0.032	2.946
0.542	0.999	0.999	0.994	410.773	408.993	408.987	409.070	409.080	409.033	0.004	-0.006	0.003	0.032	3.945
0.583	0.999	0.999	0.994	410.846	409.004	409.000	409.098	409.115	409.054	0.004	-0.010	0.002	0.033	3.795
0.625	0.999	0.999	0.994	410.852	408.973	408.998	409.081	409.107	409.040	0.004	-0.014	-0.014	0.033	3.933
0.667	0.999	0.999	0.994	410.874	408.998	408.984	409.059	409.073	409.028	0.004	-0.008	0.008	0.033	3.653
0.708	0.999	0.999	0.994	410.785	409.064	409.043	409.079	409.103	409.072	0.004	-0.014	0.012	0.032	3.655
0.750	0.999	0.999	0.994	410.822	409.001	409.088	409.104	409.128	409.080	0.004	-0.014	-0.050	0.032	4.373
0.792	0.999	0.999	0.994	410.833	409.028	409.009	409.044	409.062	409.036	0.004	-0.010	0.010	0.033	3.633
0.833	0.999	0.999	0.994	410.830	408.980	408.994	409.028	409.056	409.015	0.004	-0.015	-0.008	0.033	3.820
0.875	0.999	0.999	0.994	410.860	408.928	408.990	409.037	409.052	409.002	0.005	-0.008	-0.034	0.033	4.170
0.917	0.999	0.999	0.994	410.871	408.972	408.989	409.022	409.040	409.006	0.005	-0.009	-0.009	0.033	3.870
0.958	0.999	0.999	0.994	410.872	408.925	408.976	409.019	409.037	408.989	0.005	-0.009	-0.027	0.034	4.059
1.000	0.999	0.999	0.994	410.826	408.967	408.968	409.006	409.032	408.993	0.004	-0.014	0.000	0.033	3.697

Five-hole Probe Reduced Data for IFA = 35° and Re = 380,000

Y/S	Cpt1	Cpt2	Cps1	P1	P2	P3	P4	P5	Pavg	Beta	Gamma	Delta	X	PSI
0.000	0.999	0.999	0.989	412.324	408.880	408.902	409.011	409.014	408.952	0.008	-0.001	-0.007	0.046	1.982
0.042	0.999	0.998	0.989	412.287	408.889	408.889	408.998	409.010	408.947	0.008	-0.003	0.000	0.046	1.867
0.083	0.999	0.998	0.989	412.264	408.919	408.890	408.996	409.013	408.954	0.008	-0.005	0.009	0.046	1.713
0.125	0.999	0.998	0.989	412.241	408.925	408.864	408.984	409.002	408.944	0.008	-0.005	0.018	0.046	1.515
0.167	0.999	0.998	0.989	412.234	408.947	408.871	408.992	409.011	408.955	0.008	-0.006	0.023	0.045	1.426
0.208	0.999	0.998	0.989	412.016	408.963	408.897	408.986	409.010	408.964	0.007	-0.008	0.022	0.044	1.698
0.250	0.998	0.997	0.989	411.537	409.055	409.028	409.115	409.160	409.090	0.006	-0.018	0.011	0.039	2.550
0.292	0.999	0.997	0.989	411.524	408.952	408.865	408.972	408.991	408.945	0.006	-0.007	0.034	0.040	2.001
0.333	0.998	0.997	0.989	411.801	409.067	409.000	409.097	409.109	409.068	0.007	-0.004	0.025	0.041	2.055
0.375	0.998	0.998	0.989	412.004	408.985	409.026	409.096	409.109	409.054	0.007	-0.004	-0.014	0.043	2.547
0.417	0.999	0.998	0.989	412.195	408.924	408.905	408.996	408.999	408.956	0.008	-0.001	0.006	0.045	1.880
0.458	0.998	0.998	0.989	412.179	408.917	408.930	409.016	409.021	408.971	0.008	-0.001	-0.004	0.045	2.103
0.500	0.998	0.998	0.989	412.019	409.006	409.036	409.106	409.110	409.064	0.007	-0.001	-0.010	0.043	2.507
0.542	0.998	0.998	0.989	411.995	408.997	409.035	409.104	409.102	409.060	0.007	0.001	-0.013	0.043	2.591
0.583	0.998	0.998	0.989	411.998	409.022	409.054	409.113	409.126	409.079	0.007	-0.004	-0.011	0.043	2.531
0.625	0.998	0.998	0.989	412.035	408.965	409.022	409.095	409.106	409.047	0.007	-0.004	-0.019	0.043	2.593
0.667	0.998	0.998	0.989	412.015	408.890	408.970	409.030	409.043	408.983	0.007	-0.004	-0.026	0.044	2.651
0.708	0.998	0.998	0.989	412.138	408.978	409.029	409.090	409.109	409.052	0.007	-0.006	-0.017	0.044	2.424
0.750	0.998	0.998	0.989	412.053	408.988	409.037	409.090	409.119	409.059	0.007	-0.010	-0.016	0.043	2.486
0.792	0.998	0.998	0.989	412.050	408.957	409.025	409.079	409.094	409.039	0.007	-0.005	-0.023	0.043	2.611
0.833	0.998	0.998	0.989	412.029	408.945	409.011	409.067	409.087	409.027	0.007	-0.007	-0.022	0.043	2.598
0.875	0.998	0.998	0.989	412.070	408.880	408.989	409.014	409.035	408.979	0.007	-0.007	-0.035	0.044	2.705
0.917	0.998	0.998	0.989	412.133	408.953	409.011	409.047	409.062	409.018	0.008	-0.005	-0.018	0.044	2.434
0.958	0.998	0.998	0.989	412.050	408.995	409.036	409.076	409.107	409.053	0.007	-0.011	-0.014	0.043	2.437
1.000	0.998	0.998	0.989	412.050	408.985	409.022	409.060	409.130	409.049	0.007	-0.023	-0.012	0.043	2.289

Five-hole Probe Reduced Data for IFA = 35° and Re = 640,000

Y/S	Cpt1	Cpt2	Cps1	P1	P2	P3	P4	P5	Pavg	Beta	Gamma	Delta	X	PSI
0.000	0.997	0.996	0.967	418.658	408.864	408.917	409.166	409.063	409.003	0.023	0.011	-0.005	0.083	-0.175
0.042	0.997	0.996	0.967	418.639	408.887	408.831	409.129	409.092	408.985	0.023	0.004	0.006	0.083	-0.395
0.083	0.997	0.996	0.967	418.596	408.952	408.763	409.165	409.157	409.009	0.023	0.001	0.020	0.082	-0.667
0.125	0.997	0.995	0.967	418.515	408.964	408.694	409.171	409.170	409.000	0.023	0.000	0.028	0.082	-0.839
0.167	0.997	0.996	0.967	418.659	409.133	408.646	409.173	409.165	409.029	0.023	0.001	0.051	0.083	-1.223
0.208	0.997	0.995	0.967	418.341	408.926	408.802	409.102	409.160	408.997	0.022	-0.006	0.013	0.081	-0.570
0.250	0.997	0.992	0.967	417.121	408.911	408.865	409.053	409.099	408.982	0.020	-0.006	0.006	0.076	-0.459
0.292	0.997	0.991	0.967	416.787	408.957	408.815	409.054	409.088	408.979	0.019	-0.004	0.018	0.074	-0.713
0.333	0.997	0.994	0.967	417.947	408.964	408.743	409.071	409.096	408.969	0.021	-0.003	0.025	0.080	-0.827
0.375	0.997	0.995	0.967	418.519	408.971	408.655	409.134	409.138	408.974	0.023	0.000	0.033	0.082	-0.924
0.417	0.997	0.996	0.967	418.738	408.943	408.770	409.164	409.153	409.008	0.023	0.001	0.018	0.083	-0.612
0.458	0.997	0.996	0.967	418.632	408.878	408.859	409.202	409.199	409.034	0.023	0.000	0.002	0.082	-0.326
0.500	0.997	0.996	0.967	418.678	408.823	408.899	409.187	409.161	409.017	0.023	0.003	-0.008	0.083	-0.128
0.542	0.997	0.995	0.967	418.649	408.786	408.915	409.191	409.155	409.012	0.023	0.004	-0.013	0.083	-0.018
0.583	0.997	0.996	0.967	418.709	408.769	408.897	409.185	409.067	408.980	0.023	0.012	-0.013	0.083	-0.016
0.625	0.997	0.996	0.967	418.704	408.762	408.886	409.163	409.045	408.964	0.023	0.012	-0.013	0.083	-0.025
0.667	0.997	0.996	0.967	418.813	408.749	408.773	409.054	408.798	408.844	0.024	0.026	-0.002	0.084	-0.201
0.708	0.997	0.996	0.967	418.937	408.799	408.884	409.095	408.918	408.924	0.024	0.018	-0.008	0.084	-0.084
0.750	0.997	0.997	0.967	418.985	408.671	408.777	409.007	408.710	408.791	0.024	0.029	-0.010	0.085	-0.028
0.792	0.997	0.997	0.967	419.072	408.820	408.917	409.130	408.937	408.951	0.024	0.019	-0.010	0.085	-0.053
0.833	0.997	0.997	0.967	418.994	408.632	408.785	408.957	408.643	408.754	0.024	0.031	-0.015	0.085	0.059
0.875	0.997	0.997	0.968	419.081	408.783	408.869	409.116	408.857	408.906	0.024	0.025	-0.008	0.085	-0.068
0.917	0.997	0.997	0.967	419.005	408.680	408.769	409.037	408.598	408.771	0.024	0.043	-0.009	0.085	-0.053
0.958	0.997	0.997	0.967	418.972	408.927	408.907	409.150	408.939	408.981	0.024	0.021	0.002	0.084	-0.282
1.000	0.997	0.997	0.968	418.956	408.786	408.698	409.153	408.670	408.827	0.024	0.048	0.009	0.084	-0.377

THIS PAGE INTENTIONALLY LEFT BLANK

APPENDIX E: LDV INLET SURVEY REDUCED DATA

LDV Inlet Survey for IFA = 33° and Re = 280,000

Vref = 29.6371 m/s **Blade Spacing 152.4 mm**

Y/S (mm)	Z (mm)	U/Vref	V/Vref	u'/Vref	v'/Vref	UVmean/Vref	UV Re	UVx corr
0.0000	-36.6	0.7908	0.5275	2.4972	1.9092	0.9505	0.0330	0.0787
0.0417	-36.6	0.8004	0.5405	2.5658	1.9817	0.9658	0.0658	0.1472
0.0833	-36.6	0.8123	0.5510	2.4919	1.8397	0.9815	0.0360	0.0894
0.1250	-36.6	0.8246	0.5613	2.4301	2.1282	0.9975	0.0299	0.0659
0.1667	-36.6	0.8381	0.5681	2.1814	1.9776	1.0125	0.0236	0.0622
0.2083	-36.6	0.8495	0.5726	2.1499	1.9511	1.0244	0.0223	0.0604
0.2500	-36.6	0.8577	0.5676	2.1060	1.7034	1.0285	0.0203	0.0645
0.2917	-36.6	0.8615	0.5644	1.9707	1.9272	1.0299	0.0111	0.0333
0.3333	-36.6	0.8668	0.5589	2.0364	1.7003	1.0314	0.0322	0.1058
0.3750	-36.6	0.8681	0.5520	2.1705	1.7390	1.0288	0.0471	0.1421
0.4167	-36.6	0.8686	0.5472	2.1136	1.7947	1.0266	0.0249	0.0749
0.4583	-36.6	0.8720	0.5465	2.2065	2.0215	1.0291	0.0145	0.0369
0.5000	-36.6	0.8695	0.5411	2.1114	1.9290	1.0241	0.0084	0.0234
0.5417	-36.6	0.8683	0.5356	1.9200	2.1190	1.0202	0.0320	0.0896
0.5833	-36.6	0.8632	0.5312	2.0764	2.0116	1.0135	0.0329	0.0897
0.6250	-36.6	0.8518	0.5252	2.0268	2.0580	1.0007	0.0299	0.0815
0.6667	-36.6	0.8409	0.5178	2.0528	2.1250	0.9876	0.0090	0.0235
0.7083	-36.6	0.8315	0.5141	2.1184	2.3585	0.9776	0.0195	0.0444
0.7500	-36.6	0.8219	0.5147	2.3050	1.8503	0.9698	0.0221	0.0590
0.7917	-36.6	0.8233	0.5210	2.5145	2.0446	0.9742	0.0499	0.1104
0.8333	-36.6	0.8248	0.5284	2.4177	2.0867	0.9796	0.0160	0.0360
0.8750	-36.6	0.8246	0.5375	2.2387	4.4323	0.9843	0.0065	0.0075
0.9167	-36.6	0.8264	0.5390	2.1335	1.8414	0.9866	0.0381	0.1104
0.9583	-36.6	0.8202	0.5434	2.0411	1.7435	0.9838	0.0288	0.0922
1.0000	-36.6	0.8226	0.5533	2.0911	1.7784	0.9914	0.0193	0.0589

LDV Inlet Survey for IFA = 33° and Re = 380,000

Vref = 40.1873 m/s **Blade Spacing = 152.4 mm**

Y/S (mm)	Z (mm)	U/Vref	V/Vref	u'/Vref	v'/Vref	UVmean/Vref	UV Re	UV x corr.
0.0000	-36.6	0.7986	0.5338	2.4322	1.8547	0.9606	0.1046	0.1436
0.0417	-36.6	0.8059	0.5455	2.4514	2.3559	0.9732	0.0434	0.0465
0.0833	-36.6	0.8158	0.5565	2.5700	2.5122	0.9875	0.0774	0.0743
0.1250	-36.6	0.8312	0.5673	2.2242	1.9421	1.0063	0.0565	0.0810
0.1667	-36.6	0.8408	0.5713	2.9181	1.9913	1.0165	0.0359	0.0383
0.2083	-36.6	0.8504	0.5729	1.9858	1.8876	1.0254	0.0456	0.0753
0.2500	-36.6	0.8574	0.5671	1.9479	1.8308	1.0280	0.0440	0.0763
0.2917	-36.6	0.8648	0.5629	1.8980	2.4172	1.0319	0.0776	0.1047
0.3333	-36.6	0.8687	0.5559	1.9567	1.8541	1.0314	0.0493	0.0841
0.3750	-36.6	0.8697	0.5526	1.9961	1.8560	1.0304	0.0466	0.0779
0.4167	-36.6	0.8745	0.5481	2.0887	1.9051	1.0320	0.0163	0.0254
0.4583	-36.6	0.8773	0.5456	2.1023	2.2201	1.0331	0.0867	0.1151
0.5000	-36.6	0.8751	0.5404	1.9403	1.9935	1.0285	0.0594	0.0951
0.5417	-36.6	0.8707	0.5375	1.8428	2.3314	1.0232	0.0685	0.0987
0.5833	-36.6	0.8573	0.5277	1.9160	2.2417	1.0067	0.1102	0.1588
0.6250	-36.6	0.8403	0.5195	1.8886	2.2421	0.9879	0.1011	0.1478
0.6667	-36.6	0.8336	0.5124	2.0602	2.1752	0.9785	0.0127	0.0176
0.7083	-36.6	0.8252	0.5106	2.2514	2.2120	0.9704	-0.0041	-0.0051
0.7500	-36.6	0.8257	0.5141	2.5040	2.2846	0.9727	0.0859	0.0930
0.7917	-36.6	0.8240	0.5188	2.5008	1.9430	0.9737	0.0432	0.0550
0.8333	-36.6	0.8268	0.5263	2.4251	2.9483	0.9801	0.0080	0.0069
0.8750	-36.6	0.8270	0.5269	1.9625	2.5634	0.9806	0.0204	0.0251
0.9167	-36.6	0.8221	0.5342	1.9172	1.8809	0.9804	0.0095	0.0163
0.9583	-36.6	0.8141	0.5383	1.9532	1.8594	0.9760	0.0243	0.0415
1.0000	-36.6	0.8171	0.5505	2.0858	2.1690	0.9853	0.0360	0.0492

LDV Inlet Survey for IFA = 33° and Re = 640,000

Vref = 68.7834 m/s **Blade Spacing = 152.4 mm**

Y/S (mm)	Z (mm)	U/Vref	V/Vref	u'/Vref	v'/Vref	UVmean/Vref	UV Re	UVx corr
0.0000	-36.6	0.8028	0.5253	2.3533	1.8690	0.9594	0.1201	0.0577
0.0417	-36.6	0.8081	0.5388	2.5509	1.6093	0.9713	0.1087	0.0560
0.0833	-36.6	0.8197	0.5500	2.2338	1.7626	0.9871	0.0179	0.0096
0.1250	-36.6	0.8300	0.5589	2.0322	1.5848	1.0006	0.0827	0.0543
0.1667	-36.6	0.8409	0.5628	1.9644	1.6058	1.0118	0.0844	0.0566
0.2083	-36.6	0.8547	0.5666	2.1735	1.4681	1.0255	0.0893	0.0592
0.2500	-36.6	0.8655	0.5646	1.8950	1.5064	1.0334	0.1207	0.0893
0.2917	-36.6	0.8691	0.5615	1.6181	1.5405	1.0347	0.0914	0.0775
0.3333	-36.6	0.8720	0.5562	1.7199	1.5325	1.0343	0.0594	0.0476
0.3750	-36.6	0.8747	0.5546	1.7831	1.6682	1.0357	0.0851	0.0605
0.4167	-36.6	0.8767	0.5506	1.9099	1.4552	1.0353	0.1158	0.0881
0.4583	-36.6	0.8737	0.5432	1.7591	1.4534	1.0288	0.0250	0.0207
0.5000	-36.6	0.8700	0.5385	1.7630	1.6956	1.0232	0.1284	0.0908
0.5417	-36.6	0.8637	0.5337	1.6792	1.7336	1.0153	0.2191	0.1591
0.5833	-36.6	0.8496	0.5261	1.8866	1.8170	0.9993	0.1875	0.1156
0.6250	-36.6	0.8361	0.5202	1.8245	1.9578	0.9847	0.0716	0.0424
0.6667	-36.6	0.8265	0.5120	1.9891	1.7435	0.9723	0.1007	0.0614
0.7083	-36.6	0.8249	0.5124	2.1817	1.6245	0.9711	0.1031	0.0615
0.7500	-36.6	0.8240	0.5172	2.4351	1.7964	0.9729	0.0606	0.0293
0.7917	-36.6	0.8229	0.5215	2.4563	1.5516	0.9742	0.0913	0.0507
0.8333	-36.6	0.8315	0.5277	2.0533	1.9120	0.9848	0.1333	0.0718
0.8750	-36.6	0.8274	0.5324	1.7814	1.5908	0.9839	0.0566	0.0422
0.9167	-36.6	0.8264	0.5365	1.8530	1.4561	0.9853	0.1151	0.0901
0.9583	-36.6	0.8204	0.5460	1.8349	1.4917	0.9855	0.0194	0.0150
1.0000	-36.6	0.8189	0.5557	1.9839	1.1434	0.9897	0.0431	0.0402

LDV Inlet Survey for IFA = 31° and Re = 380,000

Vref = 39.9467 m/s **Blade Spacing = 152.4 mm**

Y/S (mm)	Z (mm)	U/Vref	V/Vref	u'/Vref	v'/Vref	UVmean/Vref	UV Re	UV x corr.
0.0000	-36.6	0.8085	0.5162	1.8170	1.6525	0.9592	0.0495	0.1033
0.0417	-36.6	0.8124	0.5252	1.8787	1.7557	0.9673	0.0687	0.1305
0.0833	-36.6	0.8203	0.5309	1.9671	1.7145	0.9771	0.0311	0.0578
0.1250	-36.6	0.8235	0.5342	2.2270	1.7330	0.9816	0.0679	0.1103
0.1667	-36.6	0.8381	0.5418	2.2566	1.6589	0.9980	0.0551	0.0923
0.2083	-36.6	0.8501	0.5455	2.1949	1.7410	1.0101	0.0144	0.0236
0.2500	-36.6	0.8673	0.5431	1.9066	1.8943	1.0233	0.0852	0.1478
0.2917	-36.6	0.8742	0.5426	1.7652	1.6750	1.0289	0.0486	0.1031
0.3333	-36.6	0.8862	0.5370	1.8222	1.6219	1.0361	0.0342	0.0726
0.3750	-36.6	0.8861	0.5328	1.7940	1.7667	1.0340	0.0333	0.0657
0.4167	-36.6	0.8878	0.5249	1.6540	1.9408	1.0314	0.0417	0.0814
0.4583	-36.6	0.8856	0.5194	1.7104	1.6447	1.0266	0.0260	0.0579
0.5000	-36.6	0.8919	0.5121	1.7422	1.6049	1.0285	0.0421	0.0945
0.5417	-36.6	0.8861	0.5096	1.6778	1.6127	1.0222	0.0326	0.0755
0.5833	-36.6	0.8762	0.5023	1.6177	1.6019	1.0100	0.0465	0.1124
0.6250	-36.6	0.8717	0.5011	1.6356	1.6859	1.0055	0.0470	0.1068
0.6667	-36.6	0.8625	0.4974	1.5448	1.6341	0.9956	0.0479	0.1190
0.7083	-36.6	0.8532	0.4947	1.6825	1.6605	0.9863	0.0697	0.1563
0.7500	-36.6	0.8471	0.4945	1.7067	1.7062	0.9808	0.0545	0.1173
0.7917	-36.6	0.8483	0.4977	1.9491	1.5780	0.9835	0.0416	0.0849
0.8333	-36.6	0.8501	0.5025	1.9367	1.7233	0.9875	0.0551	0.1034
0.8750	-36.6	0.8441	0.5082	1.8630	1.7799	0.9853	0.0571	0.1079
0.9167	-36.6	0.8344	0.5091	1.7843	1.7835	0.9774	0.0583	0.1148
0.9583	-36.6	0.8301	0.5187	1.7517	1.7185	0.9788	0.0702	0.1462
1.0000	-36.6	0.8298	0.5307	1.8104	1.6885	0.9850	0.0365	0.0747

LDV Inlet Survey for IFA = 35° and Re = 380,000

Vref = 41.6141 m/s **Blade Spacing = 152.4 mm**

Y/S (mm)	Z (mm)	U/Vref	V/Vref	u'/Vref	v'/Vref	UVmean/Vref	UV Re	UVx corr
0.0000	-36.6	0.7832	0.5800	1.6500	1.4454	0.9746	0.0351	0.0849
0.0417	-36.6	0.7895	0.5890	1.7823	1.4778	0.9850	0.0422	0.0925
0.0833	-36.6	0.7982	0.5970	1.9262	1.7150	0.9967	0.0761	0.1331
0.1250	-36.6	0.8139	0.6064	1.7414	1.4678	1.0149	0.0532	0.1201
0.1667	-36.6	0.8235	0.6085	1.8246	1.5978	1.0239	0.0658	0.1304
0.2083	-36.6	0.8342	0.6041	1.5551	1.5458	1.0300	0.0456	0.1094
0.2500	-36.6	0.8480	0.5974	1.8909	1.7089	1.0373	0.0535	0.0956
0.2917	-36.6	0.8490	0.5899	1.6510	1.5134	1.0338	0.0035	0.0081
0.3333	-36.6	0.8521	0.5868	1.6375	1.5173	1.0346	0.0209	0.0487
0.3750	-36.6	0.8464	0.5785	1.7785	1.6135	1.0252	0.0237	0.0477
0.4167	-36.6	0.8522	0.5756	1.6992	1.6974	1.0284	0.0376	0.0752
0.4583	-36.6	0.8545	0.5695	1.9234	1.6656	1.0269	0.0401	0.0723
0.5000	-36.6	0.8472	0.5653	1.8065	1.5855	1.0185	0.0633	0.1275
0.5417	-36.6	0.8423	0.5599	1.6441	1.8782	1.0114	0.0698	0.1305
0.5833	-36.6	0.8307	0.5540	1.6670	1.7086	0.9985	0.0506	0.1025
0.6250	-36.6	0.8226	0.5507	1.6945	1.7795	0.9899	0.0750	0.1436
0.6667	-36.6	0.8103	0.5466	1.6520	1.6305	0.9774	0.0310	0.0665
0.7083	-36.6	0.8102	0.5477	1.6779	1.5149	0.9780	0.0194	0.0442
0.7500	-36.6	0.8078	0.5490	1.8002	1.5294	0.9767	0.0309	0.0648
0.7917	-36.6	0.8016	0.5510	1.6737	1.4343	0.9728	0.0325	0.0782
0.8333	-36.6	0.7947	0.5571	1.5343	1.4182	0.9705	0.0120	0.0319
0.8750	-36.6	0.7936	0.5593	1.5876	1.7088	0.9709	0.0277	0.0590
0.9167	-36.6	0.7874	0.5655	1.5902	1.6331	0.9694	0.0537	0.1194
0.9583	-36.6	0.7840	0.5743	1.7339	1.6562	0.9718	0.0705	0.1417
1.0000	-36.6	0.7935	0.5802	1.7846	1.6581	0.9830	0.0290	0.0566

THIS PAGE INTENTIONALLY LEFT BLANK

APPENDIX F: HOT-WIRE REDUCED DATA

Hot-wire Blade 4 Wake Survey for IFA = 31° and Re = 380,000

Vref = 39.9467 m/s

Y/S	Umean/Vref	u'/Vref		Y/S	Umean/Vref	u'/Vref
-0.25000	0.73698	1.71577		0.00833	0.17984	4.48095
-0.24167	0.74422	1.65224		0.01667	0.14068	5.62101
-0.23333	0.73821	1.61830		0.02500	0.47438	8.47768
-0.22500	0.73538	1.63394		0.03333	0.62671	7.06114
-0.21667	0.73626	1.80729		0.04167	0.70486	6.91141
-0.20833	0.72562	1.97440		0.05000	0.77468	4.90134
-0.20000	0.72764	1.74045		0.05833	0.82367	2.43206
-0.19167	0.73666	1.71015		0.06667	0.82520	1.83632
-0.18333	0.72865	1.82059		0.07500	0.83241	1.71152
-0.17500	0.73460	1.77877		0.08333	0.82895	1.70582
-0.16667	0.73743	1.91858		0.09167	0.82452	1.61763
-0.15833	0.73558	1.97761		0.10000	0.83626	1.86060
-0.15000	0.73220	2.08589		0.10833	0.82663	1.46668
-0.14167	0.73611	2.32006		0.11667	0.82885	1.62969
-0.13333	0.74196	2.64607		0.12500	0.82961	1.61159
-0.12500	0.73320	2.27799		0.13333	0.82490	1.55708
-0.11667	0.73433	3.07970		0.14167	0.82873	1.56290
-0.10833	0.74324	2.71929		0.15000	0.82830	1.71757
-0.10000	0.73593	4.02996		0.15833	0.83994	1.61790
-0.09167	0.73711	4.43141		0.16667	0.83634	1.69718
-0.08333	0.73558	4.65894		0.17500	0.82628	1.61669
-0.07500	0.72699	5.64372		0.18333	0.83151	1.61279
-0.06667	0.72742	5.34755		0.19167	0.84182	1.71100
-0.05833	0.72537	6.30706		0.20000	0.84137	1.68308
-0.05000	0.71227	6.91967		0.20833	0.83208	1.68189
-0.04167	0.71958	6.33752		0.21667	0.83822	1.86587
-0.03333	0.72967	6.14450		0.22500	0.83043	1.79656
-0.02500	0.71903	5.75320		0.23333	0.84455	1.70954
-0.01667	0.72957	6.44862		0.24167	0.84095	2.02231
-0.00833	0.74459	6.36991		0.25000	0.84227	1.69415
0.00000	0.50640	10.42120				

Hot-wire Blade 4 Wake Survey for IFA = 33° and Re = 380,000

Vref = 40.1873 m/s

Y/S	Umean/Vref	u'/Vref		Y/S	Umean/Vref	u'/Vref
-0.25000	0.81401	2.01257		0.00833	0.65506	7.10738
-0.24167	0.81444	1.97151		0.01667	0.76012	7.05099
-0.23333	0.82349	2.35058		0.02500	0.84066	6.11499
-0.22500	0.81314	1.95544		0.03333	0.91984	3.88762
-0.21667	0.82621	2.04949		0.04167	0.93972	2.11513
-0.20833	0.81630	1.79766		0.05000	0.95697	1.83413
-0.20000	0.82016	1.75826		0.05833	0.94833	1.74664
-0.19167	0.83459	2.07480		0.06667	0.94968	1.80999
-0.18333	0.83069	1.94148		0.07500	0.95889	1.83588
-0.17500	0.81884	2.09533		0.08333	0.94634	1.67200
-0.16667	0.83148	1.80814		0.09167	0.95786	1.56668
-0.15833	0.83069	1.90401		0.10000	0.95438	1.77372
-0.15000	0.84049	2.32858		0.10833	0.95774	1.77211
-0.14167	0.84487	2.20604		0.11667	0.95665	1.57665
-0.13333	0.84223	1.93528		0.12500	0.95408	1.51069
-0.12500	0.84696	2.05074		0.13333	0.95963	1.62389
-0.11667	0.84999	2.11130		0.14167	0.95174	1.88750
-0.10833	0.85726	2.18276		0.15000	0.94943	1.63197
-0.10000	0.85582	2.57053		0.15833	0.96063	1.72192
-0.09167	0.85823	2.47196		0.16667	0.97068	1.62676
-0.08333	0.86575	3.43104		0.17500	0.96023	1.72640
-0.07500	0.85975	5.36630		0.18333	0.96735	1.57735
-0.06667	0.85569	4.87950		0.19167	0.96115	1.73180
-0.05833	0.85291	5.06430		0.20000	0.96732	1.66215
-0.05000	0.85355	4.76624		0.20833	0.97200	1.51651
-0.04167	0.85019	4.53043		0.21667	0.97210	1.76815
-0.03333	0.85029	5.34350		0.22500	0.97297	1.70046
-0.02500	0.86079	5.49712		0.23333	0.97844	1.71736
-0.01667	0.57792	10.41583		0.24167	0.96227	1.59640
-0.00833	0.19646	5.50233		0.25000	0.96448	1.61445
0.00000	0.42506	8.77323				

Hot-wire Blade 4 Wake Survey for IFA = 35° and Re = 380,000

Vref = 41.6141 m/s

Y/S	Umean/Vref	u'/Vref		Y/S	Umean/Vref	u'/Vref
-0.25000	0.70664	1.29215		0.00833	0.13716	3.39998
-0.24167	0.70152	1.23979		0.01667	0.13423	3.81263
-0.23333	0.70462	1.14902		0.02500	0.19293	7.84973
-0.22500	0.70368	1.27774		0.03333	0.38710	7.59614
-0.21667	0.69686	1.20026		0.04167	0.53371	7.26330
-0.20833	0.68813	1.25563		0.05000	0.66028	6.47550
-0.20000	0.68931	1.14880		0.05833	0.74523	3.73448
-0.19167	0.69330	1.19996		0.06667	0.76318	2.06363
-0.18333	0.68258	1.15192		0.07500	0.76587	1.51382
-0.17500	0.69750	1.29338		0.08333	0.76496	1.26990
-0.16667	0.68969	1.32676		0.09167	0.76873	1.48111
-0.15833	0.68571	1.18579		0.10000	0.76851	1.37041
-0.15000	0.68926	1.15038		0.10833	0.77267	1.50678
-0.14167	0.69044	1.21351		0.11667	0.76133	1.22376
-0.13333	0.68051	1.11182		0.12500	0.77068	1.53056
-0.12500	0.68801	1.22996		0.13333	0.76433	1.32229
-0.11667	0.68893	1.15381		0.14167	0.76210	1.30776
-0.10833	0.69440	1.18118		0.15000	0.77519	1.59806
-0.10000	0.69017	1.21402		0.15833	0.76681	1.33700
-0.09167	0.69779	1.15471		0.16667	0.76426	1.35144
-0.08333	0.70217	1.15408		0.17500	0.76729	1.47687
-0.07500	0.70962	1.22103		0.18333	0.75808	1.29958
-0.06667	0.70990	1.29905		0.19167	0.76094	1.28500
-0.05833	0.70822	1.11396		0.20000	0.76717	1.43169
-0.05000	0.70769	1.24002		0.20833	0.76722	1.50075
-0.04167	0.72057	1.15083		0.21667	0.76760	1.44815
-0.03333	0.72348	1.34690		0.22500	0.76284	1.43193
-0.02500	0.72250	1.80002		0.23333	0.76753	1.49637
-0.01667	0.72283	2.32152		0.24167	0.77135	1.44065
-0.00833	0.70005	2.94133		0.25000	0.77226	1.48668
0.00000	0.69318	3.51621				

Hot-wire Blade 4 Wake Survey for IFA = 33° and Re = 280,000

Vref = 29.6371 m/s

Y/S	Umean/Vref	u'/Vref		Y/S	Umean/Vref	u'/Vref
-0.25000	0.84725	1.64231		0.00833	0.66029	7.97891
-0.24167	0.83601	1.57731		0.01667	0.67372	8.58921
-0.23333	0.84647	1.78174		0.02500	0.74909	7.84377
-0.22500	0.83875	1.86915		0.03333	0.84188	6.93527
-0.21667	0.83972	1.86679		0.04167	0.89989	5.37322
-0.20833	0.83986	1.82384		0.05000	0.92752	2.74240
-0.20000	0.84377	1.99476		0.05833	0.93808	2.18188
-0.19167	0.84121	1.88574		0.06667	0.93049	1.55261
-0.18333	0.85045	1.94848		0.07500	0.93042	1.44392
-0.17500	0.83807	1.65670		0.08333	0.93194	1.43696
-0.16667	0.84438	2.01782		0.09167	0.93245	1.40259
-0.15833	0.84637	2.01987		0.10000	0.93336	1.56552
-0.15000	0.85298	2.15703		0.10833	0.92938	1.42408
-0.14167	0.84846	1.89598		0.11667	0.93248	1.53384
-0.13333	0.84320	2.04063		0.12500	0.93815	1.42749
-0.12500	0.85821	1.92592		0.13333	0.93774	1.66731
-0.11667	0.85130	1.76900		0.14167	0.93940	1.57715
-0.10833	0.85784	1.66447		0.15000	0.94412	1.63078
-0.10000	0.85514	2.17241		0.15833	0.94240	1.55882
-0.09167	0.85501	2.43190		0.16667	0.93852	2.16338
-0.08333	0.85352	3.90769		0.17500	0.94976	1.69959
-0.07500	0.84880	3.63677		0.18333	0.94949	1.71430
-0.06667	0.84708	4.39550		0.19167	0.93855	1.75556
-0.05833	0.84060	5.08194		0.20000	0.93754	1.67482
-0.05000	0.84293	4.62221		0.20833	0.94253	1.60778
-0.04167	0.83966	4.54162		0.21667	0.94959	1.60271
-0.03333	0.84472	4.90469		0.22500	0.94257	1.72217
-0.02500	0.79191	7.69763		0.23333	0.95654	1.70532
-0.01667	0.21869	5.23913		0.24167	0.94895	1.60438
-0.00833	0.20156	5.83491		0.25000	0.95576	1.87520
0.00000	0.23304	8.73443				

Hot-wire Blade 4 Wake Survey for IFA = 33° and Re = 640,000

Vref = 68.7834 m/s

Y/S	Umean/Vref	u'/Vref		Y/S	Umean/Vref	u'/Vref
-0.25000	0.81783	1.69045		0.00833	0.64414	6.74090
-0.24167	0.81985	1.64683		0.01667	0.77802	5.17649
-0.23333	0.82632	1.85599		0.02500	0.88463	3.55887
-0.22500	0.82060	1.74141		0.03333	0.92774	1.94918
-0.21667	0.82683	1.85259		0.04167	0.92796	1.71505
-0.20833	0.82952	1.83249		0.05000	0.92819	1.61208
-0.20000	0.82013	1.71349		0.05833	0.93306	1.56101
-0.19167	0.82680	1.80383		0.06667	0.93008	1.59899
-0.18333	0.83290	1.82906		0.07500	0.93863	1.63528
-0.17500	0.82924	1.92857		0.08333	0.94079	1.62089
-0.16667	0.83109	1.93286		0.09167	0.93576	1.52679
-0.15833	0.83596	1.95923		0.10000	0.94130	1.66752
-0.15000	0.83894	1.80061		0.10833	0.93930	1.57257
-0.14167	0.83776	1.91504		0.11667	0.93438	1.49258
-0.13333	0.83817	1.89753		0.12500	0.94242	1.63850
-0.12500	0.84083	2.03430		0.13333	0.94492	1.57887
-0.11667	0.85224	2.05356		0.14167	0.94341	1.52314
-0.10833	0.85230	2.00205		0.15000	0.94171	1.54535
-0.10000	0.86029	2.58217		0.15833	0.94399	1.56665
-0.09167	0.85132	2.68780		0.16667	0.94300	1.58085
-0.08333	0.85409	2.75563		0.17500	0.94406	1.55034
-0.07500	0.85528	3.44318		0.18333	0.94476	1.54034
-0.06667	0.85064	3.61829		0.19167	0.94422	1.52436
-0.05833	0.84939	3.88027		0.20000	0.95381	1.64732
-0.05000	0.84462	4.19972		0.20833	0.95144	1.68128
-0.04167	0.84278	4.03066		0.21667	0.94827	1.68412
-0.03333	0.83802	4.15315		0.22500	0.95000	1.77697
-0.02500	0.83639	5.15495		0.23333	0.94856	1.54473
-0.01667	0.56168	11.39360		0.24167	0.94655	1.72528
-0.00833	0.27216	5.10570		0.25000	0.94453	1.64594
0.00000	0.31891	7.75504				

THIS PAGE INTENTIONALLY LEFT BLANK

APPENDIX G: LDV WAKE SURVEY REDUCED DATA

LDV Blade 4 Wake Survey at IFA = 33° and Re = 280,000

Vref = 29.6371 m/s

Y/S	Z (mm)	UVmean/Vref	Non-Dim TI%	UV Re	UVx corr
-0.0833	133.0	0.8353	2.0413	0.0923	0.2521
-0.0750	133.0	0.8241	1.9749	0.0739	0.2156
-0.0667	133.0	0.8224	1.8885	0.0595	0.1900
-0.0583	133.0	0.8199	1.7441	0.0368	0.1376
-0.0500	133.0	0.8181	2.2537	0.0411	0.0924
-0.0417	133.0	0.7699	5.2371	0.2953	0.1227
-0.0333	133.0	0.3526	10.9476	-1.3378	-0.1280
-0.0250	133.0	0.8628	4.8293	-0.0005	-0.0016
-0.0167	133.0	0.8781	5.3661	0.0121	0.0569
-0.0083	133.0	0.8870	4.2983	-0.0014	-0.0061
0.0000	133.0	0.8935	1.7152	0.0228	0.0916
0.0083	133.0	0.9051	1.7943	0.0197	0.0727
0.0167	133.0	0.9131	1.6433	0.0165	0.0719
0.0250	133.0	0.9149	1.6863	0.0124	0.0505
0.0333	133.0	0.9126	1.6872	0.0215	0.0865
0.0417	133.0	0.9073	1.6213	0.0170	0.0747
0.0500	133.0	0.9021	1.5842	0.0139	0.0641
0.0583	133.0	0.8943	1.6320	0.0285	0.1236
0.0667	133.0	0.8907	1.5968	0.0223	0.1014
0.0750	133.0	0.8908	1.5132	0.0080	0.0404
0.0833	133.0	0.8824	1.6555	0.0161	0.0674
0.0917	133.0	0.8720	1.6710	0.0258	0.1052
0.1000	133.0	0.8628	1.7876	0.0312	0.1111
0.1083	133.0	0.8476	1.7990	0.0368	0.1296
0.1167	133.0	0.8425	1.7880	0.0222	0.0797

LDV Blade 4 Wake Survey for IFA = 33° and Re = 380,000

Vref = 40.1873 m/s

Y/S	Z	UVmean/Vref	Non-Dim TI%	UVRe	UVx corr.
-0.0667	133.0	0.8197	3.6491	0.3069	0.1464
-0.0583	133.0	0.7999	4.3923	0.0588	0.0196
-0.0500	133.0	0.7766	5.3932	0.4970	0.1085
-0.0417	133.0	0.7527	6.4326	0.6014	0.0951
-0.0333	133.0	0.6525	8.8316	1.3145	0.1081
-0.0250	133.0	0.4917	11.9201	2.6978	0.1179
-0.0167	133.0	0.4238	13.0247	0.1484	0.0055
-0.0083	133.0	0.5407	10.9657	-1.0066	-0.0518
0.0000	133.0	0.6626	8.3143	-0.6281	-0.0574
0.0083	133.0	0.7582	7.2819	-0.4835	-0.0568
0.0167	133.0	0.8559	4.0667	-0.1056	-0.0399
0.0250	133.0	0.8885	2.3649	-0.0132	-0.0146
0.0333	133.0	0.9437	2.9988	0.0856	0.0078
0.0417	133.0	0.9040	2.0020	0.0099	0.0155
0.0500	133.0	0.9115	1.5070	-0.0009	-0.0026
0.0583	133.0	0.9139	1.4934	0.0119	0.0336

LDV Blade 4 Wake Survey for IFA = 33° and Re = 640,000

Vref = 68.7834 m/s

Y/S	Z	Uvmean/Vref	Non-Dim TI%	UV Re	UV x corr.
-0.1083	133.0	0.8028	1.5102	0.1261	0.0577
-0.1000	133.0	0.7936	2.0164	0.0976	0.0560
-0.0917	133.0	0.7906	2.4029	0.0989	0.0096
-0.0833	133.0	0.7573	2.1014	0.0805	0.0543
-0.0750	133.0	0.7246	3.1251	0.1266	0.0566
-0.0667	133.0	0.6948	4.1394	0.3420	0.0592
-0.0583	133.0	0.6184	4.9445	-0.5652	0.0893
-0.0500	133.0	0.5784	6.3938	0.0001	0.0775
-0.0417	133.0	0.4795	9.2702	0.0277	0.0476
-0.0333	133.0	0.4531	9.2741	0.0090	0.0605
-0.0250	133.0	0.3824	10.8393	0.0215	0.0881
-0.0167	133.0	0.4812	6.5945	-0.0007	0.0207
-0.0083	133.0	0.5647	5.5684	0.0360	0.0908
0.0000	133.0	0.5875	9.8379	0.0411	0.1591
0.0083	133.0	0.6460	2.7739	0.0403	0.1156
0.0167	133.0	0.7488	2.3304	0.0253	0.0424
0.0250	133.0	0.7975	1.8826	0.0242	0.0614
0.0333	133.0	0.8249	2.5048	0.0132	0.0615
0.0417	133.0	0.8240	2.2526	0.0489	0.0293
0.0500	133.0	0.8229	2.3281	0.0296	0.0507
0.0583	133.0	0.8315	2.0421	0.0420	0.0718
0.0667	133.0	0.8419	1.9527	0.0383	0.0422
0.0750	133.0	0.8554	1.8023	0.0743	0.0901
0.0833	133.0	0.8785	1.4475	0.0476	0.0150

LDV Blade 4 Wake Survey for IFA = 31° and Re = 380,000

Vref = 39.9467 m/s

Y/S	Z	Uvmean/Vref	Non-Dim TI%	UV Re	UV x corr.
-0.0500	133.0	0.8290	5.3996	0.6095	0.1315
-0.0417	133.0	0.8238	5.0988	0.2316	0.0558
-0.0333	133.0	0.8019	6.5688	0.5295	0.0776
-0.0250	133.0	0.7845	7.5231	0.9667	0.1077
-0.0167	133.0	0.7128	9.3779	2.1719	0.1563
-0.0083	133.0	0.5069	15.0265	8.2910	0.2308
0.0000	133.0	0.3743	12.2174	-0.4401	-0.0186
0.0083	133.0	0.5053	9.2832	-1.2011	-0.0888
0.0167	133.0	0.6624	7.3976	-1.2515	-0.1466
0.0250	133.0	0.8035	5.6267	-0.1983	-0.0399
0.0333	133.0	0.8849	2.6712	0.0111	0.0097
0.0417	133.0	0.8955	1.7766	0.0135	0.0272
0.0500	133.0	0.8990	1.6443	0.0315	0.0749
0.0583	133.0	0.9077	1.5183	0.0090	0.0252
0.0667	133.0	0.9105	1.4961	0.0203	0.0585
0.0750	133.0	0.9124	1.4323	0.0158	0.0496

LDV Blade 4 Wake Survey for IFA = 35° and Re = 380,000

Vref = 41.6141 m/s

Y/S	Z (mm)	UVmean/Vref	Non-Dim TI%	UV Re	UV x corr.
-0.0417	130.1	0.8332	1.6351	0.1172	0.2532
-0.0333	130.1	0.8277	1.6486	0.0931	0.1978
-0.0250	130.1	0.8275	1.6543	0.1069	0.2255
-0.0167	130.1	0.8263	1.6611	0.0918	0.1921
-0.0083	130.1	0.7542	1.5837	0.0474	0.1094
0.0000	130.1	0.5057	4.0827	0.2227	0.0779
0.0083	130.1	0.5168	7.2283	-0.5909	-0.0671
0.0167	130.1	0.5614	4.8620	-0.0092	-0.0635
0.0250	130.1	0.5809	7.5843	-0.0095	-0.0983
0.0333	130.1	0.6835	1.7657	0.0140	0.0176
0.0417	130.1	0.7982	1.4426	0.0223	0.0634
0.0500	130.1	0.8582	1.4756	0.0123	0.0445
0.0583	130.1	0.8882	1.4448	0.0246	0.0534
0.0667	130.1	0.8921	1.4844	0.0093	0.0625
0.0750	130.1	0.8972	1.4403	0.0223	0.0554
0.0833	130.1	0.8982	1.4568	0.0293	0.0634

THIS PAGE INTENTIONALLY LEFT BLANK

LIST OF REFERENCES

1. Gelder, T.F., Schmidt, J.F., Suder, K.L., and Hathaway, M.D., "Design and Performance of Controlled-Diffusion Stator Compared With Original Double-Circular-Arc Stator", NASA Technical Paper 2852, March 1989.
2. Sanger, N.L., "The Use of Optimization Techniques to Design Controlled-Diffusion Compressor Blading", *ASME Journal Of Engineering For Power,* Vol. 105, pp.256-264, 1983.
3. Hansen, D.J., "Investigation of Second Generation Controlled-Diffusion Compressor Blades in Cascade", Master's Thesis, Naval Postgraduate School, Monterey, California, September 1995.
4. Schnorenberg, D.G., "Investigation of the Effect of Reynolds Number on Laminar Separation Bubbles on Controlled-Diffusion Compressor Blades in Cascade", Master's Thesis, Naval Postgraduate School, Monterey, California, June 1996.
5. Grove, D.V., "Experimental and Numerical Investigation of Second Generation, Controlled-Diffusion, Compressor Blades in Cascade", Master's Thesis, Naval Postgraduate School, Monterey, California, June 1997.
6. Nicholls, J.L., "Investigation of Flow Over Second Generation Controlled-Diffusion Blades in a Linear Cascade", Master's Thesis, Naval Postgraduate School, Monterey, California, September 1999.
7. Carlson, J.R., "Experimental and Computational Investigation of the End Wall Flow in a Cascade of Compressor Blades", Master's Thesis, Naval Postgraduate School, Monterey, California, September 2000.
8. Caruso, T.M., "Three-Component LDV Measurements of Corner Vortices Over Second-Generation, Controlled-Diffusion, Compressor Blades in Cascade", Master's Thesis, Naval Postgraduate School, Monterey, California, September 2001.
9. Sanger, N.L., and Shreeve, R.P., "Comparison of Calculated and Experimental Cascade Performance for Controlled-Diffusion Compressor Stator Blading", *ASME Journal of Turbomachinery,* Vol. 108, pp.42-50, July 1986.
10. Grubb, C., Grubbs, L.W., Neuser, M.D., Muller, J., O'Brien, J., "Subsonic Five-Hole Probe Calibration in Non Null-Yaw Mode", AA3802 Term Project, Naval Postgraduate School, Monterey, California, December 1999.
11. Grossman, B.L., "Testing and Analysis of a Transonic Axial Compressor", Master's Thesis, Naval Postgraduate School, Monterey, California, September 1997.
12. Roshko, A., "On the Development of Turbulent Wakes From Vortex Streets", *NACA Rep.* 1191, 1954.
13. Hah, C., Private Communication, Naval Postgraduate School, Monterey, California, January 2002.

THIS PAGE INTENTIONALLY LEFT BLANK

INITIAL DISTRIBUTION LIST

1. Defense Technical Information Center
   8725 John J. Kingman Rd., Ste 0944

2. Dudley Knox Library
   Naval Postgraduate School
   Monterey, California

3. Marine Corps Representative
   Naval Postgraduate School
   Monterey, CA

4. Director, Training and Education, MCCDC, Code C46
   Quantico, Virginia

5. Director, Marine Corps Research Center, MCCDC, Code C40RC
   Quantico, Virginia

6. Marine Corps Tactical Systems Support Activity (Attn: Operations Officer)
   Camp Pendleton, California

7. Dr. Max F. Platzer
   Department Chairman, Code AA/PL
   Department of Aeronautics and Astronautics
   Naval Postgraduate School

8. Dr. Garth V. Hobson, Code AA/HG
   Department of Aeronautics and Astronautics
   Naval Postgraduate School

9. Dr. Raymond P. Shreeve, Code AA/SF
   Department of Aeronautics and Astronautics
   Naval Postgraduate School

10. Naval Air Warfare Center
    AIR-4.4.7.1 (Attn: Mr. R. Ravindranath)
    Propulsion and Power Engineering, Building 106

11. Naval Air Warfare Center
    AIR-4.4.7.1 (Attn: Mr. M. Klein)
    Propulsion and Power Engineering, Building 106

12. NASA Glenn Research Center
MS 5-11 (Attn: Dr. C. Hah)
21000 BrookPark Rd.
Cleveland, OH

13. Peter J. Brown
229 Wintergull Lane
Annapolis, MD